

APPENDIX A

PERSONNEL CONDUCTING THE INVESTIGATION

The following Inspectors of the Air Accidents Investigation Branch conducted the investigation:

Mr M M Charles	Investigator-in-Charge
Mr D F King	Principal Inspector (Engineering)
Mr P F Sheppard	Assistant Principal Inspector (Engineering)
Mr A N Cable	Senior Inspector (Engineering)
Mr R G Carter	Senior Inspector (Engineering)
Mr P T Claiden	Senior Inspector (Engineering)
Mr P R Coombs	Senior Inspector (Engineering)
Mr S R Culling	Senior Inspector (Engineering)
Miss A Evans	Senior Inspector (Engineering)
Mr B M E Forward	Senior Inspector (Operations)
Mr P N Giles	Senior Inspector (Operations)
Mr S W Moss	Senior Inspector (Engineering)
Mr R Parkinson	Senior Inspector (Engineering)
Mr J D Payling	Senior Inspector (Operations)
Mr C G Pollard	Senior Inspector (Engineering)
Mr C A Protheroe	Senior Inspector (Engineering)
Mr A H Robinson	Senior Inspector (Engineering)
Mr A P Simmons	Senior Inspector (Engineering)
Mr R G Vance	Senior Inspector (Engineering)
Mr R StJ Whidborne	Senior Inspector (Operations)

The Air Accidents Investigation Branch would like to thank the following organisations from the United Kingdom, United States of America, France, and Canada who participated in the investigation:

Air Line Pilot's Association International
Boeing Commercial Airplane Company
British Airways
British Army
British Geological Survey
Bureau Enquete Accidents
Canadian Aviation Safety Bureau
Civil Aviation Authority
Cranfield Institute of Technology
Federal Aviation Administration
Federal Bureau of Investigation
Independent Union of Flight Attendants
National Transportation Safety Board
Pan American World Airways
Police Service
Royal Aerospace Establishment
Royal Air Force
Royal Armaments Research and Development Establishment
Royal Navy
Royal Ordnance
Royal Signals and Radar Establishment
United Technologies International Operations (Pratt and Whitney)

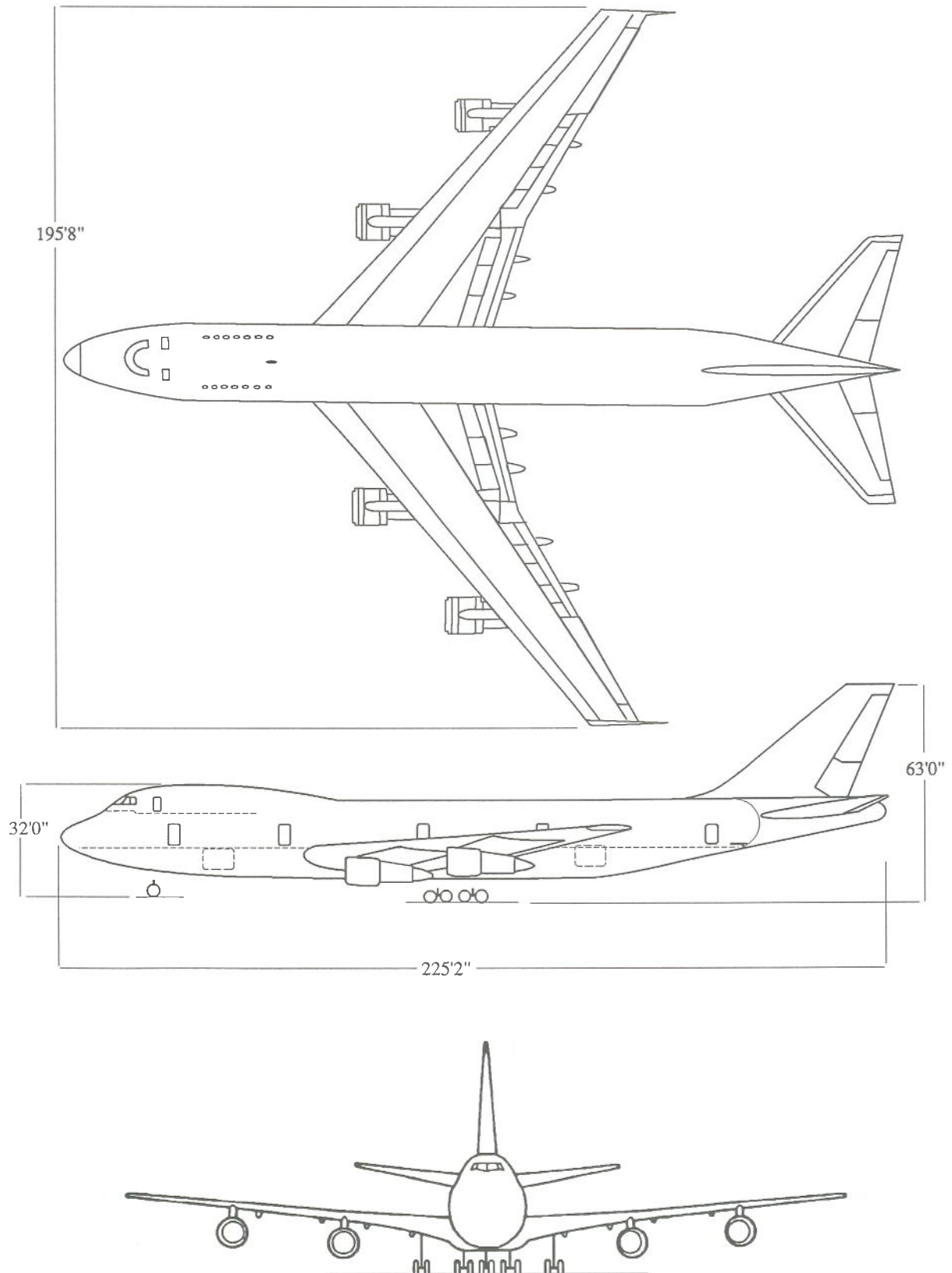
The Air Accidents Investigation Branch would also like to acknowledge the excellent work of the Dumfries & Galloway Regional Council and to thank all the many voluntary organisations who gave such unstinting support to the investigation.

APPENDIX B

PHOTOGRAPHS

AND

DIAGRAMS



Boeing 747 - 121 Leading Dimensions

Figure B-1

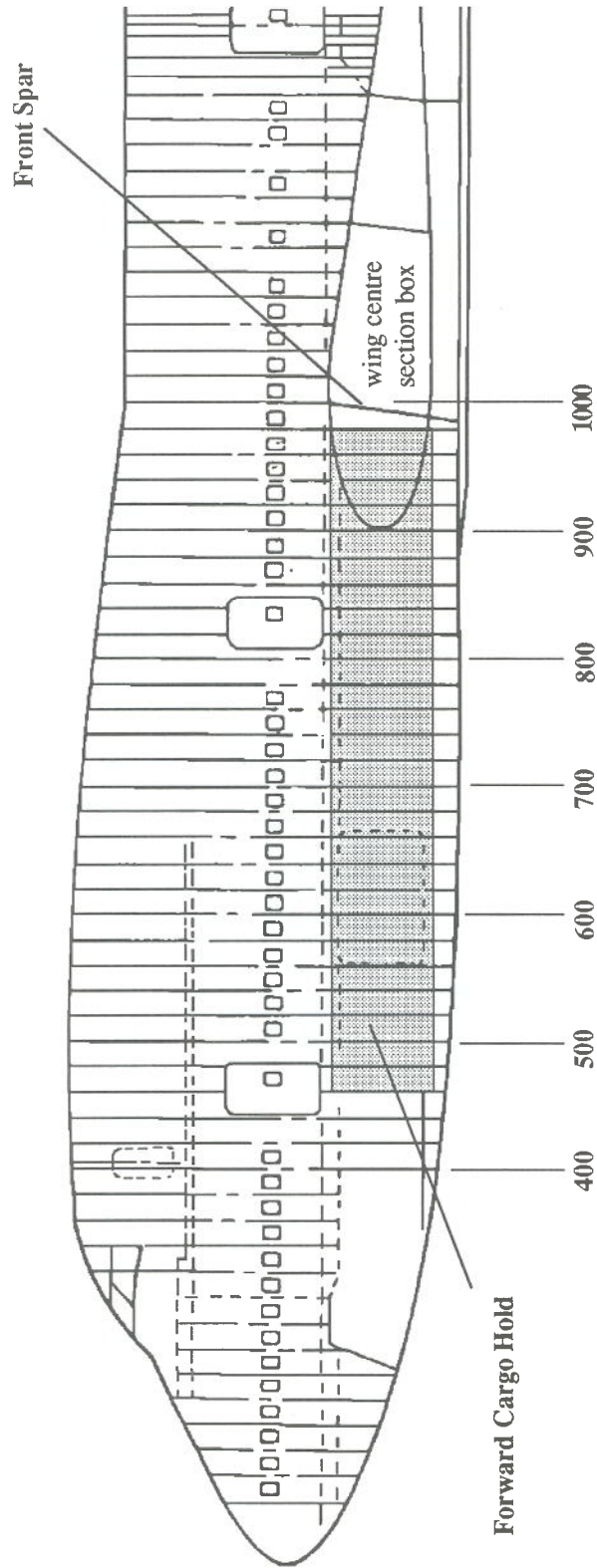
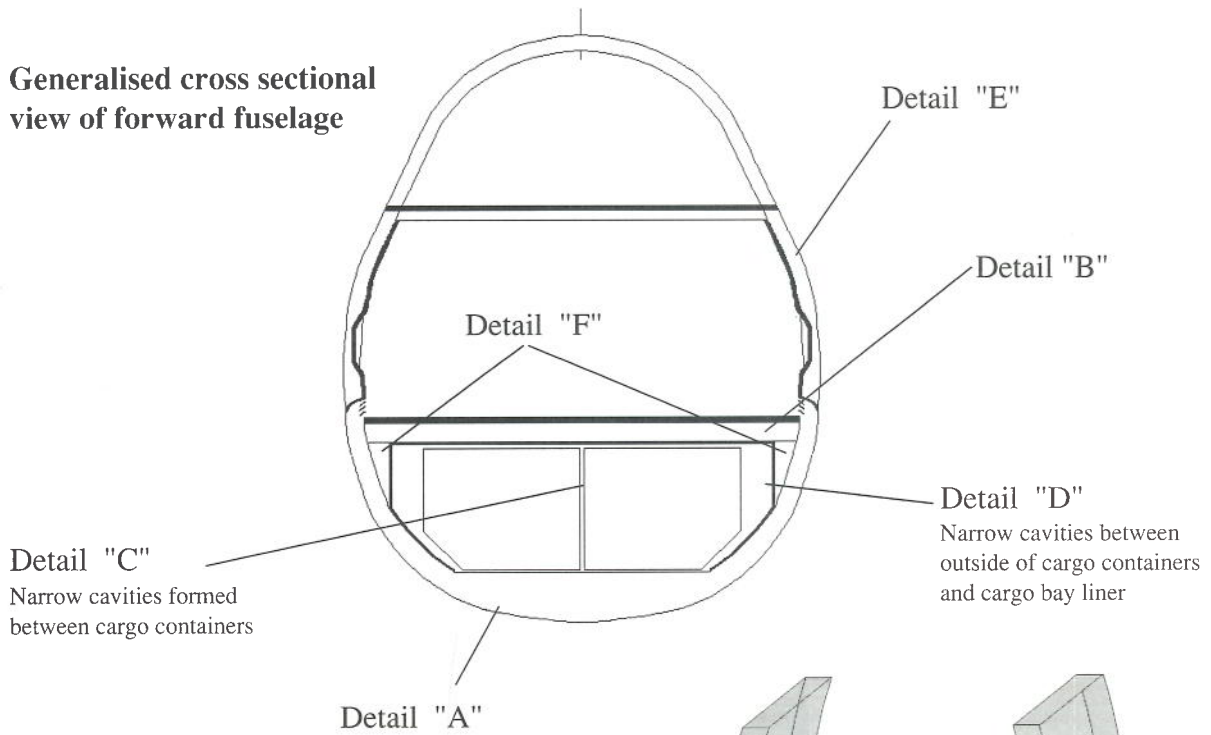


Figure B-2

Forward Fuselage Station Diagram

Generalised cross sectional view of forward fuselage



Detail "C"
Narrow cavities formed between cargo containers

Detail "D"
Narrow cavities between outside of cargo containers and cargo bay liner

Detail "E"
Vertical cavities between frames, bounded by fuselage skin and cabin side liner panel. Top of cavity largely blanked by upper deck floor panels

Detail "F"
Longitudinal 'manifold' cavity, formed in space between container side and curved fuselage side

Detail "A"

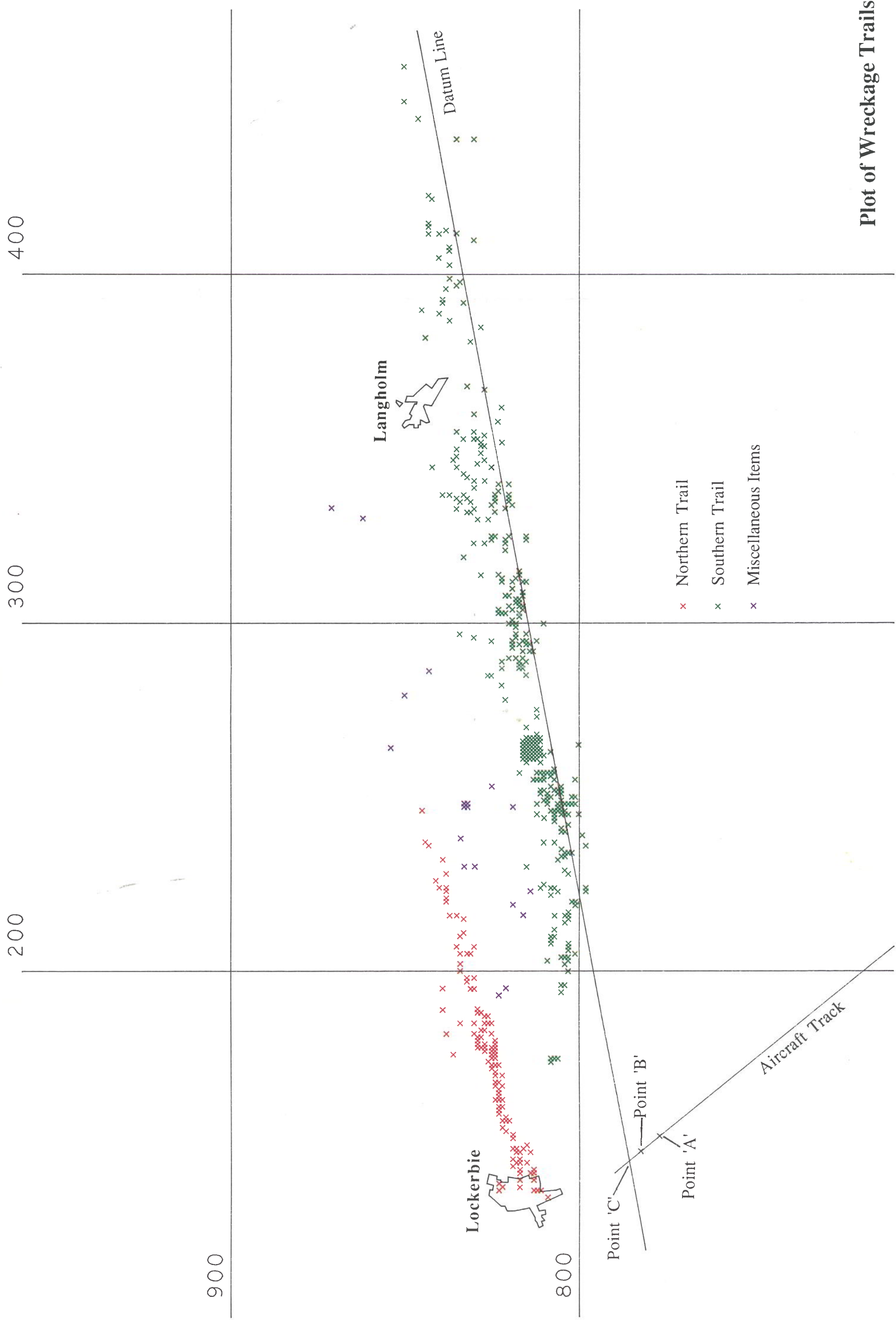
Detail "A"
Semi-circular cavity between fuselage frames in fuselage lower lobe, bounded by fuselage skin and cargo bay

Note:
Baggage containers omitted for clarity

Detail "B"
Horizontal cavity between floor beams, bounded by cabin floor panels and cargo bay liner/top panels of cargo containers

Network of Interlinked Cavities
formed within forward fuselage structure and baggage hold
(schematic representation)

Figure B-3



Plot of Wreckage Trails

Figure B-4



key:
Green : Southern wreckage trail
Red : Northern wreckage trail
Grey : Crater
Yellow : Rosebank
White : Not recovered/identified

Model showing fuselage and tail surface fracture lines
(colour coded to show location of items on the ground)

Figure B-5



key:
 Green : Southern wreckage trail
 Red : Northern wreckage trail
 Grey : Crater
 Yellow : Rosebank
 White : Not recovered/identified

Model showing fuselage and tail surface fracture lines
 (colour coded to show location of items on the ground)

Figure B-6



key:
Green : Southern wreckage trail
Red : Northern wreckage trail
Grey : Crater
Yellow : Rosebank
White : Not recovered/identified

Model showing fuselage and tail surface fracture lines
(colour coded to show location of items on the ground)

Figure B-7



key:
Green : Southern wreckage trail
Red : Northern wreckage trail
Grey : Crater
Yellow : Rosebank
White : Not recovered/identified

Model showing fuselage and tail surface fracture lines
(colour coded to show location of items on the ground)

Figure B-8



Photograph of nose and flight deck

Figure B-9

Distribution of Major Wreckage Items Located in Southern Trail.

Structure Recovered Less than 250m Beyond Datum Line

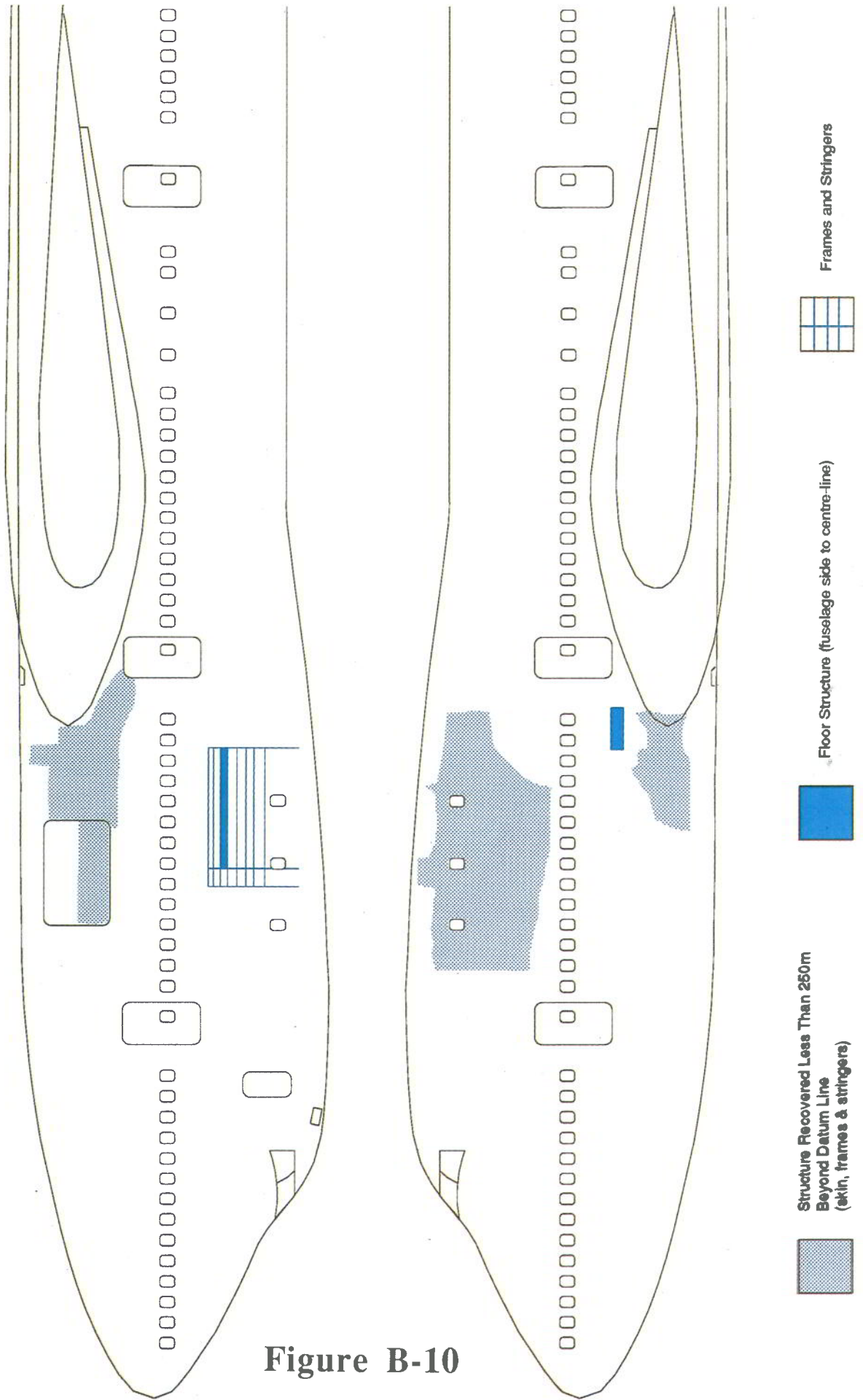


Figure B-10

Distribution of Major Wreckage Items Located in Southern Trail.

Structure Recovered Less than 300m Beyond Datum Line

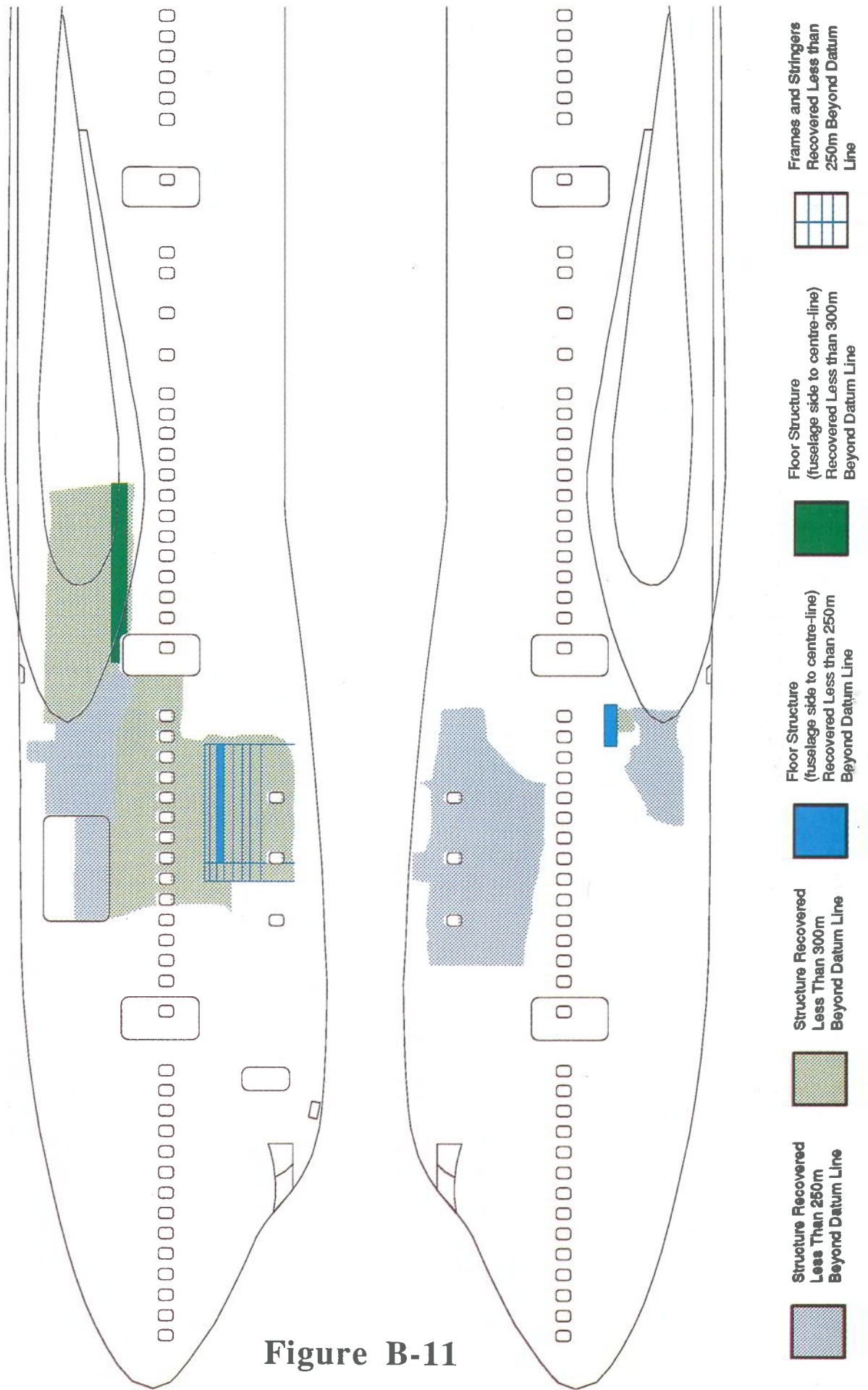


Figure B-11

Distribution of Major Wreckage Items Located in Southern Trail.

Structure Recovered Less than 600m Beyond Datum Line

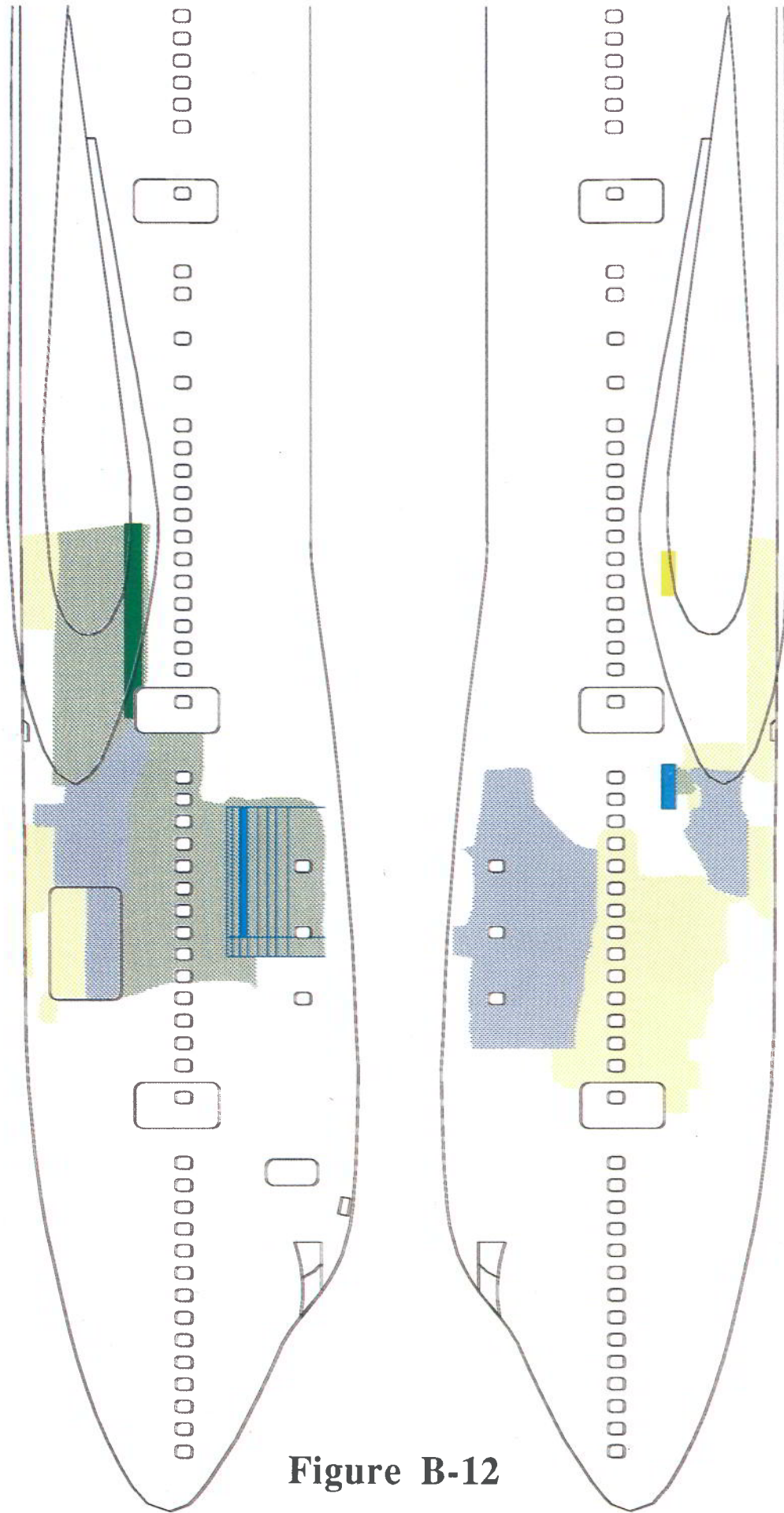












Figure B-12

-  Structure Recovered Less Than 250m Beyond Datum Line
-  Frames and Stringers Recovered Less than 250m Beyond Datum Line
-  Structure Recovered Less Than 600m Beyond Datum Line
-  Floor Structure (fuselage side to centre-line) Recovered Less than 600m Beyond Datum Line
-  Structure Recovered Less Than 250m Beyond Datum Line
-  Floor Structure (fuselage side to centre-line) Recovered Less than 300m Beyond Datum Line
-  Structure Recovered Less Than 600m Beyond Datum Line
-  Floor Structure (fuselage side to centre-line) Recovered Less than 600m Beyond Datum Line
-  Structure Recovered Less Than 250m Beyond Datum Line
-  Floor Structure (fuselage side to centre-line) Recovered Less than 300m Beyond Datum Line

Distribution of Major Wreckage Items Located in Southern Trail.

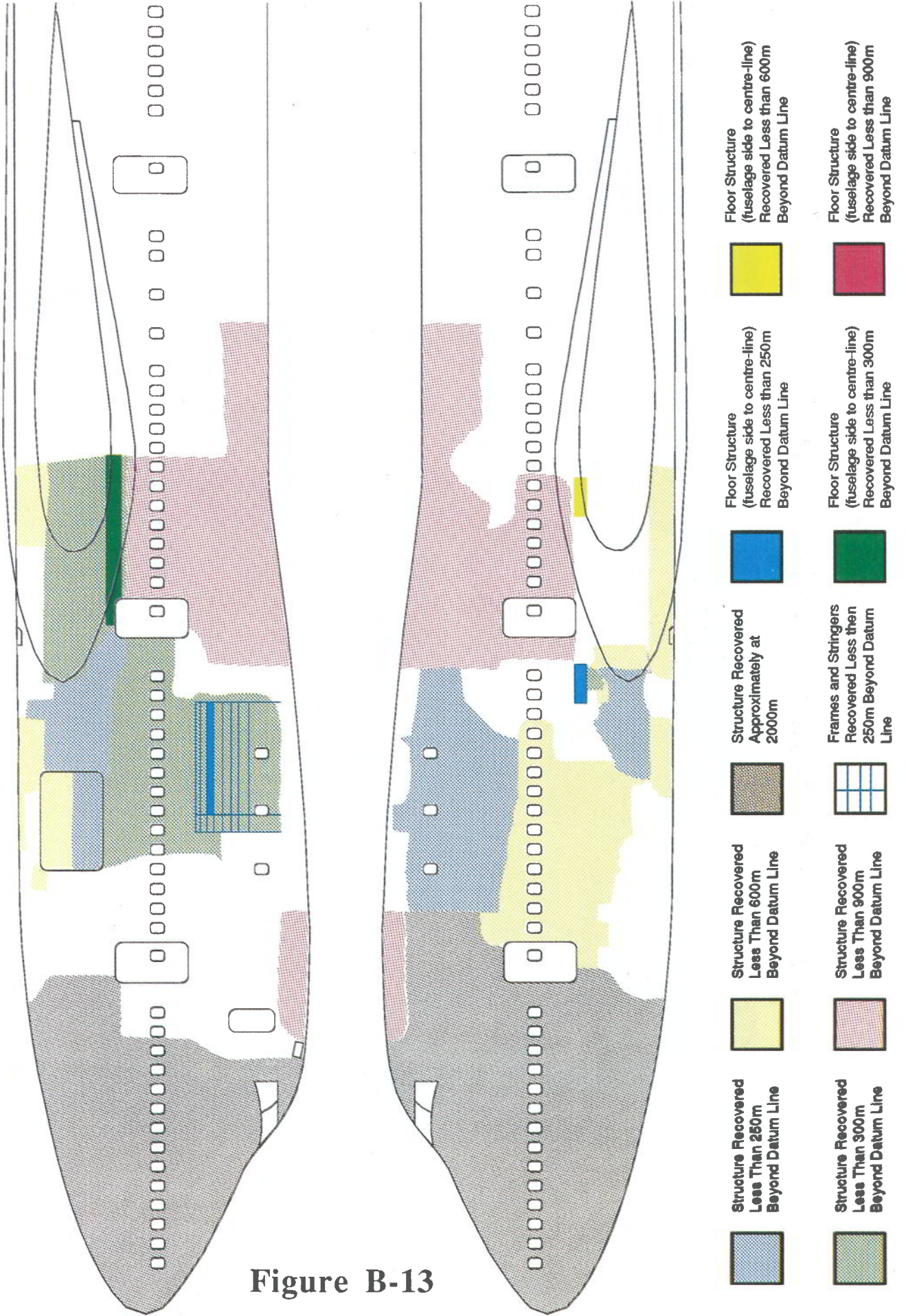


Figure B-13



Two-dimensional layout at CAD Longtown

Figure B-14



Detail of shatter zone of fuselage

Figure B-15

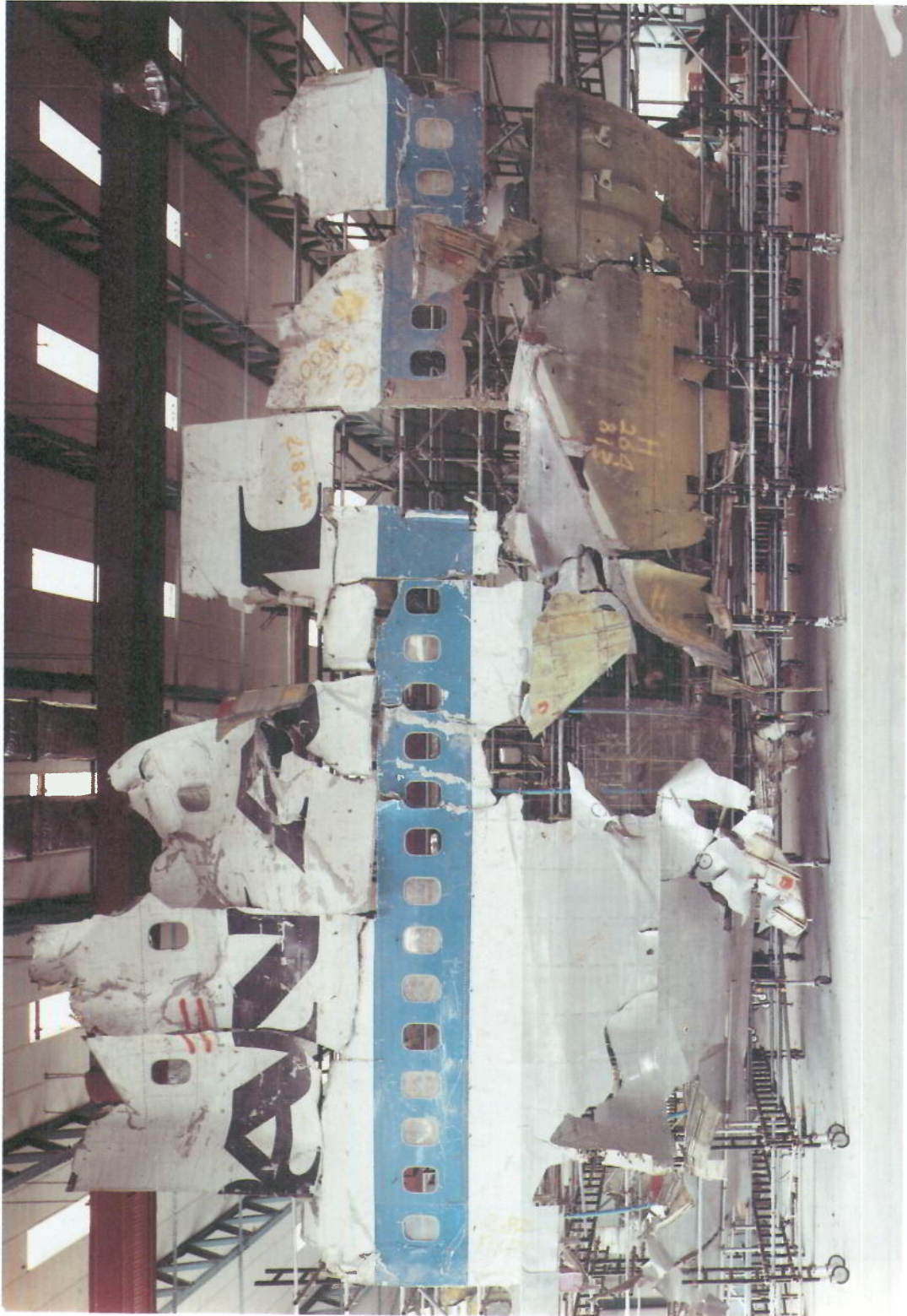


Figure B-16

Fuselage three-dimensional reconstruction

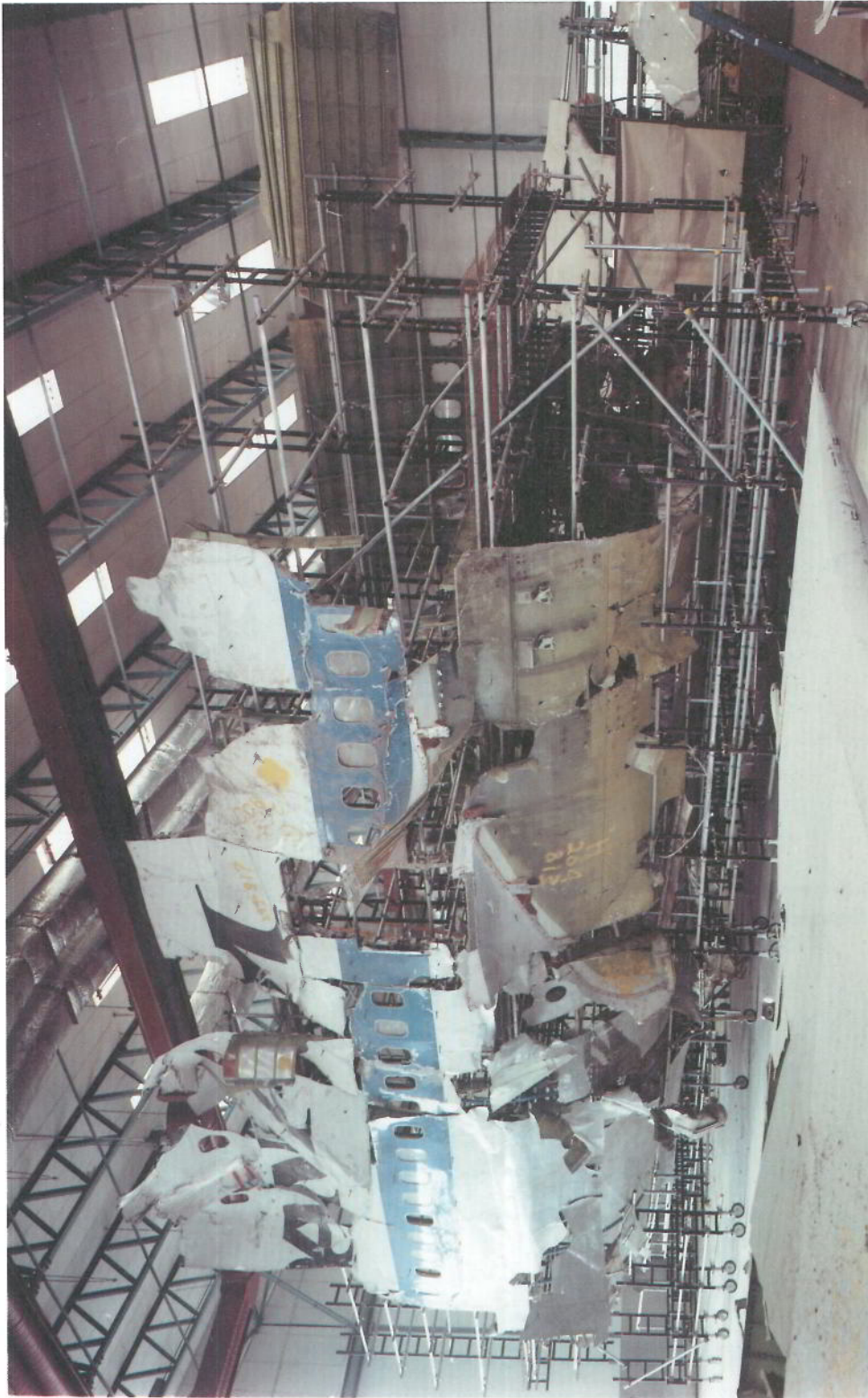
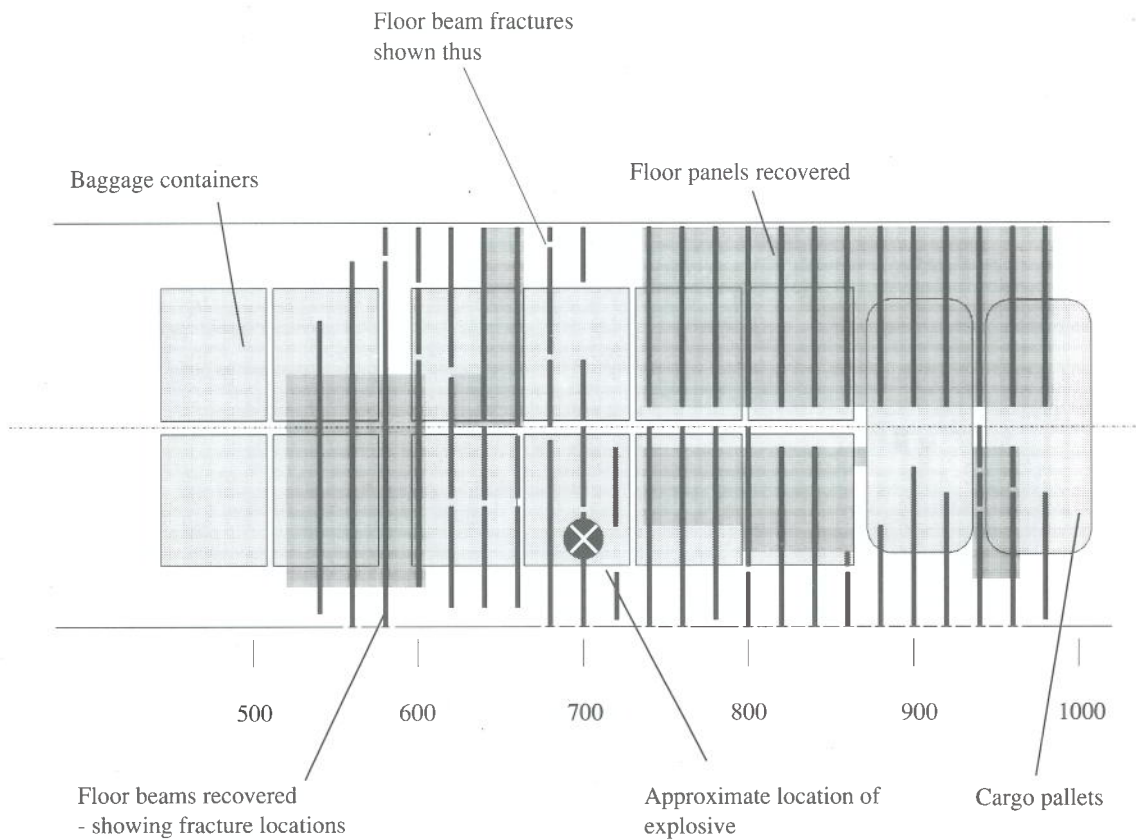


Figure B-17

Fuselage three-dimensional reconstruction

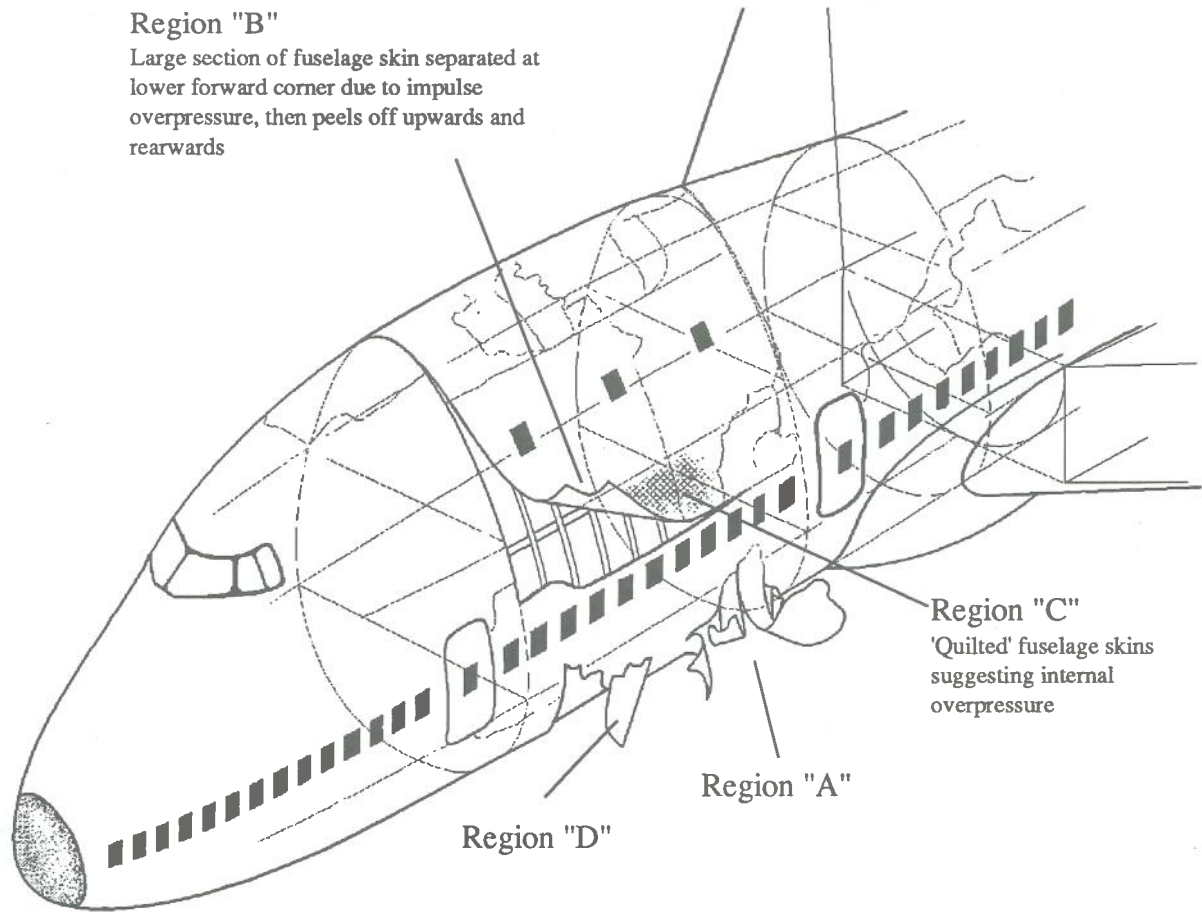


Plot of floor damage in area of explosion
 (structure & floor panel details based on those items recovered, identified, and incorporated into the three-dimensional reconstruction)

Figure B-18

Region "B"

Large section of fuselage skin separated at lower forward corner due to impulse overpressure, then peels off upwards and rearwards



Region "C"
'Quilted' fuselage skins suggesting internal overpressure

Region "A"

Region "D"

Region "A"
'Star-burst' fracture and petalled fuselage skins

Region "B"

Region "C"

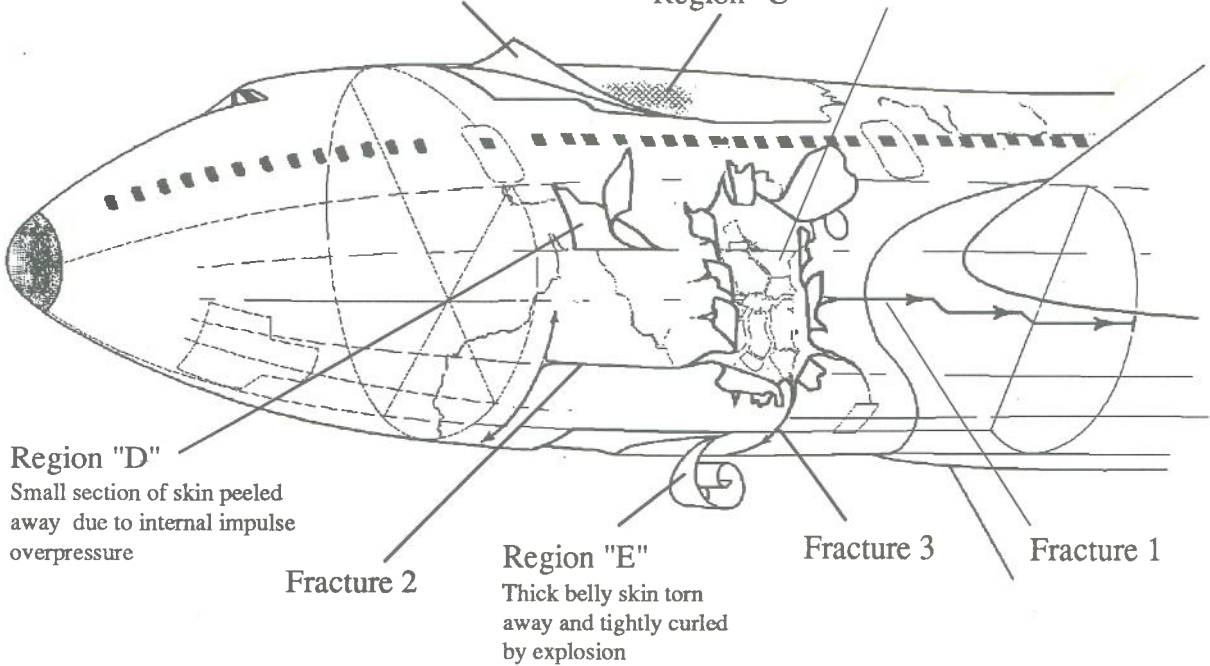
Region "D"
Small section of skin peeled away due to internal impulse overpressure

Fracture 2

Region "E"
Thick belly skin torn away and tightly curled by explosion

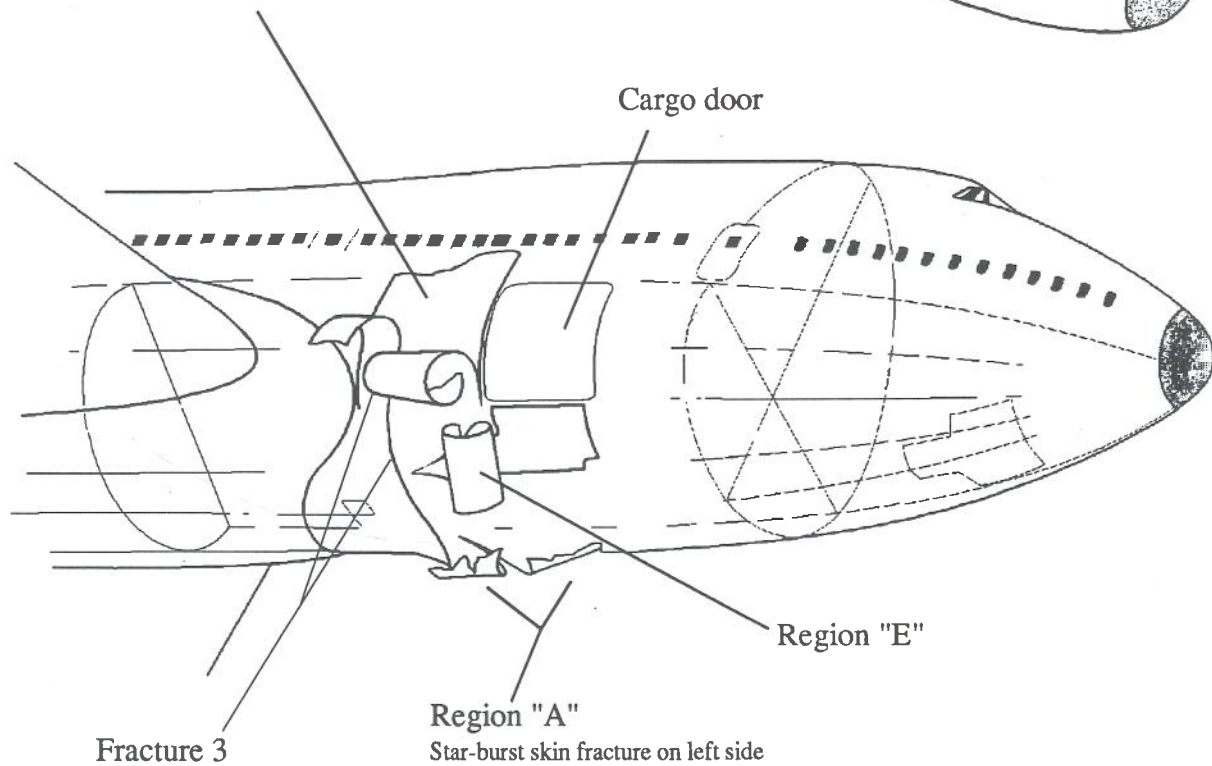
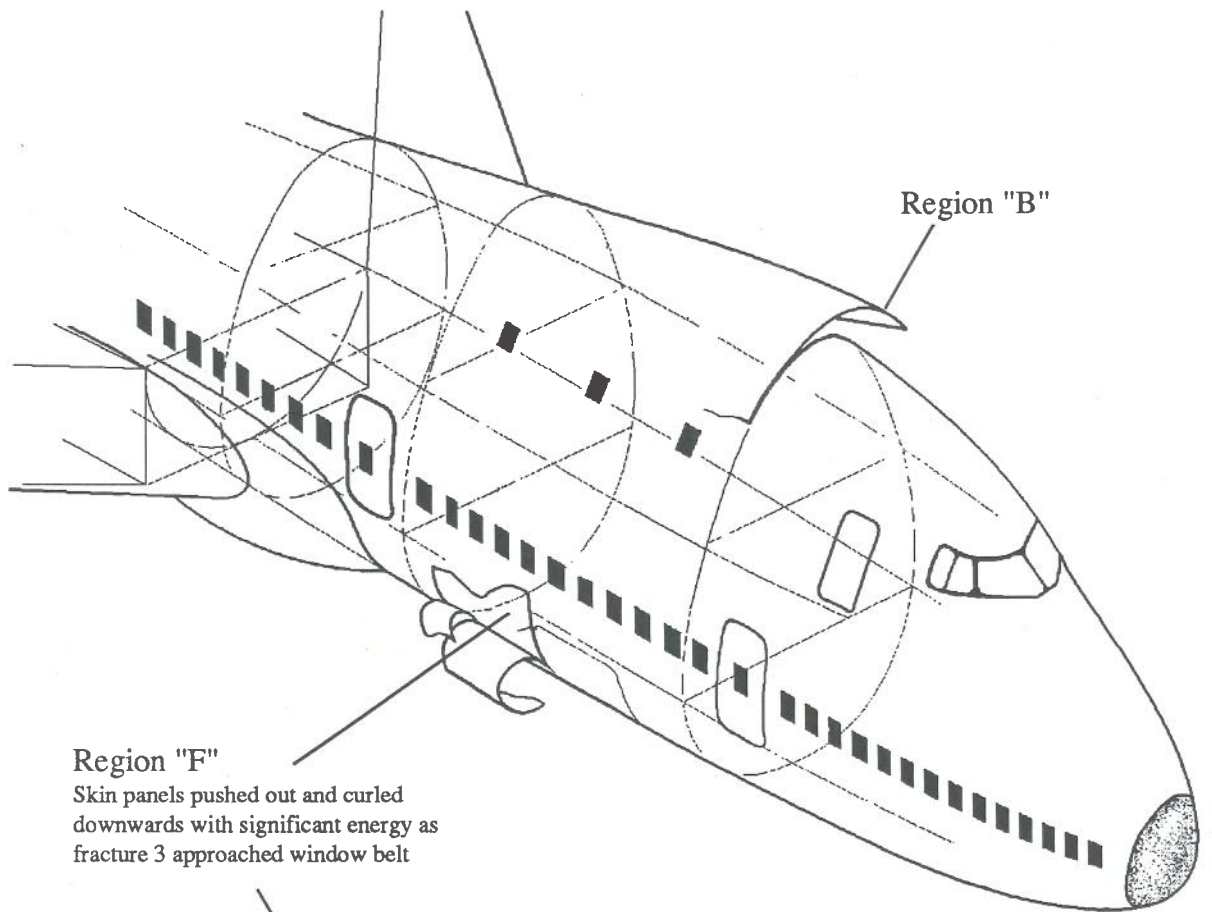
Fracture 3

Fracture 1



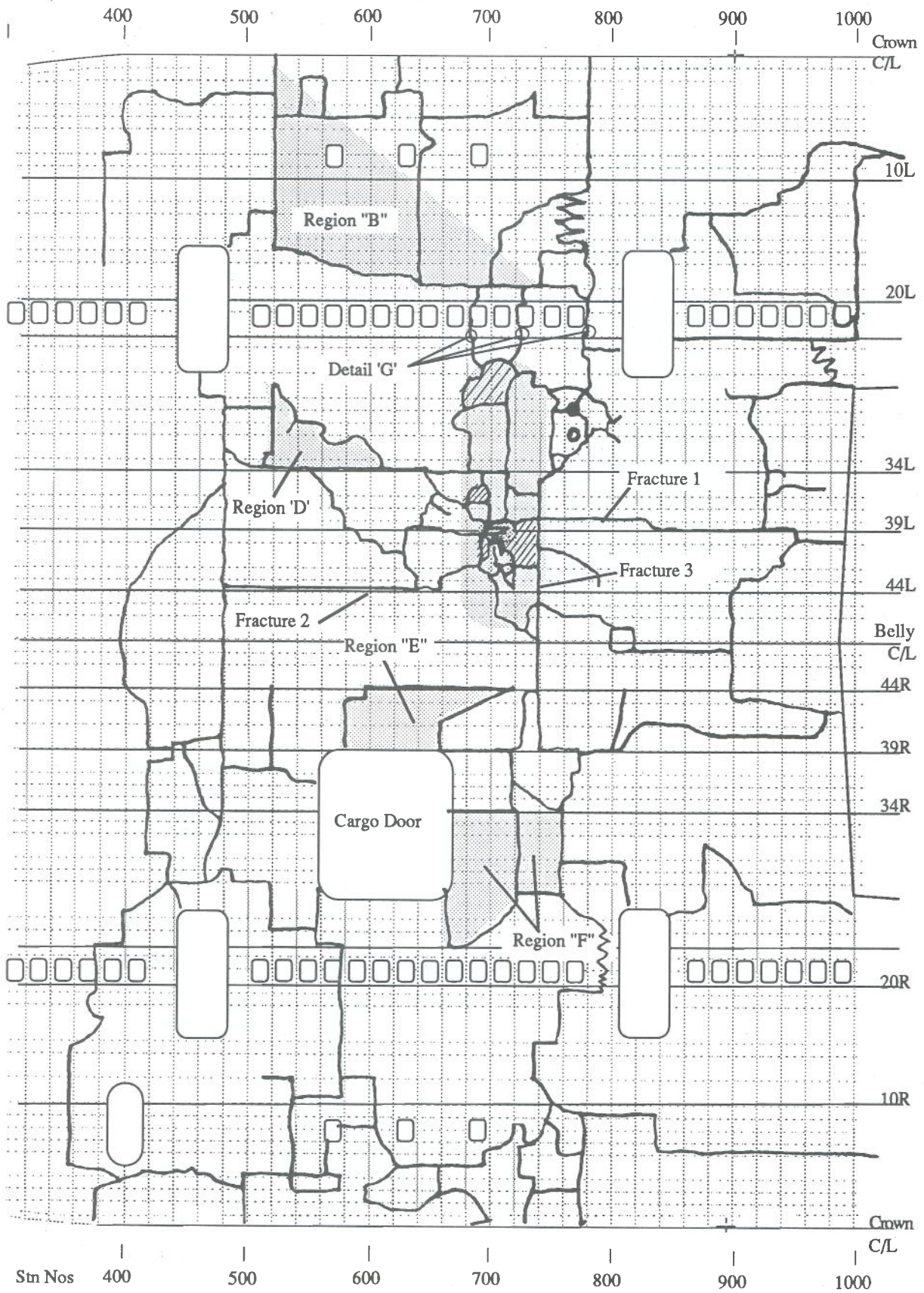
Explosive Damage - left side
(schematic representation)

Figure B-19



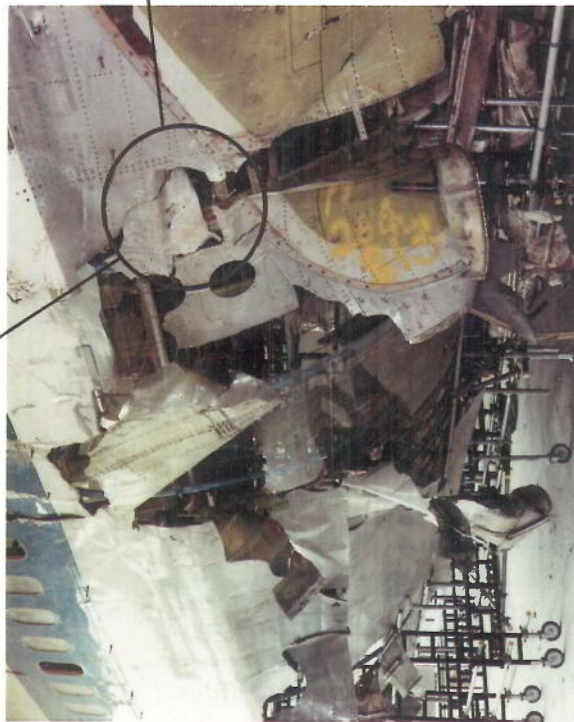
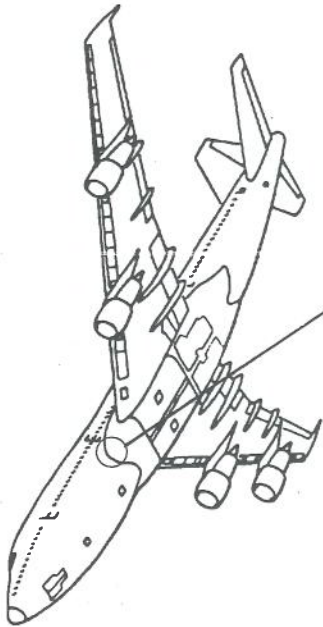
Explosive Damage - right side
(schematic representation)

Figure B-20



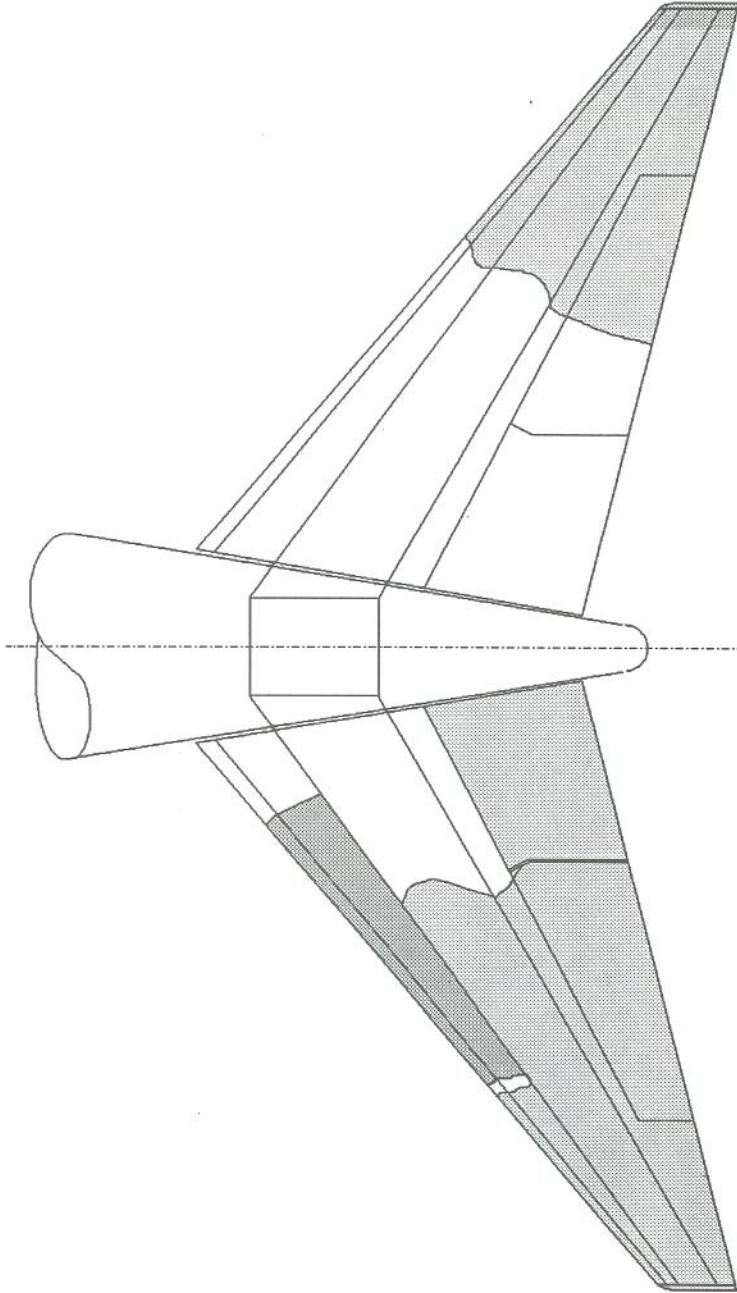
Skin Fracture Plot

Figure B-21



Spar cap embedded in fuselage

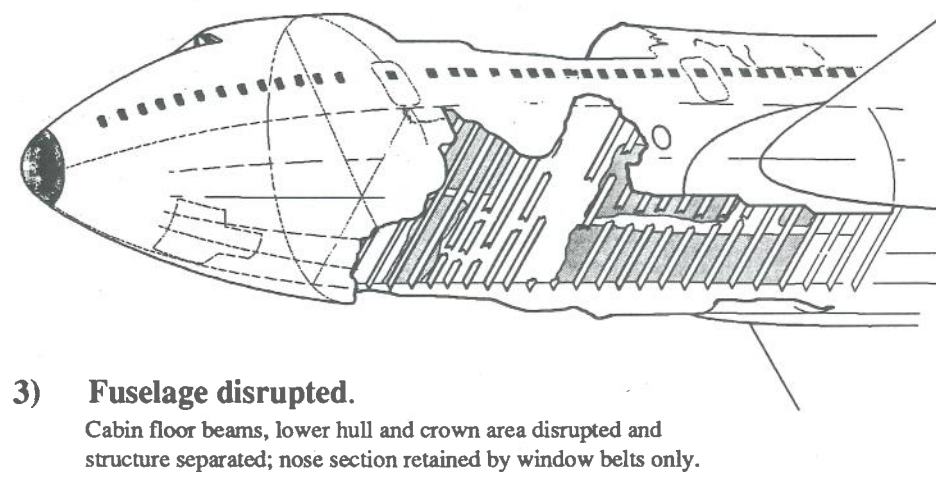
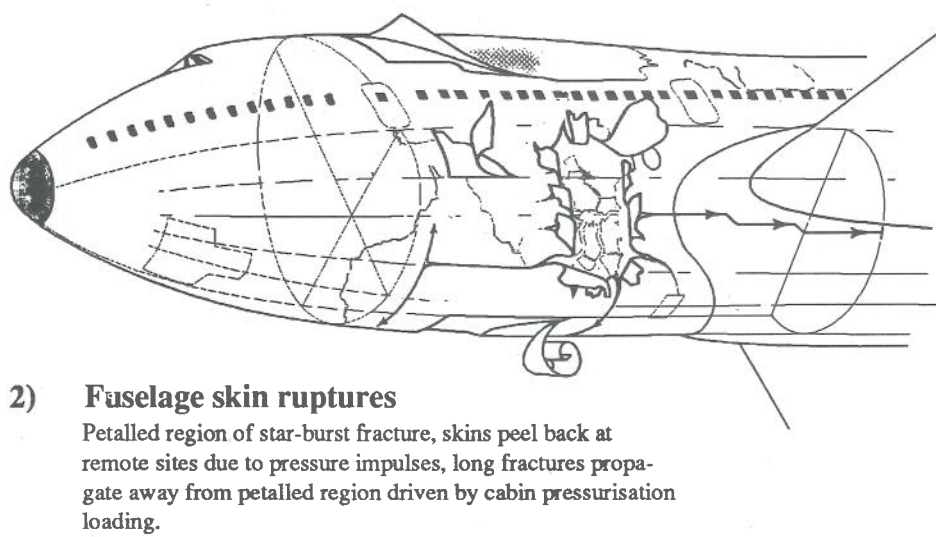
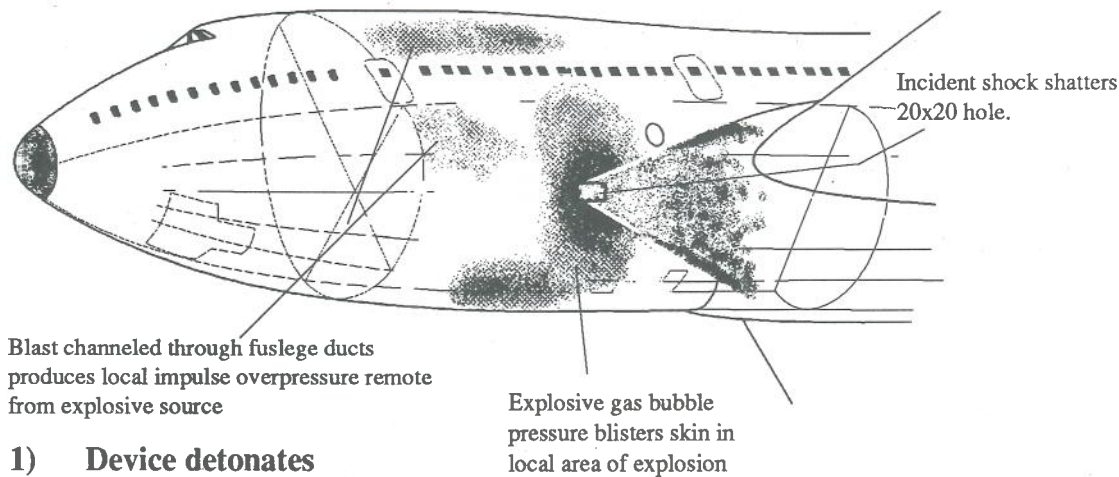
Figure B-22



Initial Damage to Tailplanes

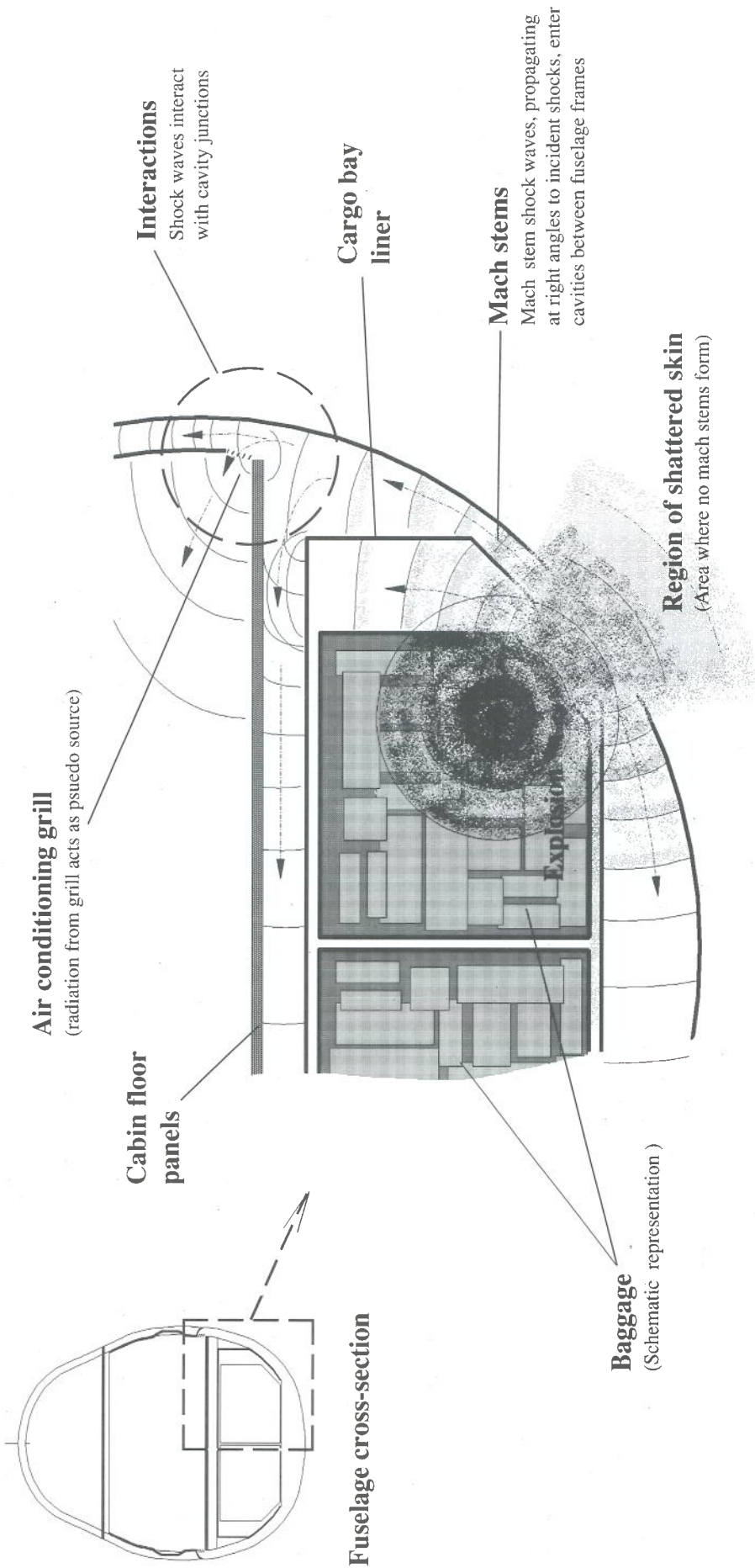
(shaded areas denote wreckage recovered from southern wreckage trail)

Figure B-23



Fuselage Initial Damage Sequence
 (schematic representation)

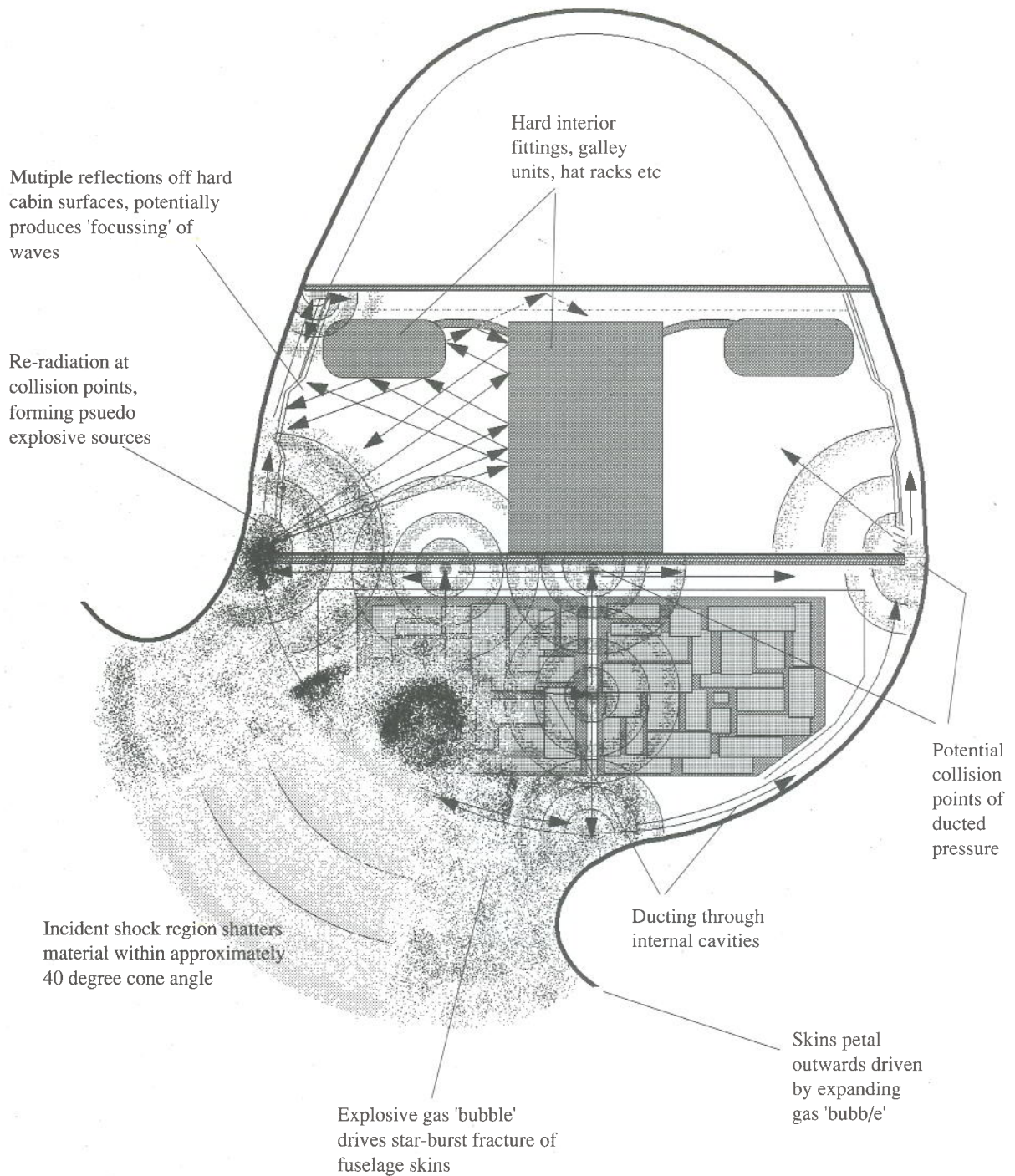
Figure B-24



Incident Shock & Regions of Mach Stem Propagation

(schematic representation)

Figure B-25



Potential Shock and Explosive Gas Propagation Paths
 (schematic representation)

Figure B-26

ANALYSIS OF RECORDED DATA

1. Introduction

This appendix describes and analyses the different types of recorded data which were examined during the investigation of the accident to Boeing 747 registration N739PA at Lockerbie on 21 December 1988. The recorded data consists of that from the Cockpit Voice Recorder (CVR), the Digital Flight Data Recorder (DFDR), Air Traffic Control (ATC) radio telephony (RTF), ATC radar, and British Geological Survey seismic records. The time correlation of the records is also discussed.

2. Digital flight data recorder

The flight data recorder installation conformed to ARINC 573B standard with a Lockheed Model 209 DFDR receiving data from a Teledyne Controls Flight Data Acquisition Unit (FDAU). The system recorded 22 analogue parameters and 27 discrete (event) parameters. The flight recorder control panel was located in the flight deck overhead panel. The FDAU was in the main equipment centre at the front end of the forward hold and the flight recorder was mounted in the aft equipment centre.

2.1 DFDR strip and examination

Internal inspection of the DFDR showed that there was considerable disruption to the control electronics circuits. The crash protection was removed and the plastic recording tape was found detached from its various guide rollers and tangled in the tape spools. There was no tension in the negator springs. This indicated that the tape had probably moved since electrical power was removed from the recorder. The position of the tape in relation to the record/replay heads was marked with a piece of splicing tape in order to quantify the movement. To ensure that no additional damage was caused to the tape it was necessary to cut the negator springs to separate the upper and lower tape reels.

The crinkling and stretching of the tape and the damage to the control electronics meant that the tape had to be replayed outside the recorder. AAIB experience has shown that the most efficient method of replaying stretched Lockheed recorder tapes is to re-spool the tape into a known serviceable recorder, in this case a Plessey 1584G.

2.2 DFDR replay

The 25 hour duration of the DFDR was satisfactorily replayed. Data relating to the accident flight was recorded on track 2. The only significant defect in the recording system was that normal acceleration was inoperative. There was one area on the tape, 2 minutes from the end, where data synchronisation was lost for 1 second.

Decoding and reduction of the data from the accident flight showed that no abnormal behaviour of the data sensors had been recorded. The recorded data simply stopped. Figure C-1 is a graphical representation of the main flight parameters.

2.3 DFDR analysis

In order to ensure that all recorded data from the accident flight had been decoded and to examine the quality of the data at the end of the recording, a section of tape, including both the most recently recorded data and the oldest data (data from 25 hours past), was replayed through an ultra-violet (UV) strip recorder. The data was also digitised and the resulting samples used to reconstruct the tape signal on a VDU.

Both methods of signal representation were used to determine the manner by which the recorder stopped. There was no gap between the most recently recorded data and the 25 hour old data. This showed that the recorder stopped while there was an incoming data stream from the FDAU. The recorder, therefore, stopped because its electrical supply was disconnected. The tape signal was examined for any transients or noise signals that would have indicated the presence of electrical disturbances prior to the recorder stopping. None was found and this indicated that there had been a quick clean break of the electrical supply.

The last seconds of data were decoded independently using both the UV record and the digitised signal. Only 17 bits of data were not recoverable (less than 23 milliseconds) and it was not possible to establish with any certainty if this data was from the accident flight or if it was old data from a previous recording.

A working group of the European Organisation for Civil Aviation Electronics (EUROCAE) was, during the period of the investigation, formulating new standards (Minimum Operational Performance Requirement for Flight Data Recorder Systems, Ref:- ED55) for future generation flight recorders which

would have permitted delays between parameter input and recording (buffering) of up to ½ second. These standards are intended to form the basis of new CAA specifications for flight recorders and may be adopted worldwide.

The analysis of the final data recorded on the DFDR was possible because the system did not buffer the incoming data. Some existing recorders use a process whereby data is stored temporarily in a memory device (buffer) before recording. The data within this buffer is lost when power is removed from the recorder and in currently designed recorders this may mean that up to 1.2 seconds of final data contained within the buffer is lost. Due to the necessary processing of the signals prior to input to the recorder, additional delays of up to 300 milliseconds may be introduced. If the accident had occurred when the aircraft was over the sea, it is very probable that the relatively few small items of structure, luggage and clothing showing positive evidence of the detonation of an explosive device would not have been recovered. However, as flight recorders are fitted with underwater location beacons, there is a high probability that they would have been located and recovered. In such an event the final milliseconds of data contained on the DFDR could be vital to the successful determination of the cause of an accident whether due to an explosive device or other catastrophic failure. Whilst it may not be possible to reduce some of the delays external to the recorder, it is possible to reduce any data loss due to buffering of data within the data acquisition unit.

It is, therefore, recommended that manufacturers of existing recorders which use buffering techniques give consideration to making the buffers non-volatile, and hence recoverable after power loss. Although the recommendation on this aspect, made to the EUROCAE working group during the investigation, was incorporated into ED55, it is also recommended that Airworthiness Authorities re-consider the concept of allowing buffered data to be stored in a volatile memory.

3. Cockpit voice recorder (CVR)

The aircraft was equipped with a 30 minute duration 4 track Fairchild Model A100 CVR, and a Fairchild model A152 cockpit area microphone (CAM). The CVR control panel containing the CAM was located in the overhead panel on the flight deck and the recorder itself was mounted in the aft equipment centre.

The channel allocation was as follows:-

Channel 1	Flight Engineer's RTF.
Channel 2	Co-Pilot's RTF.
Channel 3	Pilot's RTF.
Channel 4	Cockpit Area Microphone.

3.1 CVR strip and examination

To gain access to the recording tape it was necessary to cut away the the outer case and saw through part of the crash protected enclosure. No damage to the tape transport or the recording tape was found. The endless loop of tape was cut and the tape transferred to the replay equipment. The electronic modules in the CVR were crushed and there was evidence of long term overheating of the dropper resistors on the power supply module. The CAM had been crushed breaking internal wiring and damaging components on the printed circuit board.

3.2 CVR replay

The erase facility within the CVR was not functioning satisfactorily and low level communications from earlier recordings was audible on the RTF channels. The CAM channel was particularly noisy, this was probably due to the combination of the inherently noisy cockpit of the B747-100 in the climb and distortion from the incomplete erasure of the previous recordings. On two occasions the crew had difficulty understanding ATC, possibly indicating high cockpit noise levels. There was a low frequency sound present at irregular intervals on the CAM track but the source of this sound could not be identified as of either acoustic or electrical in origin.

The CVR tape was listened to for its full duration and there was no indication of anything abnormal with the aircraft, or unusual in crew behaviour. The tape record ended with a sudden loud sound on the CAM channel followed almost immediately by the cessation of recording. The sound occurred whilst the crew were copying their transatlantic clearance from Shanwick ATC.

3.3 Analysis of the CVR record

3.3.1 The stopping of the recorder

To determine the mechanism that stopped the recorder a bench test rig was constructed utilizing an A100 CVR and an A152 CAM. Figures C-2 to C-5 show the effect of shorting, earthing or disconnecting the CAM signal wires. Figure C-8 shows the CAM channel signal response to the event which occurred on Flight PA103. From this it can be seen that there are no characteristic transients similar to those caused by shorting or earthing the CAM signal wires. Neither does the signal stop cleanly and quickly as shown in Figure C-5, indicating that the CAM signal wires were not interrupted. The UV trace shows the recorded signal decaying in a manner similar to that shown in Figure C-6, which demonstrates the effect of disconnecting electrical power from the recorder. The tests were

repeated on other CVRs with similar results and it is therefore concluded that Flight PA103's CVR stopped because its electrical power was removed.

Figures C-9A to C-9D show the recorded signals for the Air India B747 (AI 182) accident in the North Atlantic on 23 June 1985. These show that there is a large transient on the CAM track indicating earthing or shorting of the CAM signal wires and that recorder power-down is more prolonged, indicating attempts to restore the electrical power supply either by bus switching or healing of the fault. The Flight PA103 CVR shows no attempts at power restoration with the break being clean and final.

In order to respond to events that result in the almost immediate loss of the aircraft's electrical power supply it was therefore recommended during the investigation that the regulatory authorities consider requiring CVR systems to contain a short duration (i.e. no greater than 1 minute) back-up power supply.

3.3.2 Information concerning the event

Figure C-8 is an expanded UV trace of the final milliseconds of the CVR record. Three tracks have been used, the flight engineer's RTF channel which contained similar information to the P2's channel has been replaced with a timing signal. Individual sections of interest are identified by number. On the bottom trace, the P1 RTF track, section 1 is part of the Shanwick transatlantic clearance. During this section the loud sound on the CAM channel is evident.

Examination of the DFDR event recordings shows that the Shanwick oceanic clearance was being received on VHF2, the aerial for which is on the underside of the fuselage close to the seat of the explosion. Section 2 identifies a transient, on the P1 channel, typical of an end of ATC transmission transient for this CVR. The start and finish of most of the recorded ATC transmissions were analysed and they produce a similar signature to the three shown in Figure C-10. The signature on the P1 channel more closely resembles the end of transmission signature and it is open to conjecture that this transient was caused by the explosion damaging the aerial feeder and/or its supporting structure.

Section 3 shows what is considered to be a high speed power supply transient which is evident on all the RTF channels and is probably on the CAM channel, but cannot be identified because of the automatic gain control (AGC), limiting the audio event. This transient is considered to coincide with the loss of electrical power to the CVR. Section 5 identifies the period to the end of recording and this agrees well with tests carried out by AAIB and independently by Fairchild as part of the AI 182 investigation. The typical time from removal of the electrical supply until end of recording is 110 milliseconds.

During the period identified as section 4 it is considered that the disturbances on the RTF channels are electrical transients probably channelled through the communications equipment. Section 6 identifies the 170 millisecond period from the point when the sound was first heard on the CAM until the recording stopped.

The CAM unit is of the old type which has a frequency response of 350 to 3500 Hz. The useable duration of the signal is probably confined to the first 60 milliseconds of the final 170 milliseconds and even during this period the AGC is limiting the signal. In the remaining time the sound is being distorted because power to the recorder has been disconnected. The ambient cockpit noise may have been high enough to have caused the AGC to have been active prior to the event and in this event the full volume of the sound would not be audible. Distortion from the incomplete erasure of the last recording may form part of the recorded signal.

It is not clear if the recorded sound is the result of the explosion or is from the break-up of the aircraft structure. The short period between the beginning of the event and the loss of electrical power suggests that the latter is more likely to be the case.

Additionally some of the frequencies present on the recording were not present in the original sound, but are the result of the rise in total harmonic distortion caused by the increased amplitude of the incoming signal. Outputs from a frequency analysis of the recorded signal for the same frequency of input to the CVR, but at two input amplitudes, are shown in Figures C-11 and C-12. These illustrate the effects on harmonic distortion as the signal level is increased. Finally the recorded signal does not lend itself to analysis by a digital spectrum analyser as it is, in a large measure, aperiodic and most digital signal analysis algorithms are unable to deal with a short duration signal of this type, however, it is hoped that techniques being developed in Canada will enable more information to be deduced from the end of the recording.

In the aftermath of the Air India Boeing 747 accident (AI 182) in the North Atlantic on 23 June 1985 the Royal Armaments Research and Development Establishment (RARDE) were asked informally by AAIB to examine means of differentiating, by recording violent cabin pressure pulses, between the detonation of an explosive device within the cabin (positive pulse) and a catastrophic structural failure (negative pulse). Following the Lockerbie disaster it was considered that this work should be raised to a formal research project. Therefore, in February 1989, it was recommended that the Department of Transport fund a study to devise methods of recording violent positive and negative pressure pulses, preferably utilising the aircraft's flight recorder systems.

Preliminary results from these trials indicates that if a suitable sensor can be developed its output will need to be recorded in real time and therefore it may require wiring into the CVR installation. This will further strengthen the requirement for battery back up of the CVR electrical power supply.

4. Flight recorder electrical system

4.1 CVR/DFDR electrical wiring.

The flight recorders were located in the left rear fuselage just forward of the rear pressure bulkhead. Audio information to the CVR ran along the left hand side of the aircraft, at stringer 11. Electrical power to the CVR followed a similar route on the right hand side of the aircraft crossing to the left side above the rear passenger toilets. DFDR electrical power and signal information followed the same route as the CVR audio information.

4.2 Flight recorder power supply

The DFDR, CVR and the transponders were all powered from the essential alternating current (AC) bus. This bus was capable of being powered by any generator, however, in normal operation the selector switch on the flight engineers panel is selected to "normal" connecting the essential bus to number 4 generator. When the cockpit of Flight PA103 was examined the selector switch was found in the normal position.

4.3 Aircraft alternating current power supplies

AC electrical power to the aircraft was provided by 4 engine driven generators, see Figure C-13. Each generator was driven at constant speed through a constant speed drive (CSD) and connected to a separate bus-bar through a generator control breaker (GCB). The 4 generators were connected to a parallel bus-bar (sync bus) by individual bus tie breakers (BTBs). Control and monitoring of the AC electrical system was achieved through the flight engineer's instrument panel. In normal operation the generators operated in parallel, i.e with the BTBs closed.

4.4 Fault conditions

Analysis of the CVR CAM channel signal indicated that approximately 60 milliseconds after the sound on the CAM channel an electrical transient was recorded on all 4 channels and that approximately 110 milliseconds later the CVR had ceased recording. Within the accuracy of the available timing information it is believed that the incoming VHF was lost at the same time, indicating an AC power supply fault.

The AC electrical system was protected from faults in individual systems or equipment by fuses or circuit breakers. Faults in the generators or in the distribution bus-bars and feeders were dealt with automatically by opening of the GCBs and opening or closing of the BTBs. In the event of fault conditions causing the disconnection of all 4 generators electrical power for essential services, including VHF radio, was provided by a battery located in the cockpit.

The short time interval of 55 milliseconds after which the AC supply to the flight recorders was lost limits the basis on which a fault path analysis of the AC electrical system can be undertaken. On the available information only a differential (feeder) fault could have isolated the bus-bar this quickly, with the generator field control relay taking 20 milliseconds to trip. However, in normal operation, the generators would have been operating in parallel and the essential AC bus-bar would have been supplied via the number 4 BTB from the sync bus. If the fault conditions had continued, a further 40 to 100 milliseconds would have elapsed before the BTB opened. If the BTB was open prior to the fault it would have attempted to close and restore the supply to the essential bus. Any automatic switching causes electrical transients to appear on the CVR and data losses on the FDR. Both the CVR and the FDR indicate that a clean break of the AC supply occurred with no electrical transients associated with BTBs open or closing in an attempt to restore power. In the absence of any additional information only two possibilities are apparent:

- i) That all 4 generators were simultaneously affected causing a total loss of AC electrical power. The feeders for the left and right side generators run on opposite sides of the aircraft under the passenger cabin floor. The only situation envisaged that could cause simultaneous loss of all 4 generators is the disruption of the passenger cabin floor across its entire width.
- ii) That disruption of the main equipment centre, housing the control units for the AC electrical system, caused the loss of all AC power. However, again it would have to affect both the left and right sides of the aircraft as the control equipment is located at left and right extremes of the main equipment centre.

The nature of the event may also produce effects that are not understood. It is also to be noted that a sudden loss of electrical power to the flight recorders has been reported in other B747 accidents, e.g. Air India, AI 182.

5. Seismic data

The British Geological Survey has a number of seismic monitoring stations in Southern Scotland. Stations close to Lockerbie recorded a seismic event caused by the wing section crashing on Lockerbie. The seismic monitors are time correlated with the British Telecom Rugby standard. Using this and calculating the time for the various waves to reach the recording stations it was possible for the British Geological Survey to conclude that the event occurred at 19.03:36.5 hrs \pm 1 second.

Attempts were made to correlate various smaller seismic events with other wreckage impacts. However, this was not conclusive because the nearest recording station was above ground and due to the high winds at the time of the accident had considerable noise on the trace. In addition, little of the other wreckage had the mass or impact velocity to stimulate the sensors.

6. Time correlation

6.1 Introduction

The sources of each time encoded recording were asked to provide details of their time standard and any known errors in the timings on their recordings. Although the resolution of the recorded time sources is high it was not possible to attach an accuracy of better than ± 1 second due to possible errors in synchronising the recorded time with the associated standard. The following time sources were available and used in determining the significant events in the investigation:-

i) ATC

ATC communications were recorded along with a time signal. The time source for the ATC tape was the British Telecom "Tim" signal. Any error in setting the time when individual tapes are mounted was logged.

ii) Recorded rada data

A time signal derived from the British Telecom "Rugby" standard was included on radar recordings. The Rugby and Tim times were assumed to be of equal accuracy for timing purposes.

iii) The DFDR had UTC recorded.

The source of this time was the flight engineer's clock. This clock was set manually and therefore this time was subject to a significant fixed error as well any inaccuracy in the clock.

- iv) The CVR had no time signal.

However, the CVR was correlated with the ATC time through the RTF and with the DFDR, by correlating the press to talk events on the FDR with the press to talk signature on the CVR.

- v) Seismic recordings

Seismic recordings included a timing signal derived from the British Telecom Rugby standard.

6.2 Analysis and correlation of times

The Scottish and Shanwick ATC tapes were matched with each other and with the CVR tape. The CVR recording speed was adjusted by peaking its recorded 400 Hz AC power source frequency. This correlation served as a double check on any fixed errors on the ATC recordings and to fix events on the CVR to UTC. The timing of the sound on the CAM channel of the CVR was made simpler because Shanwick was transmitting when it occurred. From this it was possible to determine that the sound on the CVR occurred at 19.02:50 hrs \pm 1 second.

With the CVR now tied to the Tim standard it was possible to match the RTF keying on the CVR with the RTF keying events on the FDR. These events on the FDR were sampled and recorded once per second, it was therefore possible for a 1 second delay to be present on the FDR. This potential error was reduced by obtaining the best fit between a number of RTF keyings and a time correlation between the FDR and CVR of $\pm\frac{1}{2}$ second was achieved. From this it was determined, within this accuracy, that electrical power was removed from the CVR and FDR at the same time.

From the recorded radar data it was possible to determine that the last recorded SSR return was at 19.02:46.9 hrs and that by the next rotation of the radar head a number of primary returns, some left and right of track, were evident. Time intervals between successive rotations of the radar head became more difficult to use as the head painted more primary returns.

The point at which aircraft wreckage impacted Lockerbie was determined using the time recorded by seismic activity detectors. A seismic event measuring 1.6 on the Richter scale was detected and, with appropriate time corrections for times of the waves to reach the sensors, it was established that this occurred at 19.03:36.5 hrs \pm 1 second. A further check was made by triangulation techniques from the information recorded by the various sensors.

7. Recorded radar information

7.1 Introduction

Recorded radar information on the aircraft was available from from 4 radar sites. Initial analysis consisted of viewing the recorded information as it was shown to the controller on the radar screen, from this it was clear that the flight had progressed in a normal manner until Secondary Surveillance Radar (SSR) was lost. There was a single primary return received by both Great Dun Fell and Claxby radars approximately 16 seconds before SSR returns were lost. The Lowther Hill and St. Annes radars did not see this return. The Great Dun Fell radar recording was watched for 1 hour both before and after this single return for any signs of other spurious returns, but none was seen. The return was only present for one paint and no explanation can be offered for its presence.

7.2 Limitations of recorded radar data

Before evaluating the recorded radar data it is important to highlight limitations in radar performance that must be taken into account when interpreting primary radar data. The radar system used for both primary and secondary radar utilised a rotating radar transmitter/receiver (Head). This means that a return was only visible whilst the radar head was pointing at the target, commonly called painting or illuminating the target. In the case of this accident the rotational speeds of the radar heads varied from approximately 10 seconds for the Lowther Hill Radar to 8 Seconds for the Great Dun Fell Radar.

Whilst it was possible to obtain accurate positional information within a resolution of 0.09° of bearing and $\pm 1/16$ nautical mile range for an aircraft from SSR, incorporating mode C height encoding, primary radar provided only slant range and bearing and therefore positional information with respect to the ground was not accurate.

The structural break-up of an aircraft releases many items which were excellent radar reflectors eg. aluminium cladding, luggage containers, sections of skin and aircraft structure. These and other debris with reflective properties produce "clutter" on the radar by confusing the radar electronics in a manner similar to chaff ejected by military aircraft to avoid radar detection.

Even when the target is not masked by clutter repetitive detection of individual targets may not be possible because detection is a function of the target effective area which, for wreckage with its irregular shape, is not constant but fluctuates wildly. These factors make it impossible to follow individual returns through successive sweeps of the radar head.

The detailed analysis of the radar information concentrated on the break-up of the aircraft. The Royal Signals and Radar Establishment (RSRE) corrected the radar returns for fixed errors and converted the SSR returns to latitude and longitude so that an accurate time and position for the aircraft could be determined. This information was correlated with the CVR and ATC times to establish a time and position for the aircraft at the initial disintegration.

For the purposes of this analysis the data from Great Dun Fell Radar has been presented. Figures C-14 to C-23 show a mosaic picture of the radar data i.e. each figure contains the information on the preceding figure together with more recently recorded information. Figure C-14 shows the radar returns from an aircraft tracking 321°(Grid) with a calculated ground speed of 434 kts. Reading along track (towards the top left of Figure C-14) there are 6 SSR returns with the sixth and final SSR return shown decoded: squawk code 0357 (identifying the aircraft as N739PA); mode C indicating FL310; and the time in seconds (68566.9 seconds from 00:00, i.e. 19.02:46.9 hrs).

At the next radar return there is no SSR data, only 4 primary returns. One return is along track close to the expected position of the aircraft if it had continued at its previous speed and heading. There are 2 returns to the left of track and 1 to the right of track. Remembering the point made earlier about clutter, it is unlikely that each of these returns are real targets. It can, however, be concluded that the aircraft is no longer a single return and, considering the approximately 1 nautical mile spread of returns across track, that items have been ejected at high speed probably to both right and left of the aircraft. Figure C-15 shows the situation after the next head rotation. There is still a return along track but it has either slowed down or the slant range has decreased due to a loss of altitude.

Each rotation of the radar head thereafter shows the number of returns increasing with those first identified across track in Figure C-14 having slowed down very quickly and followed a track along the prevailing wind line. Figure C-20 shows clearly that there has been a further break-up of the aircraft and subsequent plots show a rapidly increasing number of returns, some following the wind direction and forming a wreckage trail parallel to and north of the original break-up debris. Additionally it is possible that there was some break-up between these points with a short trail being formed between the north and south trails. From the absence of any returns travelling along track it can be concluded that the main wreckage was travelling almost vertically downwards for much of the time.

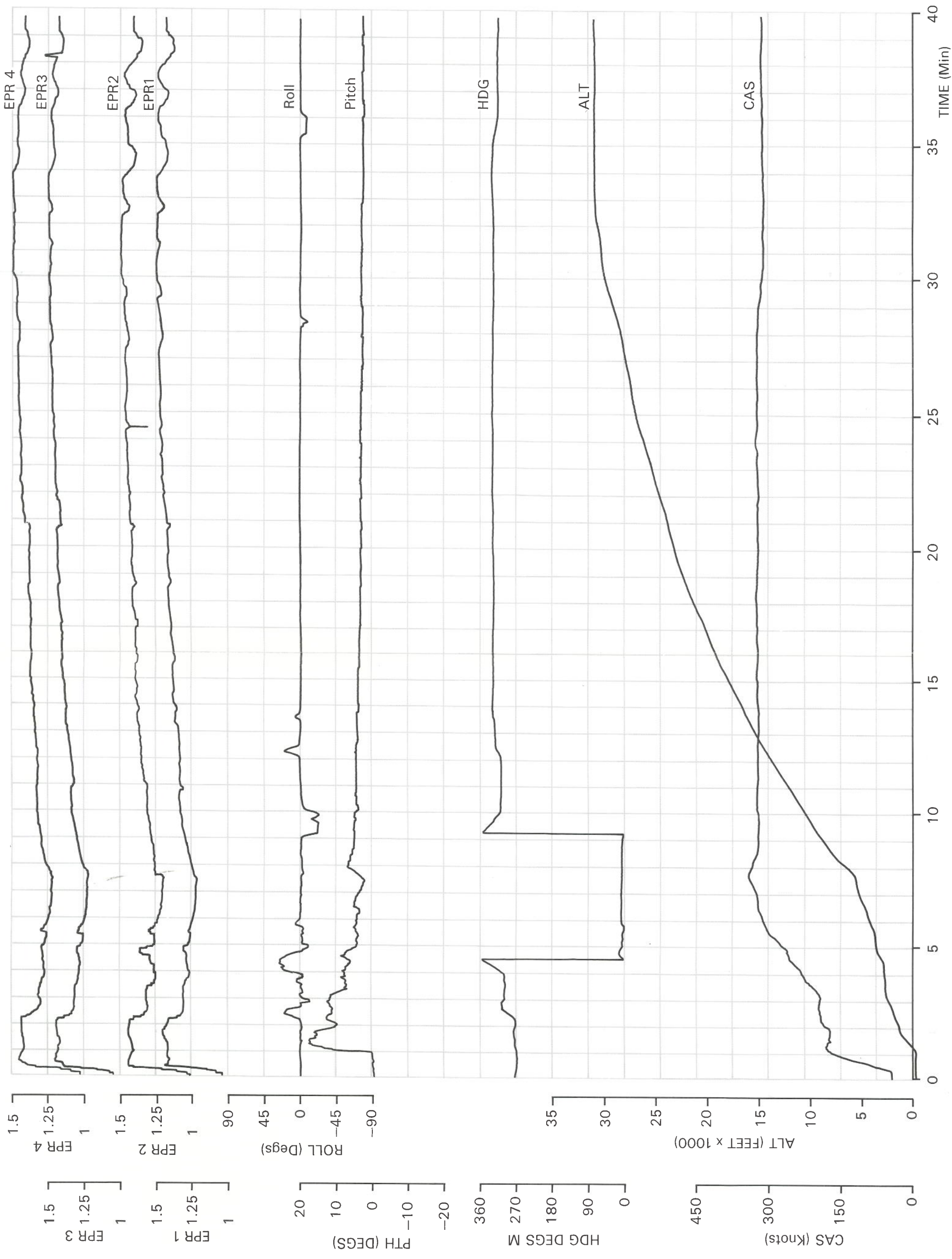
The geographical position of the final secondary return at 19.02:46.9 hrs was calculated by RSRE to be OS Grid Reference 15257772, annotated Point A in Appendix B, Figure B-4, with an accuracy considered to be better than ± 300 metres. This return was received 3.1 ± 1 seconds before the loud sound was recorded on the CVR at 19.02:50 hrs. By projecting from this position along the track of 321° (Grid) for 3.1 ± 1 seconds at the groundspeed of 434 kts, the position of the aircraft was calculated to be OS Grid Reference 14827826, annotated Point B in Appendix B, Figure B-4, within an accuracy of ± 525 metres. Based on the evidence of recorded data only, Point B therefore represents the geographical position of the aircraft at the moment the loud sound was recorded on the CVR.

8. Conclusions

The almost instant destruction of Flight PA103 resulted in no direct evidence on the cause of the accident being preserved on the DFDR. The CVR CAM track contained a loud sound 170 milliseconds before recording ceased. Sixty milliseconds of this sound were while power was applied to the recorder; after this period the amplitude decreased. It cannot be determined whether the decrease was because of reducing recorder drive or if the sound itself decreased in amplitude. Analysis of both flight recorders shows that they stopped because the electrical supply was removed and that there were valid signals available to both recorders at that time.

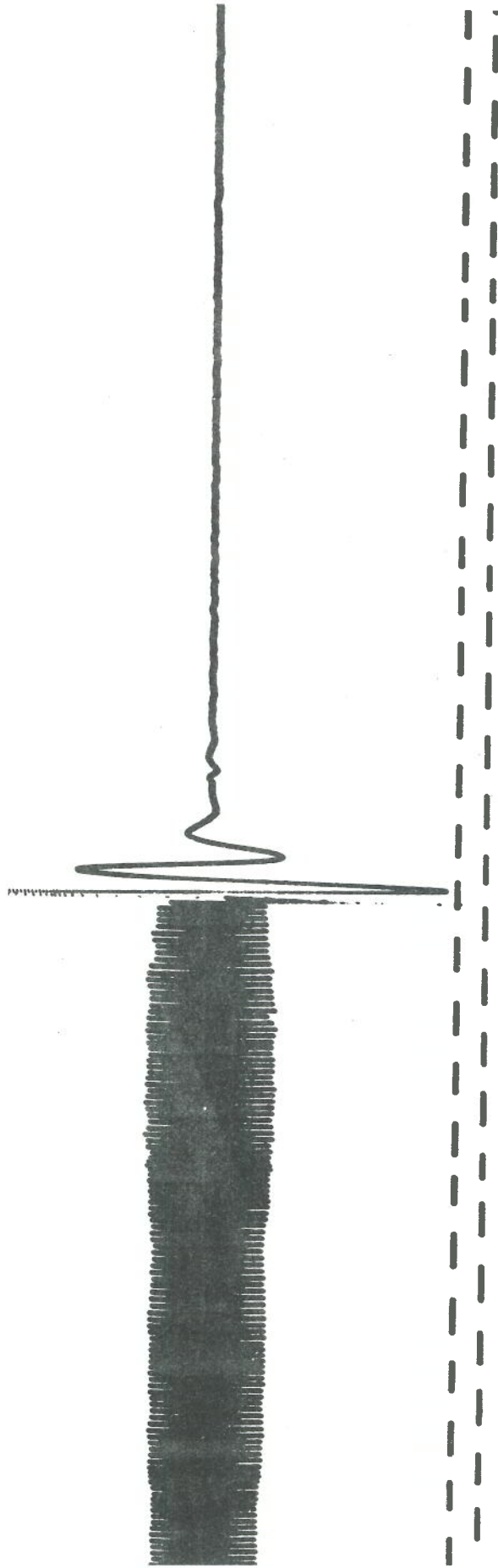
The most important contribution to the investigation that the flight recorders could make was to pinpoint the time and position of the event. As the timescale involved was so small in relation to the resolution and accuracy of many of the recorded time sources it was necessary to analyse collectively all the available recordings. From the analysis of the CVR, DFDR, ATC tapes, radar data and the seismic records it was concluded that the loud sound on the CVR occurred at 19.02:50 hrs ± 1 second and wreckage from the aircraft crashed on Lockerbie at 19.03:36.5 hrs ± 1 second, giving a time interval of 46.5 ± 2 seconds between these two events. When the loud sound was recorded on the CVR, the geographical position of the aircraft, based on the evidence of recorded data, was calculated to be within 525 metres of OS Grid Reference 14827826.

Eight seconds after the sound on the CVR the Great Dun Fell radar showed 4 primary radar returns. The returns indicated a spread of wreckage in the order of 1 nautical mile across track. On successive returns of the radar, two parallel wreckage trails are seen to develop with the second trail, to the north, becoming evident 30 to 40 seconds after the first.



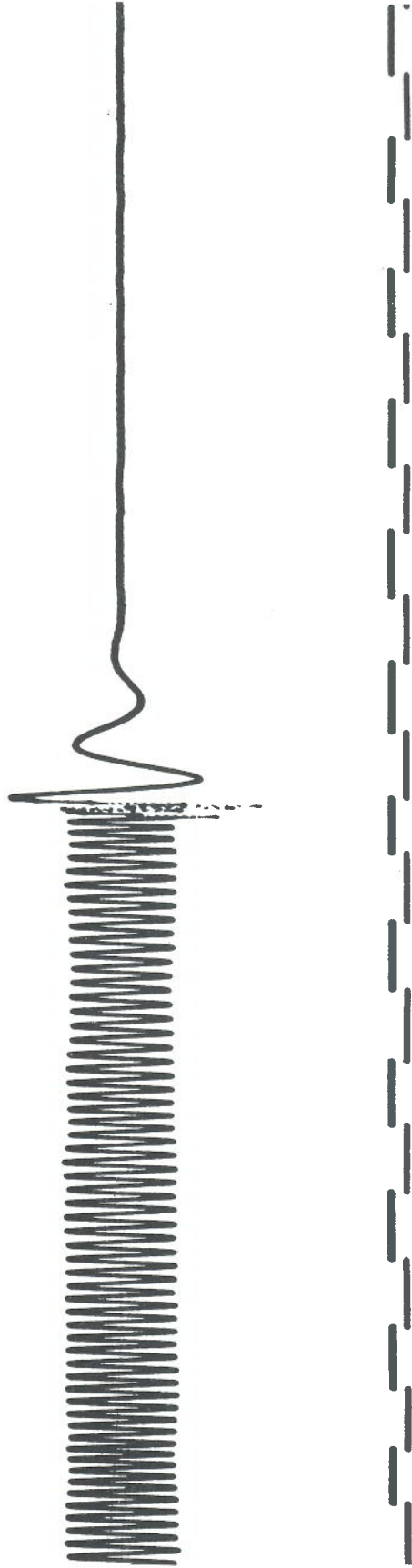
Selected DFDR parameters of final flight of N739PA

Figure C-1



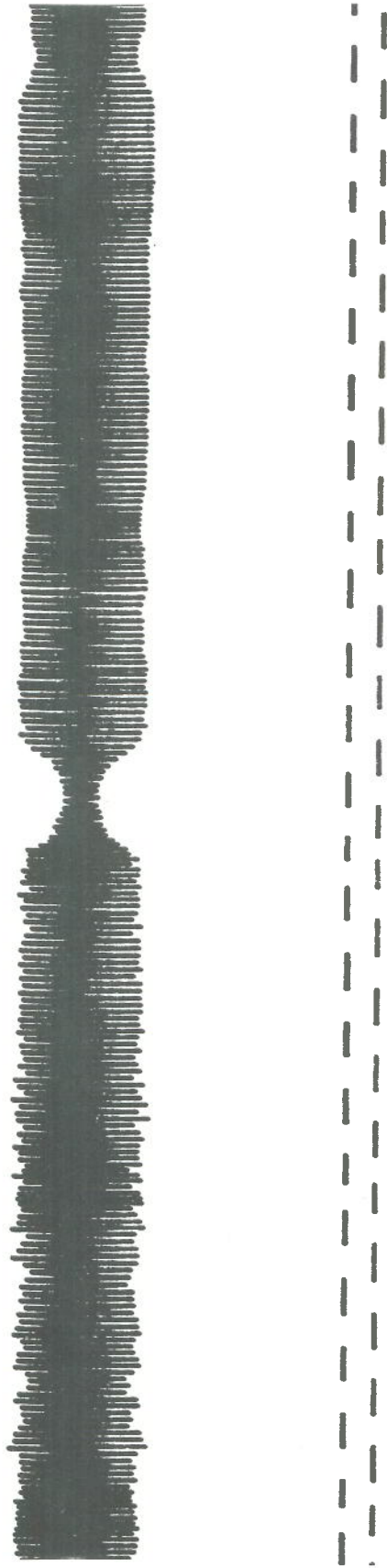
The effect on the recorded signal of shorting
the signal wires to the CAM

Figure C-2



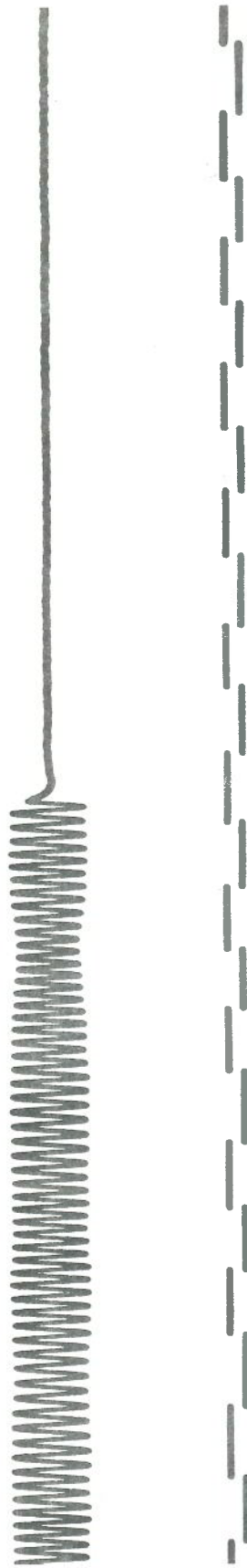
The effect on the recorded signal of earthing
the hi wire to the CAM

Figure C-3



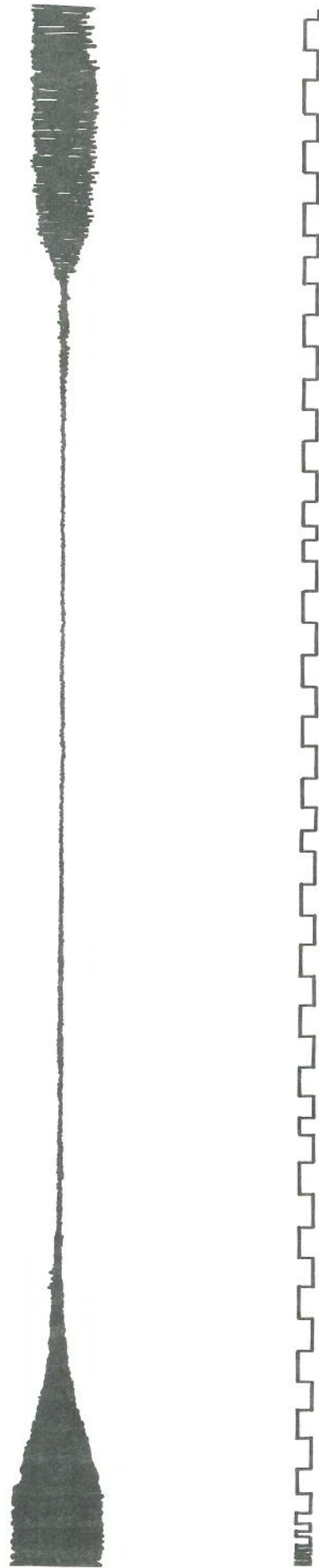
The effect on the recorded signal of earthing
the lo wire to the CAM

Figure C-4



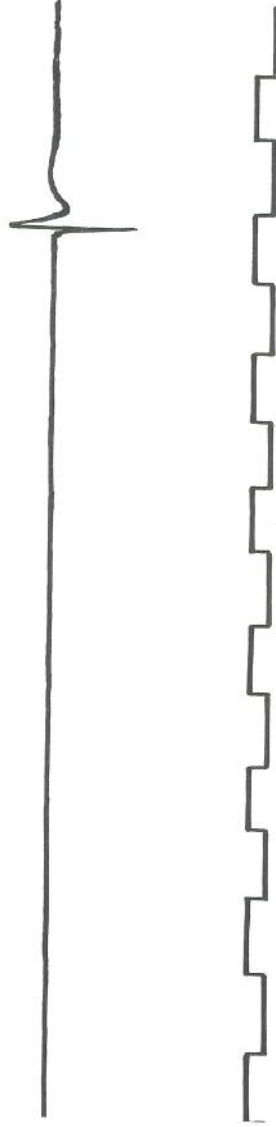
The effect on the recorded signal of disconnecting
the CAM signal wires

Figure C-5



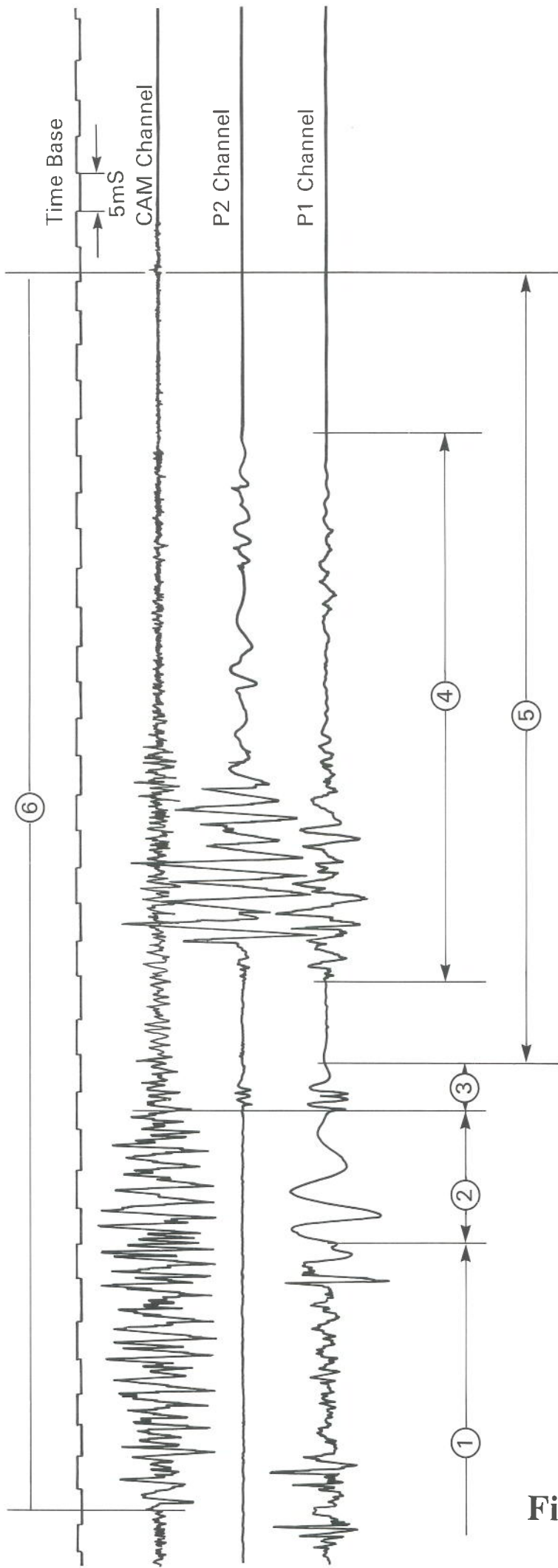
The effect on the recorded CAM signal of disconnecting
the CVR power supply

Figure C-6



The effect on the recorded CAM signal of applying power to the CVR

Figure C-7



The end of the recorded signals from the CVR of the final flight of N739PA

Figure C-8

CVR TIME HISTORY

Analogue Output of all 4 Tracks
Each Strip Approx. 410 milliseconds

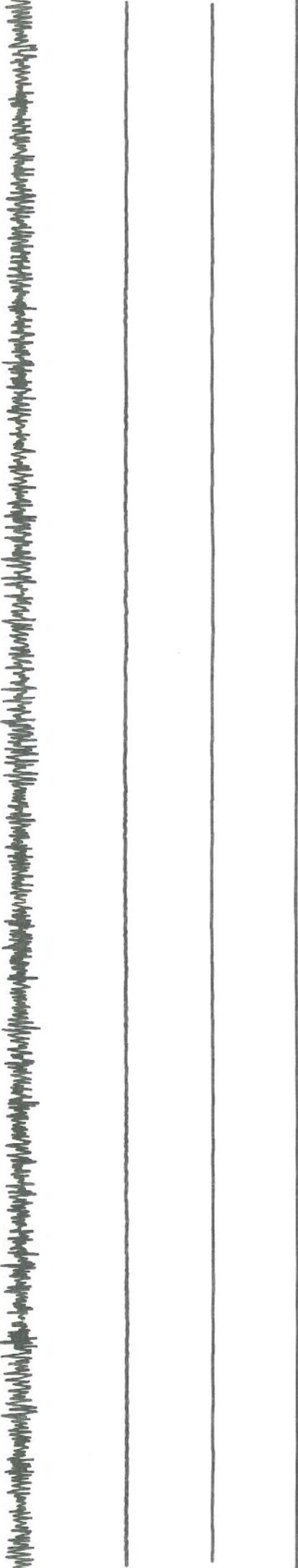
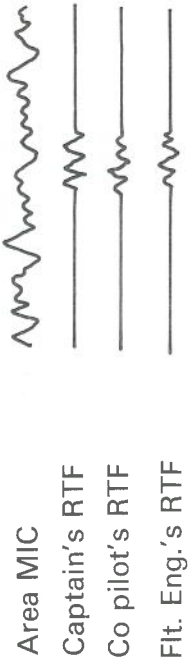


Figure C-9A

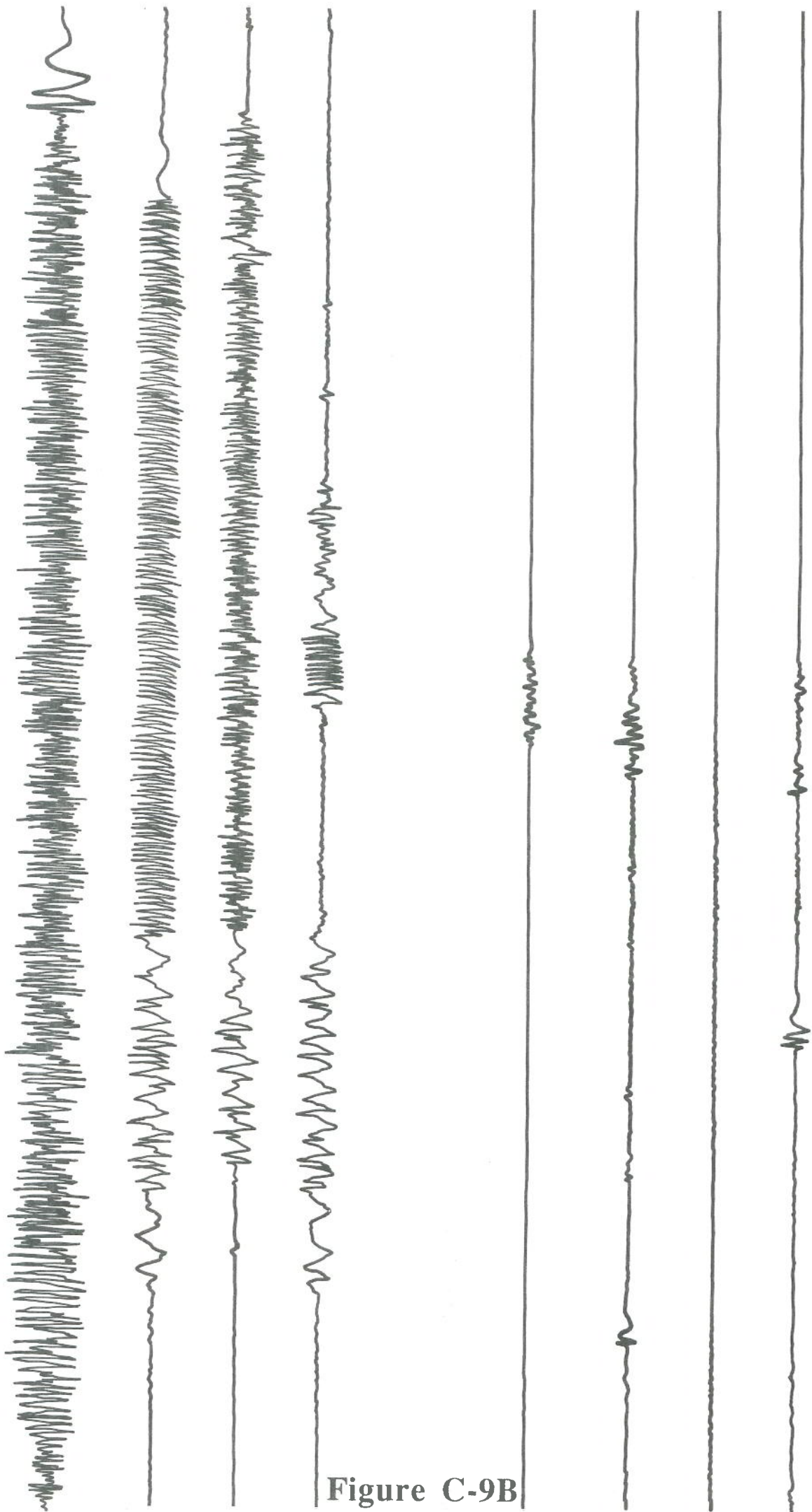


Figure C-9B

Timebase
 0 ———— 100
 mSec

The final CVR signals from Air India Flight 182

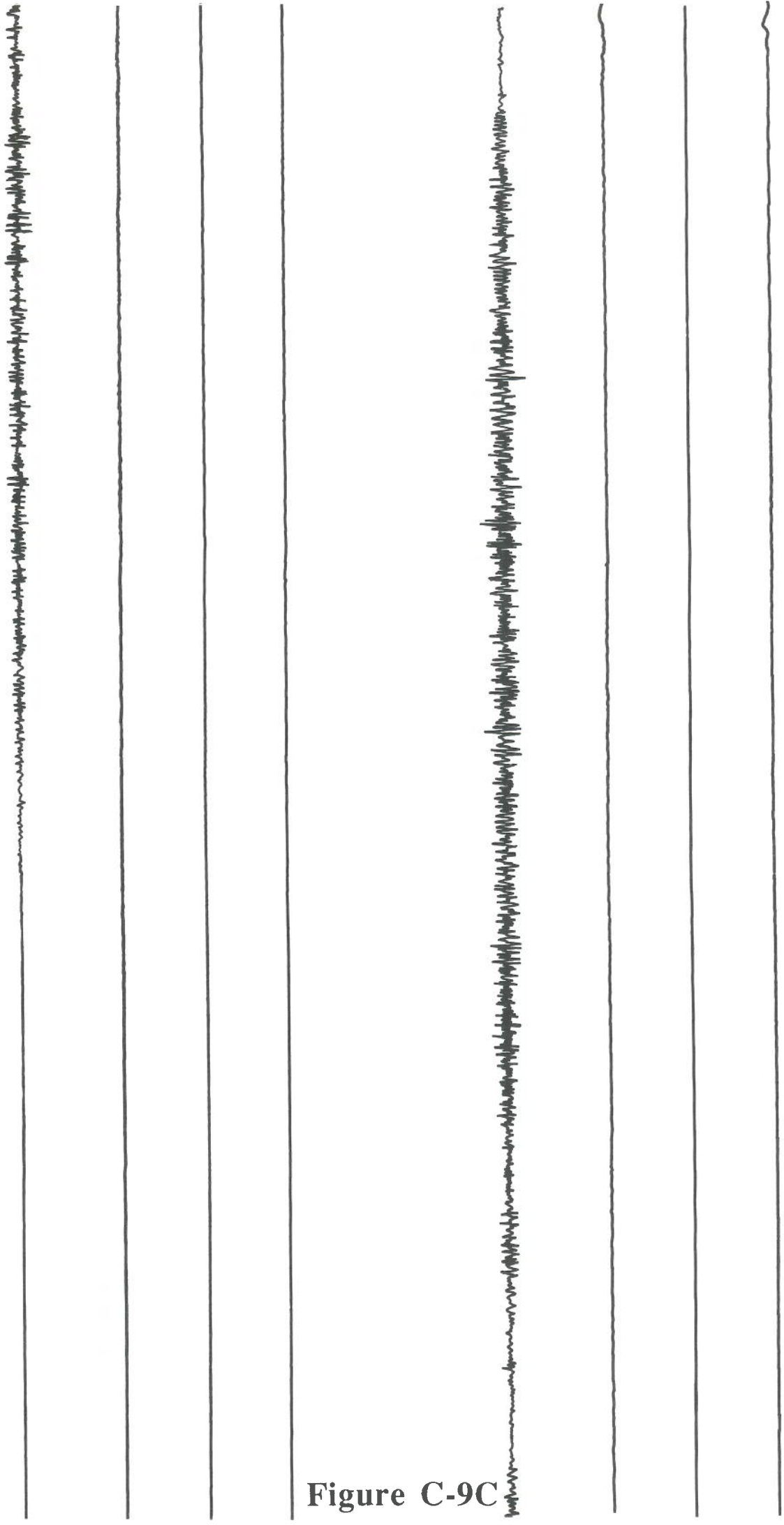


Figure C-9C

Timebase $\begin{array}{ccccccc} \text{L} & \text{L} & \text{L} & \text{L} & \text{L} & \text{L} & \text{L} \\ \hline 0 & \text{---} & \text{---} & \text{---} & \text{---} & \text{---} & \text{---} & 100 \\ \text{mSec} & & & & & & & \end{array}$

The final CVR signals from Air India Flight 182

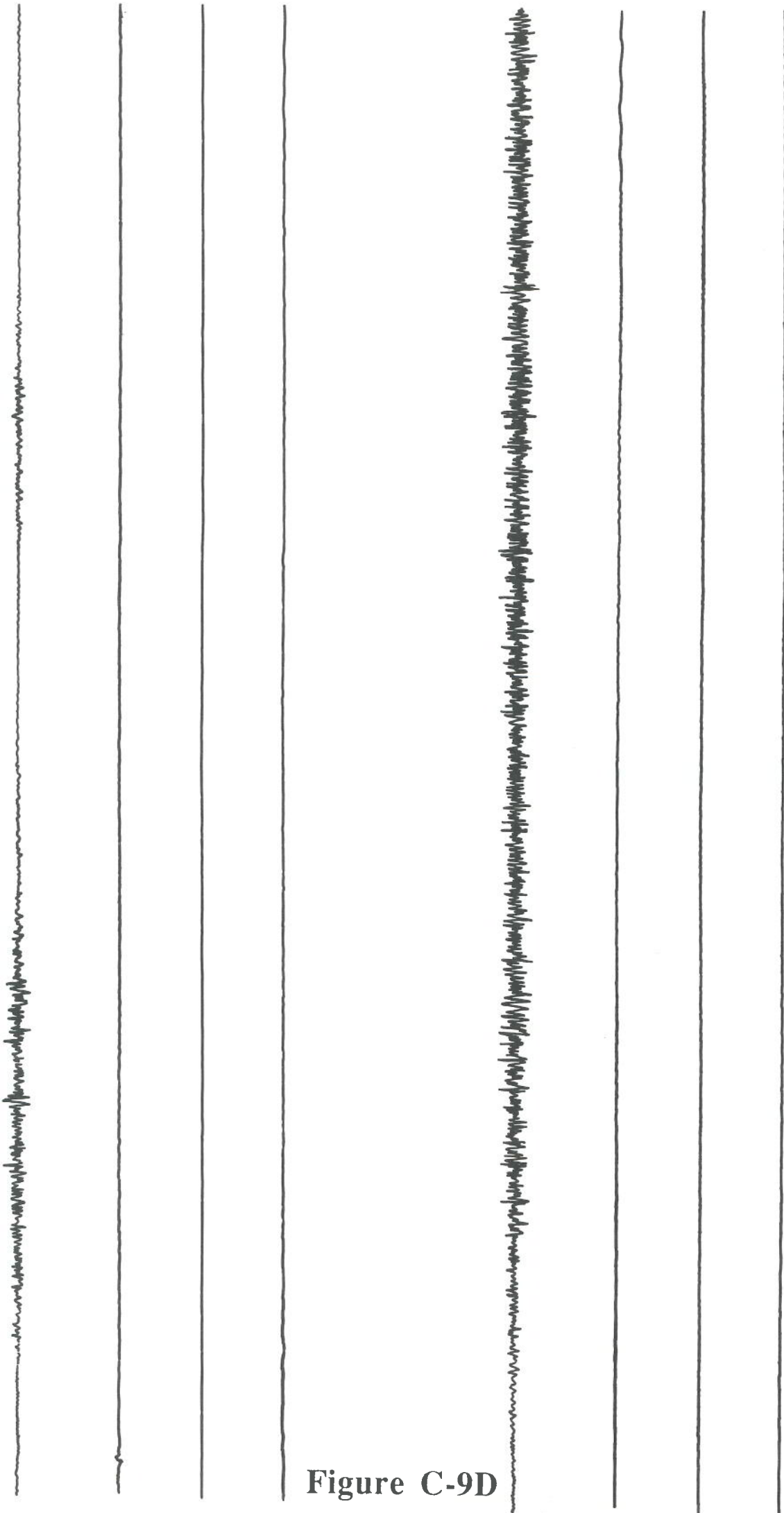
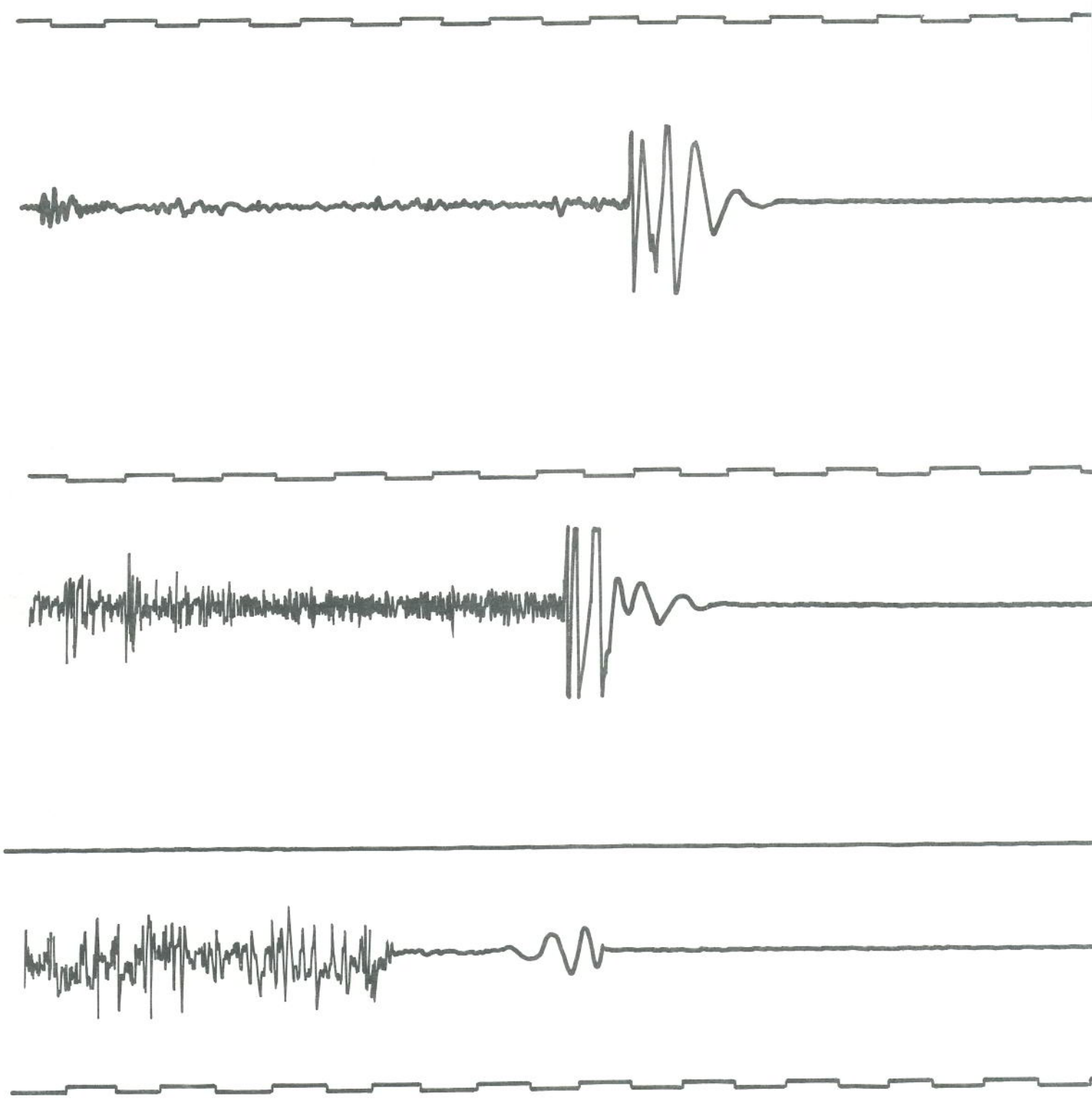


Figure C-9D

Timebase
 0 ——— L L L L L L L L L L
 mSec _____ 100

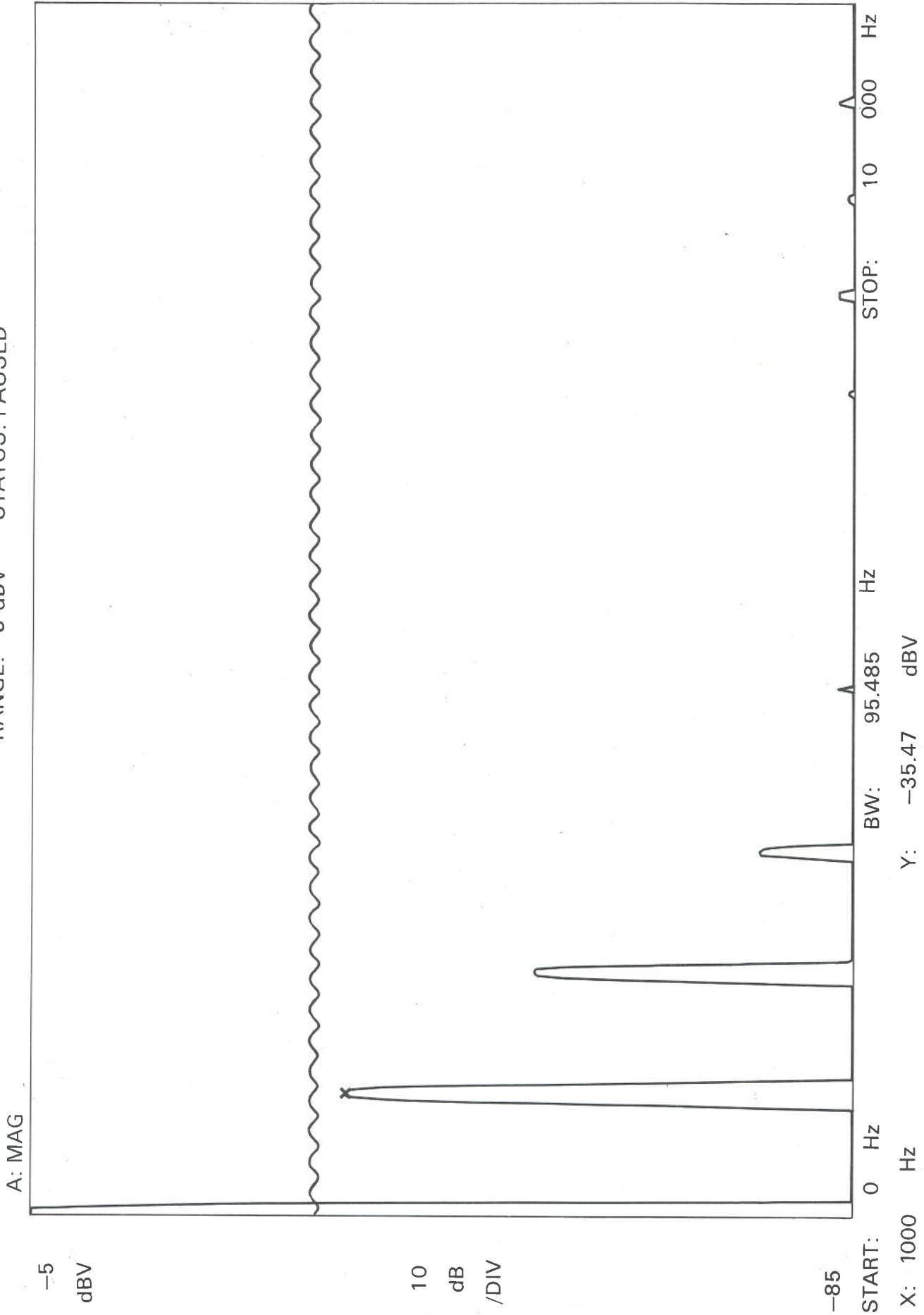
The final CVR signals from Air India Flight 182



Three typical end of RTF transmission transients
from N739PA, recorded on the CVR

Figure C-10

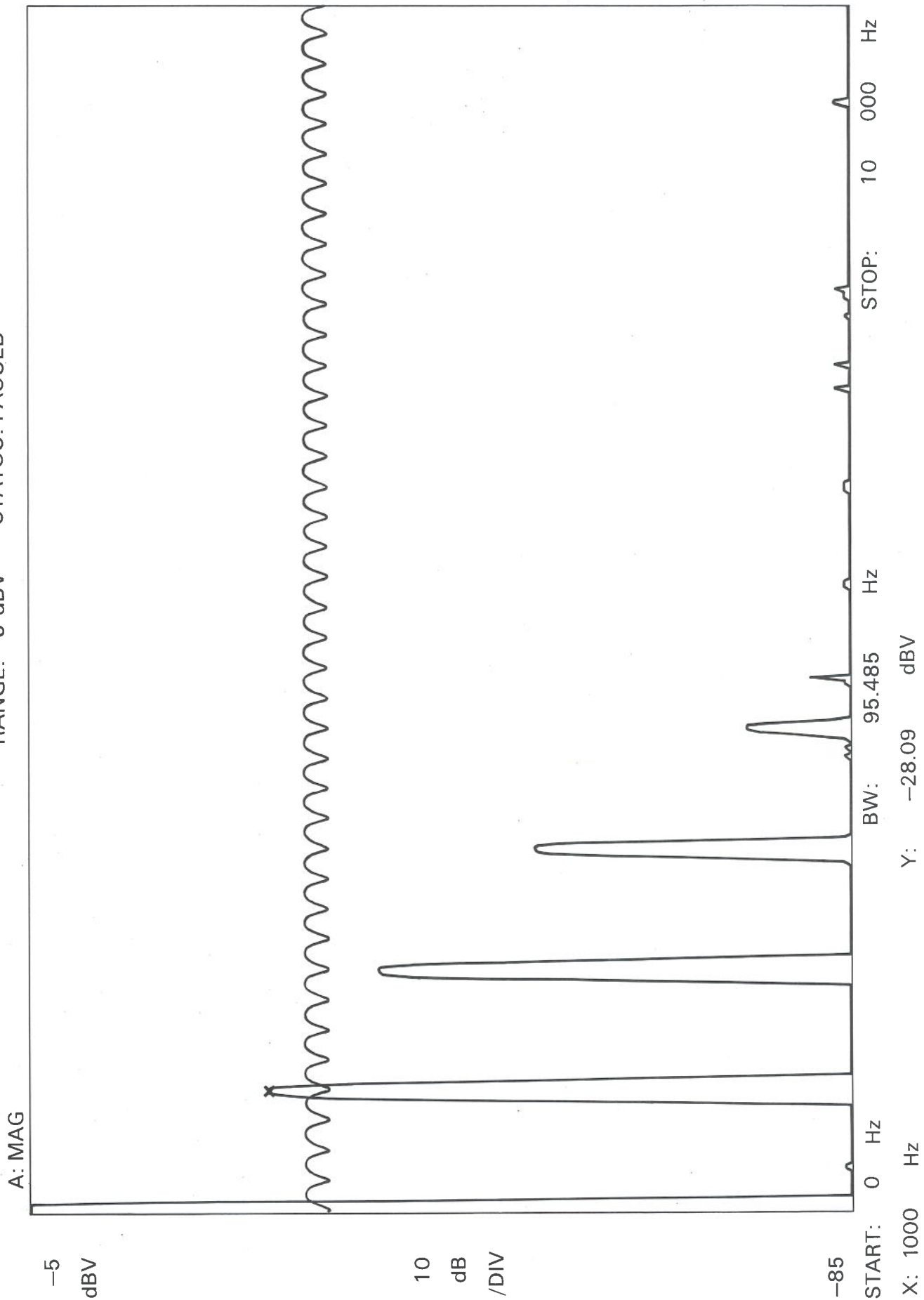
RANGE: -5 dBV STATUS: PAUSED



**Harmonic distortion of a relatively low amplitude
1 KHz signal**

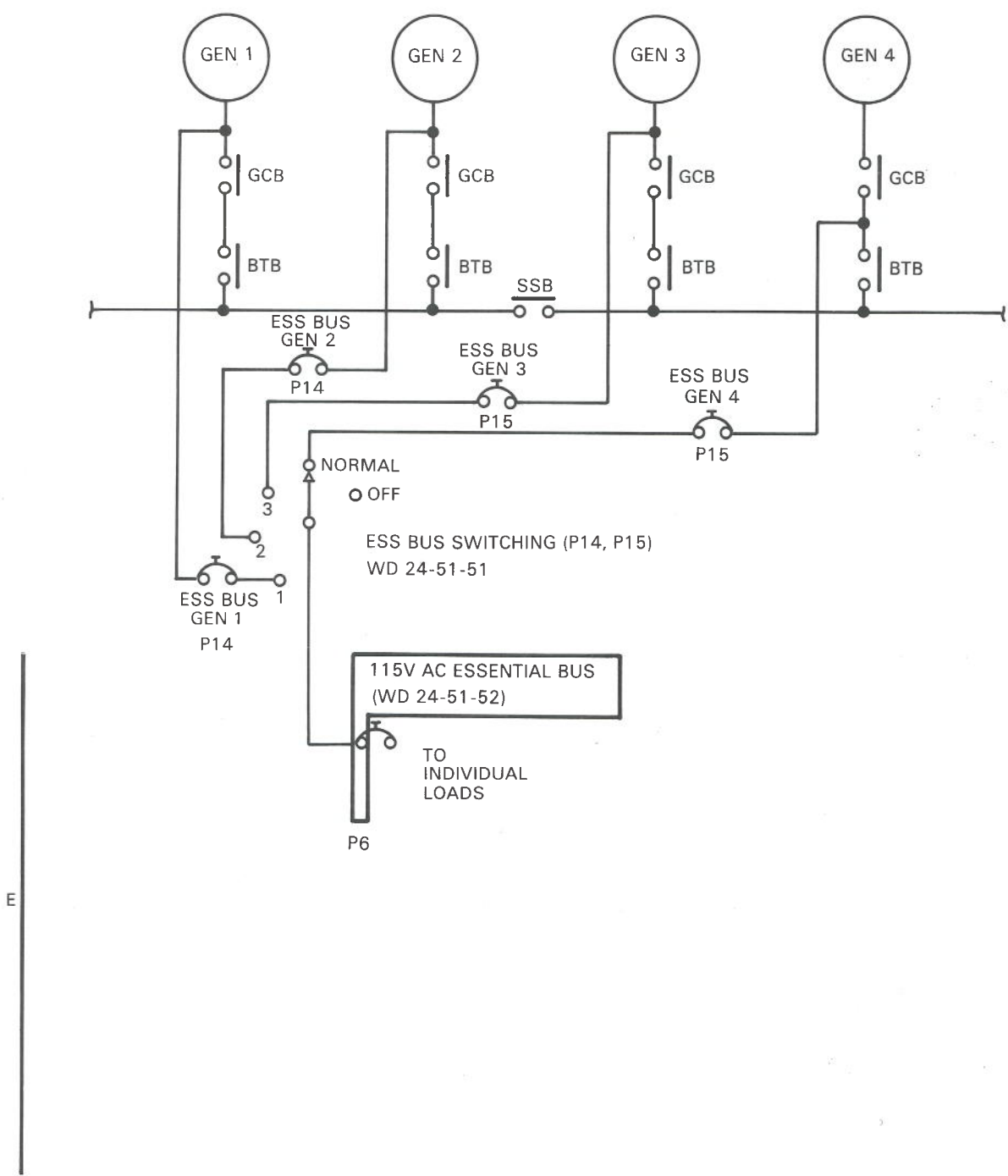
Figure C-11

RANGE: -5 dBV STATUS: PAUSED



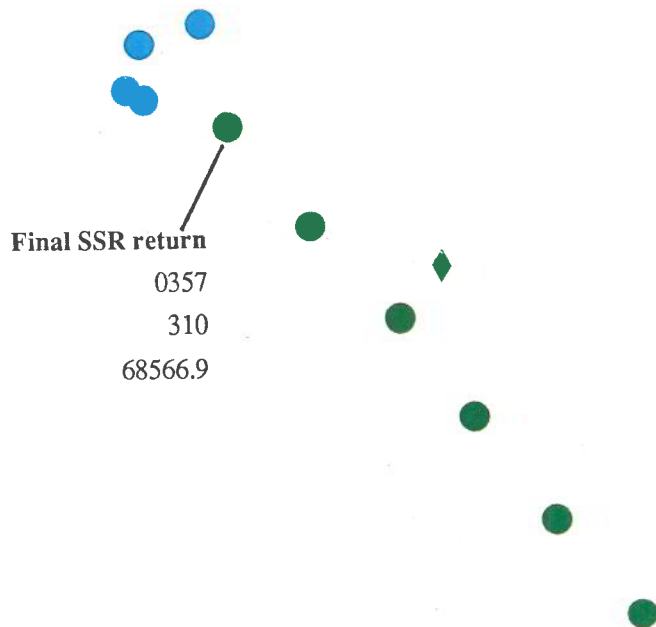
Harmonic distortion of a relatively high amplitude

Figure C-12



Boeing 747 main 115 volt AC power load distribution

Figure C-13

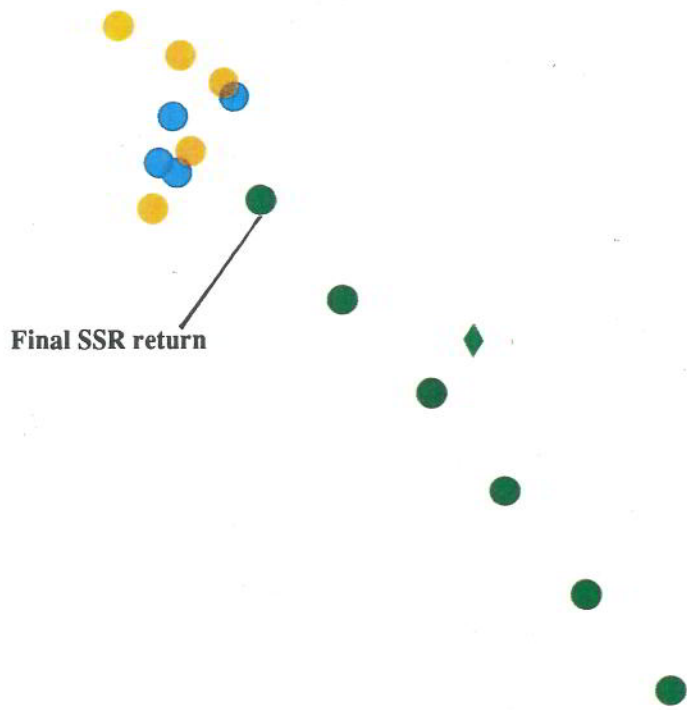


Time Secs = 68578

1st Primary Added

Radar returns from the final flight of N739PA

Figures C-14

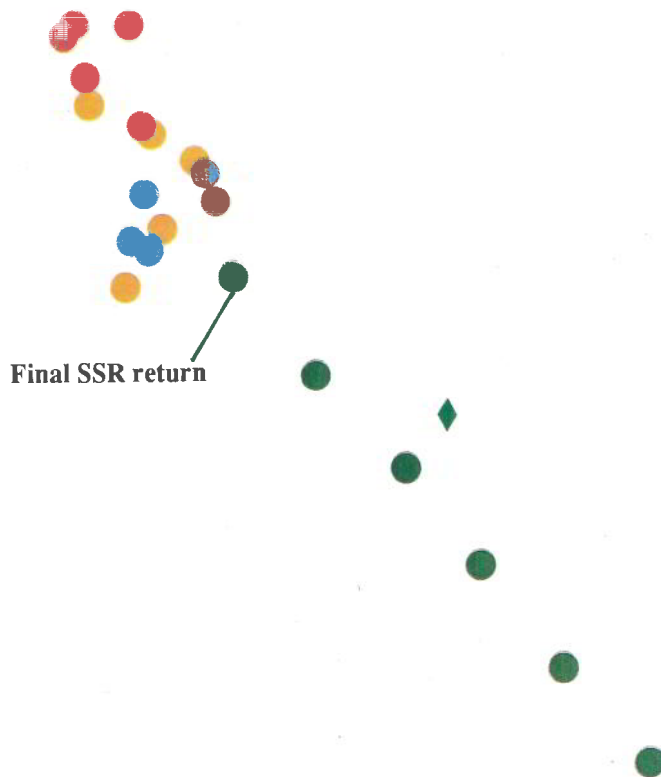


Time Secs = 68586

2nd Primary Added

Radar returns from the final flight of N739PA

Figures C-15

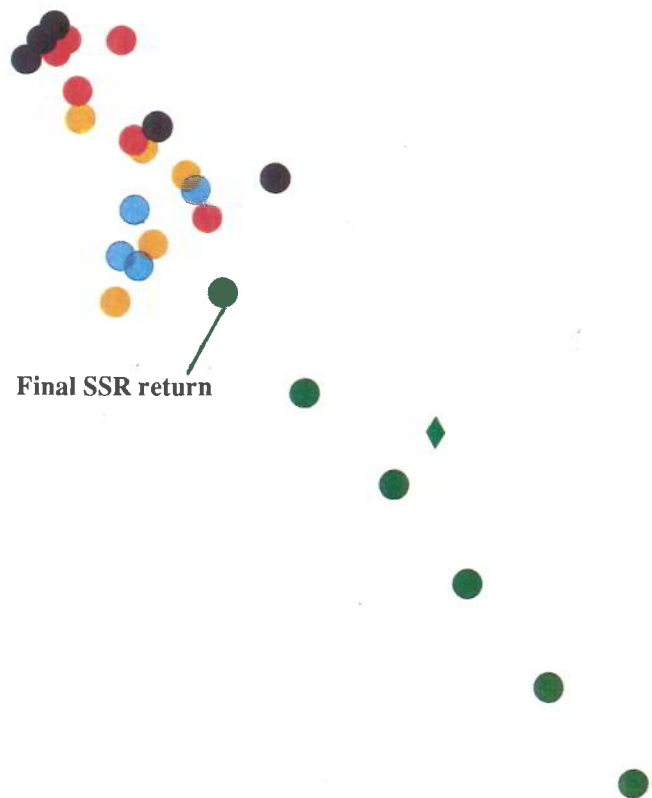


Time Secs = 68594

3rd Primary Added

Radar returns from the final flight of N739PA

Figures C-16

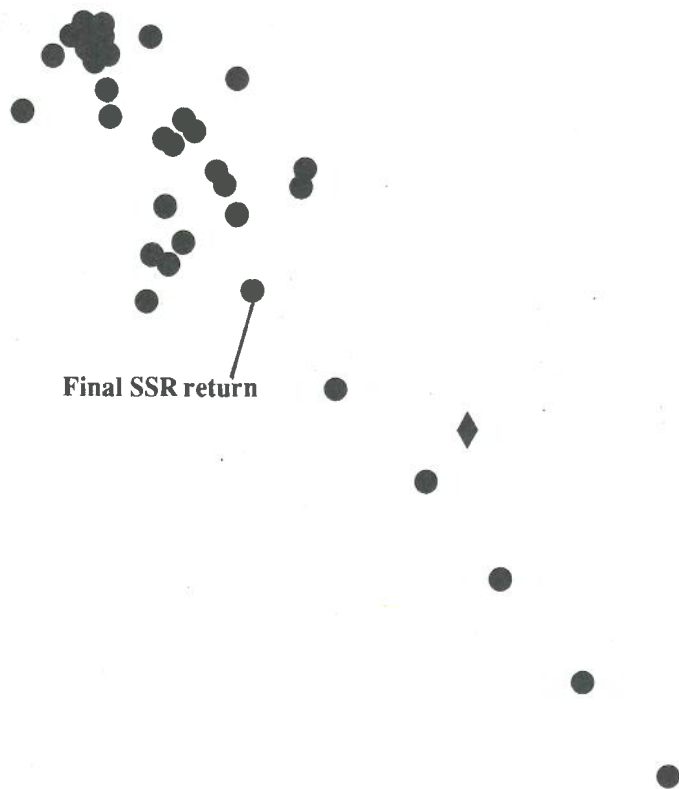


Time Secs = 68599

4th Primary Added

Radar returns from the final flight of N739PA

Figures C-17



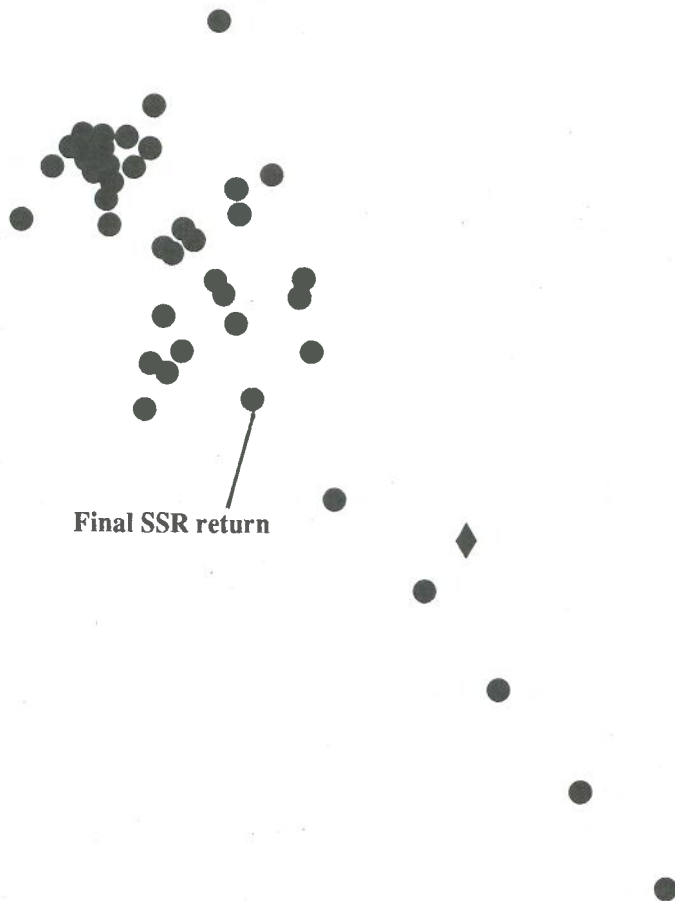
Final SSR return

Time Secs = 68610

5th Primary Added

Radar returns from the final flight of N739PA

Figures C-18

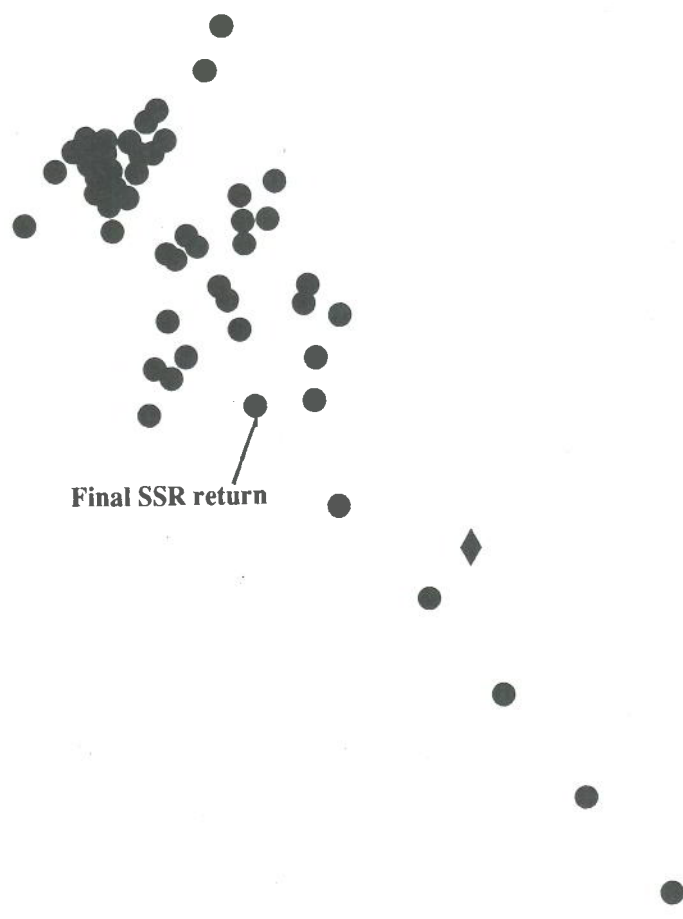


Time Secs = 68618

6th Primary Added

Radar returns from the final flight of N739PA

Figures C-19

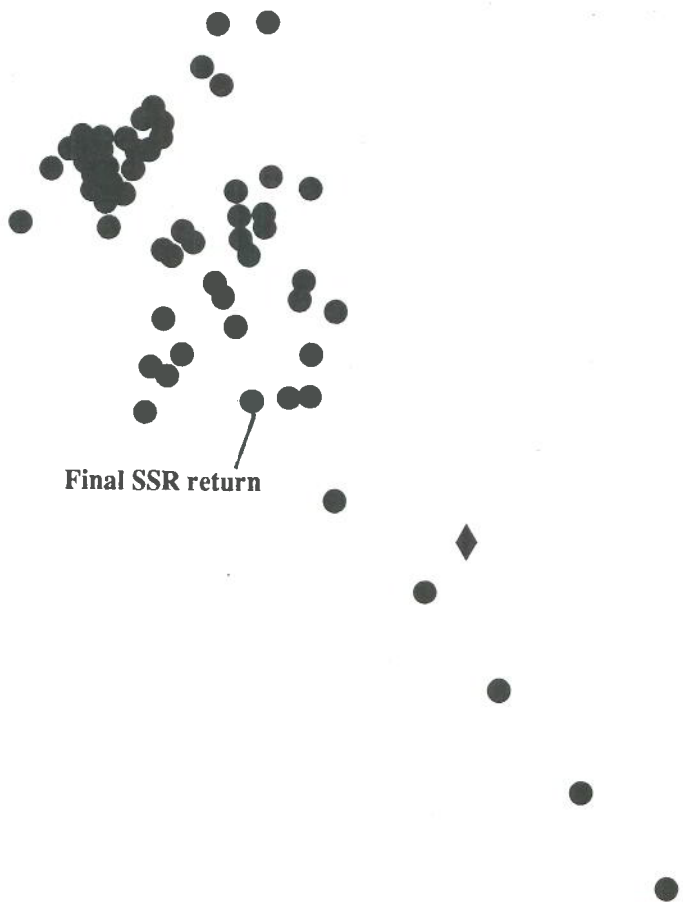


Time Secs = 68627

7th Primary Added

Radar returns from the final flight of N739PA

Figures C-20

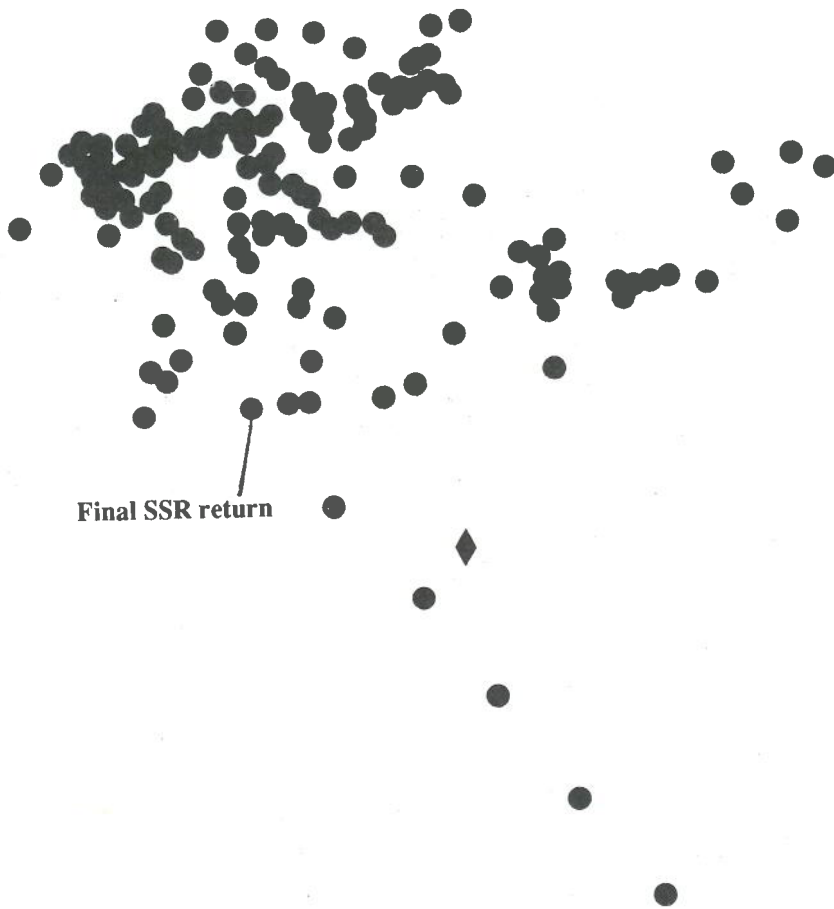


Time Secs = 68635

8th Primary Added

Radar returns from the final flight of N739PA

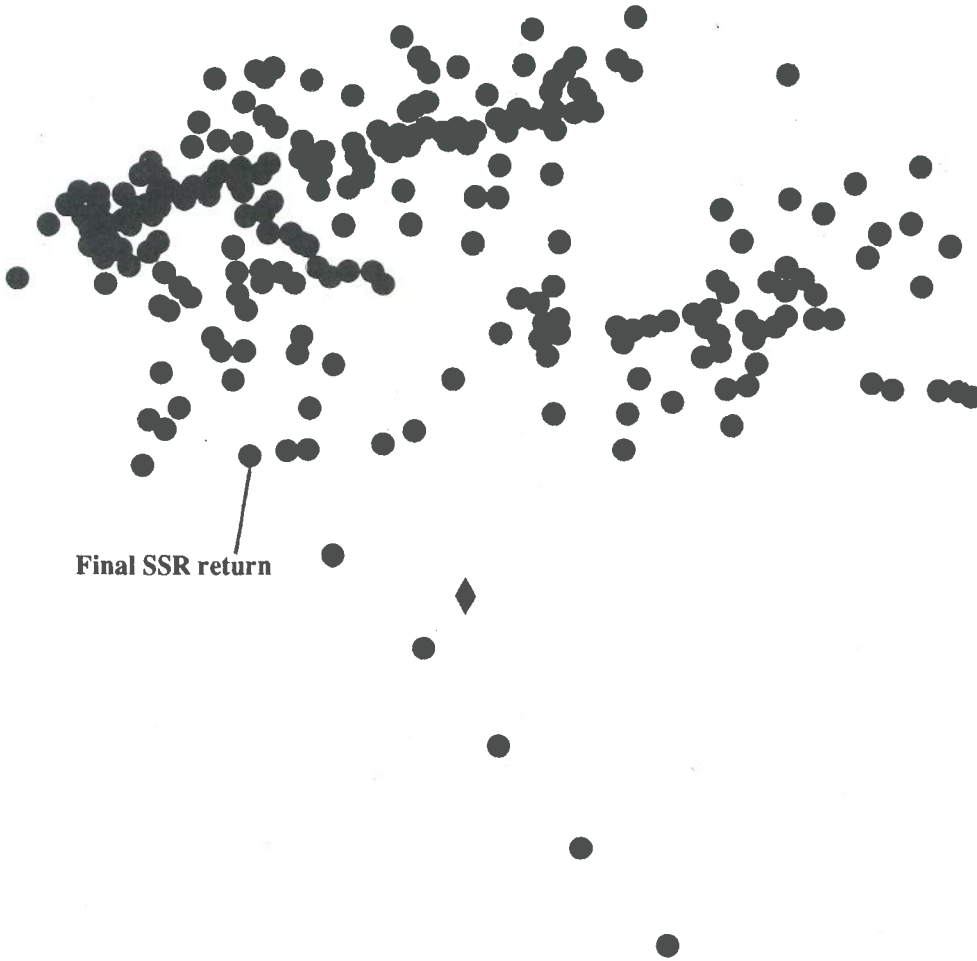
Figures C-21



Time Secs = 68753

Radar returns from the final flight of N739PA

Figures C-22



Final SSR return

Time Secs = 68816

Radar returns from the final flight of N739PA

Figures C-23

CRITICAL CRACK CALCULATIONS

It was assumed that the fuselage rupture and associated star-burst petalling process was driven by an expanding 'bubble' of high pressure gas, produced by the conversion of solid explosive material into gas products. As the explosive gas pressures reduced due to dissipation through the structure and external venting, the service differential pressure loading would have taken over from the explosive pressures as the principal force driving the skin fractures.

The high temperature gas would initially have been confined within the container where, because of the low volume, the pressure would have been extremely high (too high for containment) and the gas bubble would have expanded violently into the cavities of the fuselage between the outer skin and the container. This gas bubble would have continued to expand, with an accompanying fall in pressure due to the increasing volume combined with a corresponding drop in temperature.

The precise nature of the gas expansion process could not be determined directly from the evidence and it was therefore necessary to make a number of assumptions about its behaviour, based on the geometry of the hull and the area of fuselage skin which the high pressure bubble would have ruptured. Essentially, it was assumed that the gas bubble would expand freely in the circumferential direction, into the cavity between the fuselage skin and the container. In contrast, the freedom for the bubble to expand longitudinally would have been restricted by the presence of the fuselage frames, which would have partially blocked the passage of gas in the fore and aft directions. However, the pressures acting on the frames would have been such that they would have buckled and failed, allowing the gas to vent into the next 'bay', producing failure of the next frame. This sequential frame-failure process would have continued until the pressure had fallen to a level which the frames could withstand. During the period of frame failure and the associated longitudinal expansion of the gas bubble, this expansion rate was assumed to be half that of the circumferential rate.

It was assumed that venting would have taken place through the ruptured skin and that the boundary of the petalled hole followed behind the expanding gas bubble, just inside its outer boundary, i.e. the expanding gas bubble would have stretched and 'unzipped' the skins as it expanded. This process would have continued until the gas bubble had expanded/vented to a level where the pressure was no longer able to drive the petalling mechanism because the skin stresses had reduced to below the natural strength of the material.

The following structural model was assumed:

- (i) The pressurised hull was considered to be a cylinder of radius 128 inches, divided into regular lengths by stiff frames.
- (ii) The contributions of the stringers and frames beyond the petalled region were considered to be the equivalent of a reduction of stress in the skins by 20%, corresponding to an increase in skin thickness from 0.064 inches to 0.080 inches.
- (iii) Standing skin loads were assumed to be present due to the service differential pressure, i.e.. it was assumed that no significant venting of internal cabin pressure occurred within the relevant timescale.
- (iv) The mechanism of bubble pressure load transfer into the skins was:
 - a) Hoop direction - conventional membrane reaction into hoop stresses.
 - b) Longitudinal direction - reaction of pressures locally by the frames, restrained by the skins.

The critical crack calculations were based upon the generalised model of a plate under biaxial loading in which there was an elliptical hole with sharp cracks emanating from it. This is a good approximation of the initial condition, i.e.. the shattered hole, and an adequate representation of the subsequent phase, when the hole was enlarging in its star-burst, petalling, mode.

The analyses of critical crack dimensions in the circumferential and longitudinal directions were based on established Fracture Resistance techniques. The method utilises fracture resistance data for the material in question to establish the critical condition at which the rate of energy released by the crack just balances the rate of energy absorbed by the material in the cracking process, i.e. the instantaneous value of the parameter K_{r} , commonly referred to as the fracture toughness K_{c} . From this, the relationship between critical stress and crack length can be determined.

Using conventional Linear Elastic Fracture Mechanics (LEFM) with fracture toughness data from RAE experimental work and published geometric factors relating to cracks emanating from elliptical holes, the stress levels required to drive cracks of increasing lengths in both circumferential and longitudinal directions were calculated. The skin stresses at sequential stages of the expanding gas bubble/skin petalling process were then calculated and compared with these data.

The results of the analysis indicated that, once the large petalled hole had been produced by explosive gas overpressure, the hoop stresses generated by fuselage pressurisation loads acting alone would have been sufficient to drive cracks longitudinally for large distances beyond the boundaries of the petalled hole. Thus, with residual gas overpressure acting as well, the 43 feet (total length) longitudinal fractures observed in the wreckage are entirely understandable. The calculations also suggested that the hoop fractures, due to longitudinal stresses in the skins, would have extended beyond the boundary of the petalled hole, though the excess stress driving the fractures in this direction would have been much smaller than for the longitudinal fractures, and the level of uncertainty was greater due to the difficulty of producing an accurate model reflecting the diffusion of longitudinal loads into the skins. Nevertheless, the results suggested that the circumferential cracks would extend downwards just beyond the keel, and upwards as far as the window belt - conclusions which accord reasonably well with the wreckage evidence.

POTENTIAL REMEDIAL MEASURES

1. Introduction

In the following discussion, those damage mechanisms which appear to have contributed to the catastrophic structural failure of Flight PA103 are identified and possible ways of reducing their damaging effects are suggested. These suggestions are intended to stimulate thought and discussion by manufacturers, airworthiness authorities, and others having an interest in finding solutions to the problem; they are intended to serve as a catalyst rather than to lay claim to a definitive solution. On the basis of the Flight PA103 investigation, damage is likely to fall into two categories: direct explosive damage, and indirect explosive damage.

2. Direct explosive damage

The most serious aspect of the direct explosive damage on the structure is the large, jagged aperture in the pressure hull, combined with frame and stringer break-up, which results from the star-burst rupture of the fuselage skin. Because of its uncontrolled size and position, and the naturally radiating cracks which form as part of the petalling process, the skin's critical crack length (under pressurisation loading) is likely to be exceeded, resulting in unstable crack propagation away from the boundary of the aperture. Such cracks can lead to a critical loss of structural integrity at a time when additional loads are likely to be imposed on the structure due to reflected blast pressure and/or aircraft aerodynamic and inertial loading.

A further complicating factor is that the size of this aperture is likely to be sufficiently large to allow complete cargo containers and other debris to be ejected into the airstream, with a high probability of causing catastrophic structural damage to the empennage.

3. Indirect explosive damage

Indirect explosive damage (channelling or ducting of explosive energy in the form of both shock waves and supersonic gas flows) is likely to occur because of the network of interlinked cavities which exist, in various forms, in all large commercial aircraft, particularly below cabin floor level. This channeling mechanism can produce critical damage at significant distances from the source of the explosion.

In addition to the structural damage, aircraft flight control and other critical systems will potentially be disrupted, both by the explosive forces and as a result of structural break-up and distortions. The discussion which follows focuses on possible means of

limiting structural damage of the kind which occurred on Flight PA103. Undoubtedly, such measures will also have beneficial effects in limiting systems damage. However, system vulnerability can further be reduced by applying, wherever possible, those techniques used on military aircraft to reduce vulnerability to battle damage; multiplexed, multiply redundant systems using distributed hardware to minimise risk of a single area of damage producing major system disruption. Fly by wire flight control systems potentially offer considerable scope to achieve these goals, but the same distributed approach would also be required for the electronic and other equipment which, in current aircraft, tends to be concentrated into a small number of 'equipment centres'.

4. Remedial measures to reduce structural damage

Whilst pure containment of the explosive energy is theoretically possible, in an aviation context such a scheme would not be viable. Any unsuccessful attempt to contain the explosive will probably produce greater devastation than the original (uncontained) explosion since all the explosive energy would merely be stored until the containment finally ruptured, when the stored energy would be released together with massive fragmentation of the containment.

However, a mixed approach involving a combination of containment, venting, and energy absorption should provide useful gains provided that a systematic rather than piecemeal approach is adopted, and that the scheme also addresses blast channelling. The following scheme is put forward for discussion, primarily as means of identifying, by example, how the various elements of the problem might be approached at a conceptual level and to provide a stimulus for debate. No detailed engineering solutions are offered, but it is firmly believed that the requirements of such a scheme could be met from a technical standpoint. The proposed scheme is based on the need to counter a threat similar to that involving Flight PA103, i.e. a high explosive device placed within a baggage container, however, the principles should be applicable to other aircraft types.

Such a scheme might comprise several 'layers' of defence. The first two layers, one within the other, are essentially identical and provide partial containment of the explosive energy and the redirection of blast out from the compartment via pre-determined vent paths. Although the containment is temporary, it must provide an effective barrier to uncontrolled venting, preventing the escape of blast except via the pre-designated paths.

The third layer comprises a pre-determined area of fuselage skin, adjoining the outer end of the vent path, designed to rupture or burst in a controlled manner, providing a large vent aperture which will not tend to crack or rupture beyond the designated boundaries.

A fourth layer of protection has two elements, both intended to limit the propagation of shock waves through the internal cavities in the hull. The first element comprises the closure of any gaps between the vent apertures in the two innermost containment layers and the vent aperture in the outer skin. This effectively provides an exhaust duct connecting the inner and outer vent apertures to minimise leakage into the intervening structure and cavities around the cargo hold. The second element comprises the incorporation of an energy absorbing lining material within all the cavities in the lower hull, to absorb shock energy, limit shock reflection and limit the propagation of pressure waves which might enter the cavities, for example because of containment layer breakthrough.

5 Possible application to Boeing 747 type aircraft

5.1 Container Modification

The obvious candidates for the inner containment layer are the baggage containers themselves. Existing containers are of crude construction, typically comprising aluminium sheet sides and top attached to an aluminium frame with a fabric reinforced access curtain, or have sides and top of fibreglass laminate attached to a robust aluminium base section.

These containers are stacked in the aircraft in such a manner that on three sides (except for the endmost containers) the baggage within the adjoining containers provides an already highly effective energy absorbing barrier. If the container is modified so that loading access is via the outboard side of the container rather than at the end, i.e. the curtain is put on the faces shown in Figure E-1, then only the top and base are 'unbacked' by other containers, leaving the outboard face as a vent region.

The proposal is therefore that a modified container is developed in which the access is changed from the end to the outside face only, and which is modified to improve the resistance to internal pressures and thus encourage venting via the new access curtain only. How the container is actually modified to achieve the containment requirement is a matter of detail design, but two approaches suggest themselves, both involving the use of composite type materials. The first approach is to adopt a scheme for a rigid container which relies on a combination of energy absorption and burst strength to prevent uncontrolled breakout of explosive energy. The second approach is to use a 'flexible' container, i.e. rigid enough for normal use, but sufficiently flexible to allow gross deformation of shape without rupture. This, particularly if used with a backing blanket made from high performance material to resist fragmentation, could deform sufficiently to allow the container to bear against, and partially crush, adjoining containers. In this way, the shock energy transmission should be significantly reduced

and the inherent energy absorption capability and mass of the baggage in adjoining containers could be utilised, whilst still retaining the high pressure gas for long enough to allow venting via the side face. Clearly, care would need to be taken to ensure that the container vent aperture remained as undistorted as possible, to ensure minimal leakage at the interface.

5.2 Cargo bay liner

The existing cargo bay liner is a thin fibreglass laminate which lines the roof and sidewalls of the cargo hold. There is no floor as such; instead, the containers are supported on rails running fore and aft on the tops of the fuselage frame lower segments. In a number of areas, there are zipped fabric panels let into the liner to provide access to equipment located behind. The liner 'ceiling' is suspended on plastic pillars approximately 2 centimeters below the bottom of the main cabin floor beams. The purpose of the liner is solely to act as a general barrier to protect wiring looms and systems components.

The proposal is to produce a new liner designed to provide the second level of containment, essentially at 'floor' and 'roof' level only [Figure E-1]. The dimensional constraints are such that potentially quite thick material could be incorporated (leaving aside the weight problem), permitting not only a rigid liner design, but semi-rigid or flexible linings backed by energy absorbing blanket materials.

The liner would be designed to provide an additional barrier at the base and roof of the containers, which unlike the sides, are not protected by adjoining containers. The outside ends of these barrier elements must effectively seal against the vent apertures in the containers, to minimise leakage into the fuselage cavities.

5.3 Structural blow-out regions.

The final element in the containment/venting part of the scheme is a line of blow-out regions in the fuselage skins, coinciding exactly with the positions of the vent apertures in the cargo containers and cargo bay liner. These should extend along the length of the cargo hold, zoned in such a way that rupture due to rapid overpressure will occur in a controlled manner. The primary function of the blow-out regions would be to provide immediate pressure relief by allowing the inevitable skin rupture to take place only within pre-determined zones, limiting the extent of the skin tearing by means of careful stiffness control at the boundary of the blow-out regions.

The structural requirements of such panels are perhaps the most difficult challenge to meet, particularly for existing designs. However, it is believed that by giving appropriate consideration to the directionality of fastening strengths, and the use of

external tear straps, it should be possible to design the structure to carry the normal service loads whilst creating a pre-disposition to rupturing in a controlled manner in response to gross pressure impulse loading.

The implementation of such features will need carefully balanced design in order to provide local stiffening, sufficient to control and direct the tear processes, without creating stiffness discontinuities which could lead to fatigue problems during extended service. However, the degree of reinforcement needed at the blow-out aperture need only be sufficient to limit tearing and to sustain the aircraft long enough to complete the flight unpressurised.

All aircraft have pre-existing strength discontinuities, despite the efforts of the designers to eliminate them. By choosing the positions of butt joints, lap joints, anti-tear straps and similar structural features in future designs, so as to incorporate them into the boundary of the blow-out panel region, the natural "tear here" tendencies of such features could possibly be turned to advantage. In the case of current generation aircraft, the positions of existing lines of weakness at such features will determine the optimum position for structural blow-out areas, and hence the positions of the container and cargo bay liner blow-out panels. A limited amount of local structural reinforcement (e.g. in the form of external anti-tear straps), carried out as part of a modification program, could perhaps fine tune the tearing properties of existing lines of weakness, potentially producing significant improvements.

5.4 Closure of cavities

There are four main classes of cavity which will need to be addressed on the Boeing 747, and most other modern aircraft. These are:

- (i) The channels formed between fuselage frames
- (ii) The cross-ship cavities between cabin floor beams
- (iii) Longitudinal 'manifold' cavities on each side of the cargo deck, running fore and aft in the space behind the upper sidewall areas of the cargo bay liner.
- (iv) Air conditioning vents along the bottom of the cabin side-liner panels, which connect the side cavities below cabin floor level with the main passenger cabin.

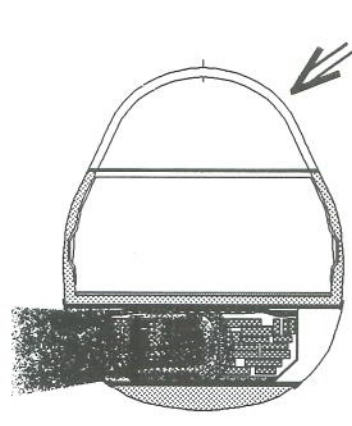
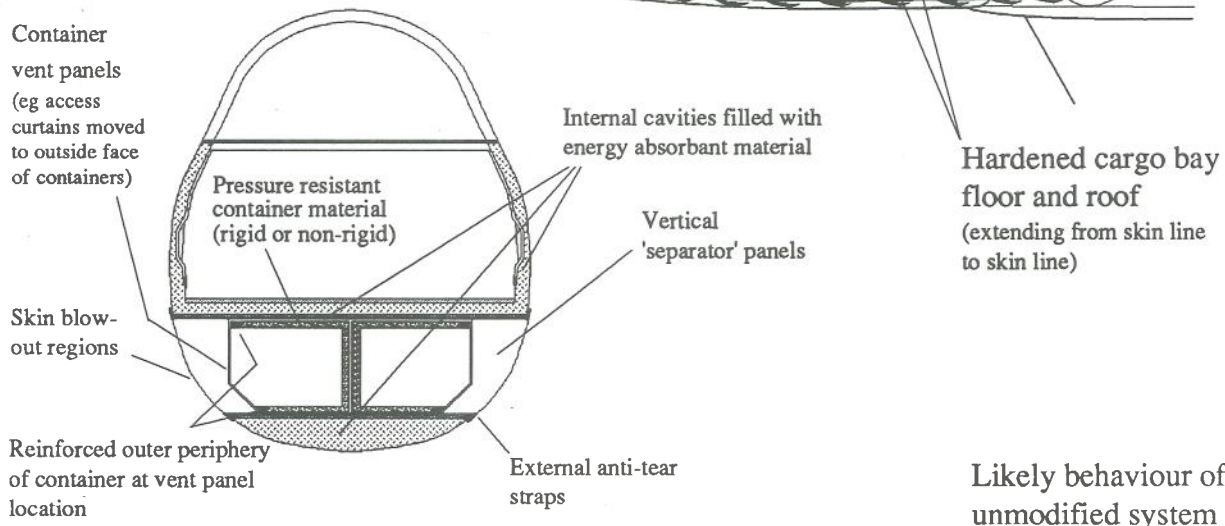
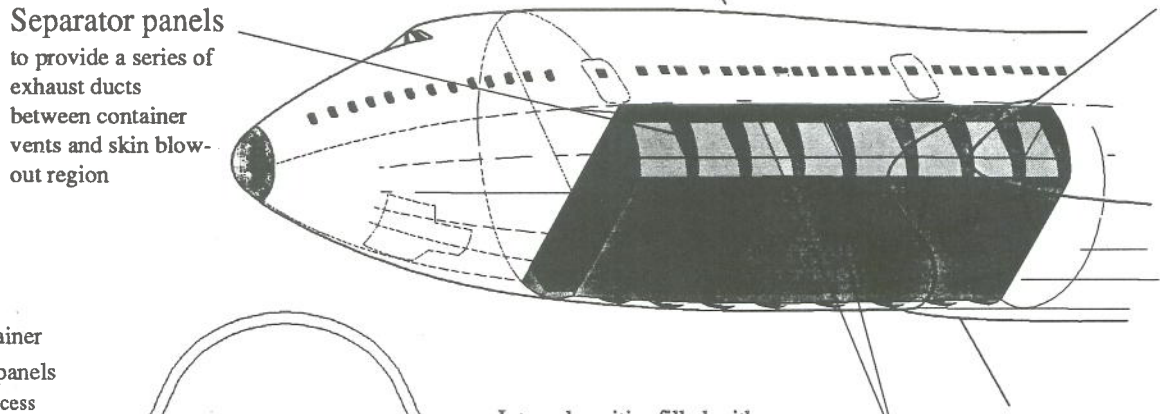
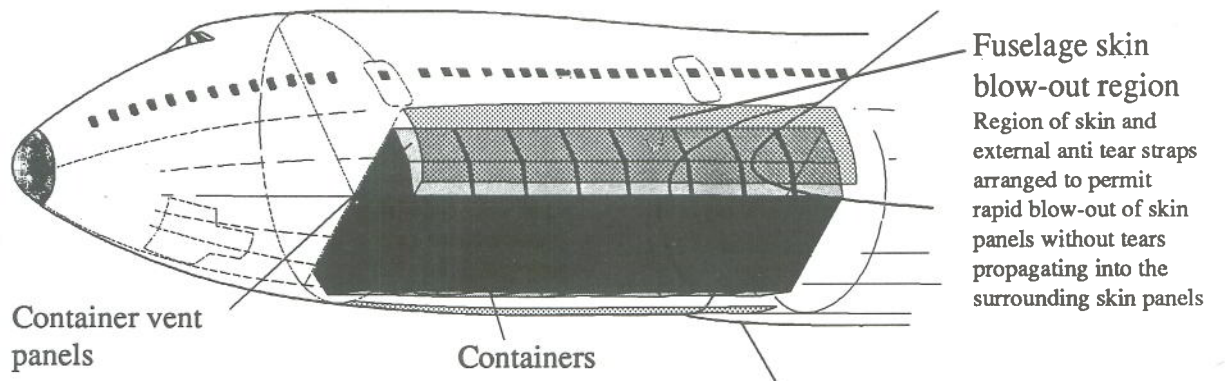
If the containment barriers (i.e. modified cargo containers and cargo hold liner) can be made to prevent blast breakthrough into these cavities directly, then the only area where

transfer can occur is at the interface between the container/cargo hold liner vent apertures and the fuselage skins at the blow-out region. This short distance will need to be sealed in order to form a short 'exhaust duct' between the container vent aperture and the fuselage skin. Since the shock and general explosive pressure will act mainly along the vent-duct axis, the pressure loading on the vent duct walls should not be excessive.

5.5 Attenuation of shock waves in structural cavities

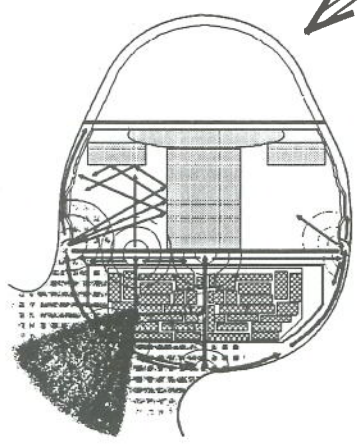
To prevent the 'ducting' of any blast which does enter the fuselage cavities, either because of partial penetration of the containment barriers or leakage at the vent duct interfaces, the scheme requires the provision of lightweight energy absorbing material within the cavities to limit reflection and propagation of pressure waves within the cavities, and radiation of shock waves into the cabin from the conditioning air vents. Materials such as vermiculite, which are of low density yet have excellent explosive energy absorption properties, may have application in this area, perhaps in lieu of the existing insulation material.

Since the existing cavities often serve as part of the air conditioning outflow circuit, some consideration will need to be given to finding an alternative route. However, the flow rates are small compared with the total cross-sectional flow potential of the cavities and this function could be served by separate air conditioning ducts, or perhaps by restricting access to one or two cavities only (thus limiting the risk), or by using some form of blast valve to close off the air conditioning vents. Similarly, the requirement to vent pressure from the cabin in the event of a cargo bay decompression would also need to be addressed.



Aim of modified system

- 1) venting through blow-out panel(s) to dissipate peak overpressure quickly
- 2) controlled size of fuselage aperture with 'clean' boundary and no extended cracks
- 3) minimal ducting through cavities
- 4) energy absorbed by baggage in adjoining containers (non-rigid container)



Likely behaviour of unmodified system

- 1) large, uncontrolled starburst rupture of fuselage with extended cracking
- 2) ducting of shock and gas overpressure through fuselage cavities
- 3) local enhancements as ducted shocks/gas overpressures re-combine
- 4) re-radiation into cabin as psuedo explosive sources
- 5) reflection off hard surfaces producing local pressure enhancements

Principal Features of Proposed Remedial Scheme

Figure E-1

**BAGGAGE CONTAINER EXAMINATION, RECONSTRUCTION AND
RELATIONSHIP TO THE AIRCRAFT STRUCTURE**

1. Introduction

During the wreckage recovery operation it became apparent that some items, identified as parts of baggage containers, exhibited blast damage. It was confirmed by forensic scientists at the Royal Armaments Research and Development Establishment (RARDE), after detailed physical and chemical examination, that these items showed conclusive evidence of a detonating high performance plastic explosive. It was therefore decided to segregate identifiable container parts and reconstruct any that showed evidence from the effect of Improvised Explosive Device (IED). It was evident, from the main wreckage layout that the IED had been located in the forward cargo hold and, although all baggage container wreckage was examined, only items from the forward hold showing the relevant characteristics were considered for the reconstruction. This Appendix documents the reconstruction of two particular containers and, from their position within the forward fuselage, defines the location of the IED.

2 Container Arrangement

Information supplied by Pan Am showed that this aircraft had been loaded with 12 baggage containers and two cargo pallets in the forward hold located as shown in Figure F-1. Three containers were recorded as being of the glass fibre reinforced plastic type (those at positions 11L, 13L and 21L) with the remaining 9 being of metal construction.

3. Container Description

All the baggage containers installed in the forward cargo hold were of the LD3 type (lower deck container, half width - cargo) and designated with the codes AVE, for those constructed from aluminum alloy, and AVA or AVN for those constructed from fibreglass. Each container was specifically identified with a four digit serial number followed by the letters PA and this nine digit identifier was present at the top of three sides of each container in black letters/numbers approximately 5 inches tall. Detail drawings and photographs of a typical metal container are shown in Figure F-2. Each container was essentially a 5 feet cube with a 17 inch extension over its full length to the left of the access aperture. In order to fit within the section of the lower fuselage this extension had a sloping face at its base joining the edge of the container floor to the left vertical sidewall at a position some 20 inches above the floor. The access aperture on the AVE type container was covered by a blue reinforced plastic curtain, fixed to the container at its top edge, braced by two wires and central and lower edge cross bars

which engaged with the aperture structure. The strength of this type of container superstructure was provided by the various extruded section edge members, attached to a robust floor panel, with a thin aluminum skin providing baggage containment and weatherproofing.

4. Container Identification

Discrimination between forward and rear cargo hold containers was relatively straightforward as the rear cargo hold wreckage was almost entirely confined to the town of Lockerbie and was characteristically different from that from the forward hold, in that it was generally severely crushed and covered in mud. The forward hold debris, by comparison, was mostly recovered from the southern wreckage trail some distance from Lockerbie and had mainly been torn into relatively large sections.

All immediately identifiable parts of the forward cargo containers were segregated into areas designated by their serial numbers and items not identified at that stage were collected into piles of similar parts for later assessment. As a result of this two containers, one metal and one fibreglass, were identified as exhibiting damage likely to have been caused by the IED. From the Pan Am records the metal container of these two had been positioned at position 14L, and the fibreglass at position 21L (adjacent positions, 4th and 5th from the front of the forward cargo hold on the left side). The serial numbers of these containers were respectively AVE 4041 PA and AVN 7511 PA.

5. Container Reconstruction

Those parts which could be positively identified as being from containers AVE 4041 PA and AVN 7511 PA were assembled onto one of three wooden frameworks; one each for the floor and superstructure of container 4041, and one for the superstructure of container 7511. Figures F-3 to F-9 show the reconstruction of container 4041 and Figure F-10 shows the reconstructed forward face of container 7511. Approximately 85% of container 4041 was identified, the main missing sections being the aft half of the sloping face skin and all of the curtain. Two items were included which could not be fracture or tear matched to container 4041, however, they showed the particular type of blast damage exhibited only by items from this container.

While this work was in progress a buckled section of skin from container 4041 was found by an AAIB Inspector to contain, trapped within its folds, an item which was subsequently identified by forensic scientists at the Royal Armaments Research and Development Establishment (RARDE) as belonging to a specific type of radio-cassette player and that this had been fitted with an improvised explosive device.

Examination of all other component parts of the remaining containers from the front and rear cargo holds did not reveal any evidence of blast damage similar to that found on containers 4041 and 7511.

5. Wreckage Distribution

Those items which were positively identified as parts of container 4041 or 7511, and for which a grid reference was available, were found to have fallen close to the southern edge of the southern wreckage trail. This indicated that one of the very early events in the aircraft break-up sequence was the blast damage to, and ejection of, parts of these two containers.

6. Fuselage Reconstruction

In order to gain a better understanding of the failure sequence, that part of the aircraft's fuselage encompassing the forward cargo hold was reconstructed at AAIB Farnborough. After all available blast damaged pieces of structure had been added, the floor of container 4041 was installed as near to its original position as the deformation of the wreckage would allow and this is shown in Figure F-11. The presence of this floor panel in the fuselage greatly assisted the three-dimensional assessment of the IED location. Witness marks between this floor and the aircraft structure, tie down rail, roller rail and relative areas of blast damage left no doubt that container 4041 had been located at position 14L at the time of detonation.

7. Analysis

The general character of damage that could be seen on the reconstructions of containers 4041 and 7511 was not of a type seen on the wreckage of any of the other containers examined. In particular, the reconstruction of the floor of container 4041 revealed an area of severe distortion, tearing and blackening localised in its aft outboard quarter which, together with the results of the forensic examination of items from this part of the container, left no doubt that the IED had detonated within this container.

Within container 4041 the lack of direct blast damage (of the type seen on the outboard floor edge member and lower portions of the aft face structural members) on most of the floor panel in the heavily distorted area suggested that this had been protected by, presumably, a piece of luggage. The downward heaving of the floor in this area was sufficient to stretch the floor material, far enough to be cut by cargo bay sub structure, and distort the adjacent fuselage frames. This supported the view that the item of baggage containing the IED had been positioned fairly close to the floor but not actually placed upon it. The installation of the floor of container 4041 into the fuselage reconstruction (Figure F-11) showed the blast to have been centered almost directly above frame 700 and that its main effects had not only been directed mostly downwards

and outboard but also rearwards. The blast effects on the aircraft skin were onto stringer 39L but centered at station 710 (Figure F-12). Downwards crushing at the top, and rearwards distortion of frame 700 was apparent as well as rearwards distortion of frame 720.

With the two container reconstructions placed together it became apparent that a relatively mild blast had exited container 4041 through the rear lower face to the left of the curtain and impinged at an angle on the forward face of container 7511. This had punched a hole, Figure F-10, approximately 8 inches square some 10 inches up from its base and removed the surface of this face inboard from the hole for some 50 inches. Radiating out from the hole were areas of sooting, and other black deposits, extending to the top of the container. No signs were present of any similar damage on other external or internal faces of container 7511 or the immediately adjacent containers 14R and 21R.

The above assessment of the directions of distortion, comparison of damage to both containers, and the related airframe damage adjacent to the container position, enabled the most probable lateral and vertical location of the IED to be established as shown in Figure F-13, centered longitudinally on station 700.

8. Conclusions

Throughout the general examination of the aircraft wreckage, direct evidence of blast damage was exhibited on the airframe only in the area bounded, approximately, by stations 700 and 720 and stringers 38L and 40L. Blast damage was found only on pieces of containers 4042 and 7511, the relative location and character of which left no doubt that it was directly associated with airframe damage. Thus, these two containers had been loaded in positions 14L and 21L as recorded on the Pan Am cargo loading documents. There was also no doubt that the IED had been located within container 14L, specifically in its aft outboard quarter as indicated in Figure F-13, centered on station 700.

Blast damage to the forward face of container 7511 was as a direct result of hot gases/fragments escaping from the aft face of container 4041. No evidence was seen to suggest that more than one IED had detonated on Flight PA103.

Baggage Container Identification and Location Forward Cargo Hold

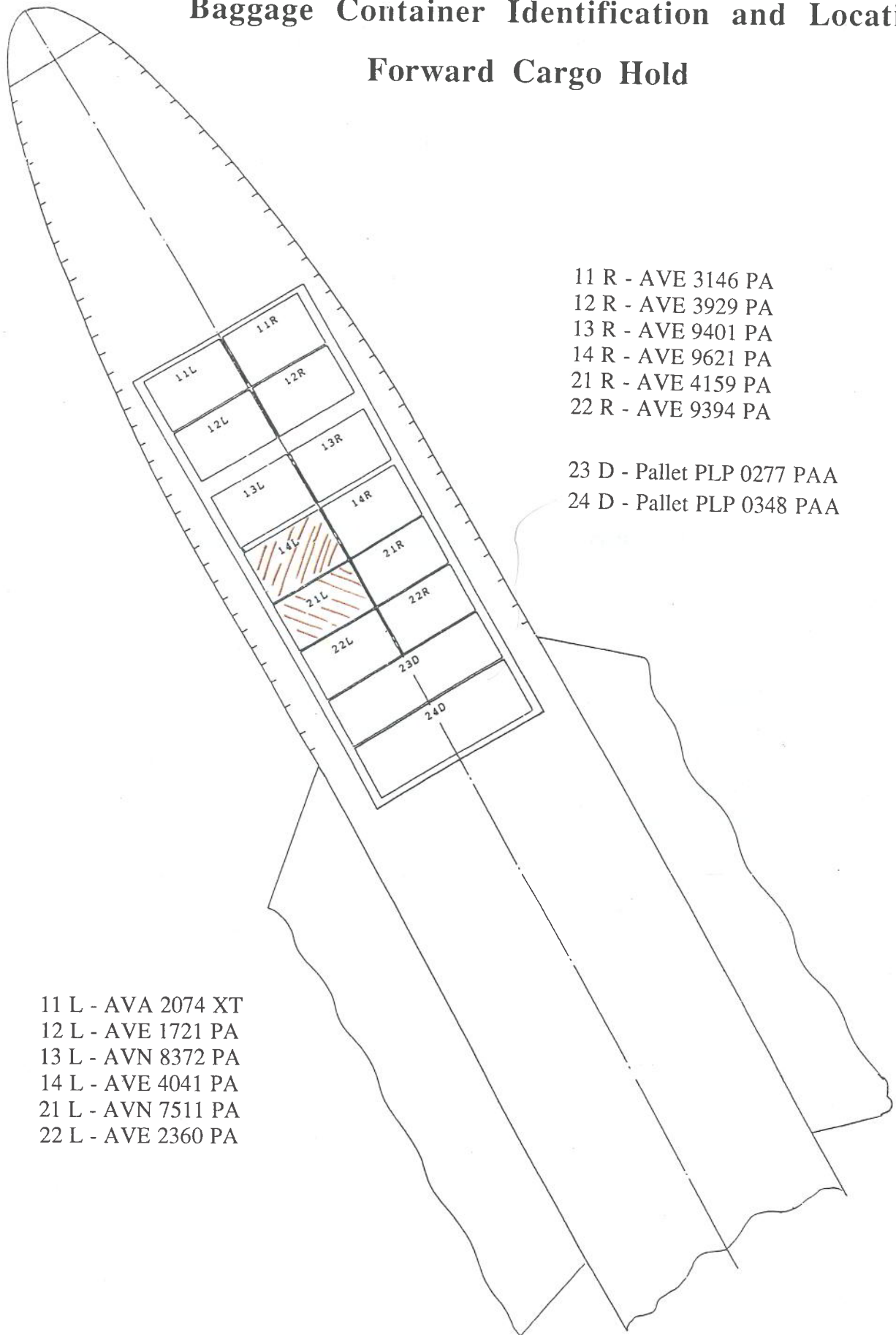


Figure F-1

PAN AM (IATA) ID CODE...AVE

OTHER CODES...LD3

RATE CLASSIFICATION

International...8

US Domestic...LD3

MAXIMUM GROSS WEIGHT (INCLUDES TARE)

3500 lb 1588 kg

TARE

240 ± 20 lb 109 ± 9 kg

Weight varies. Check weight on unit.

USABLE INTERIOR VOLUME

139 cu ft 4 cu m

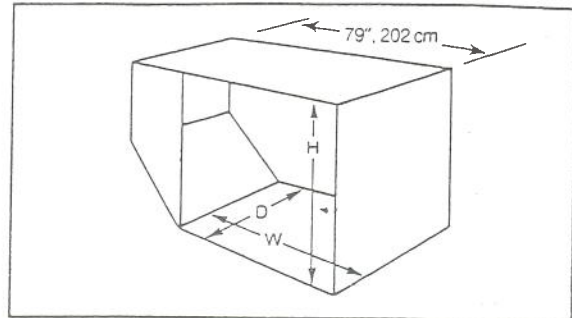
DIMENSIONS INCHES CENTIMETERS

Base Size 61 D x 62 W 153 D x 156 W

Maximum Height 64" H 163 H

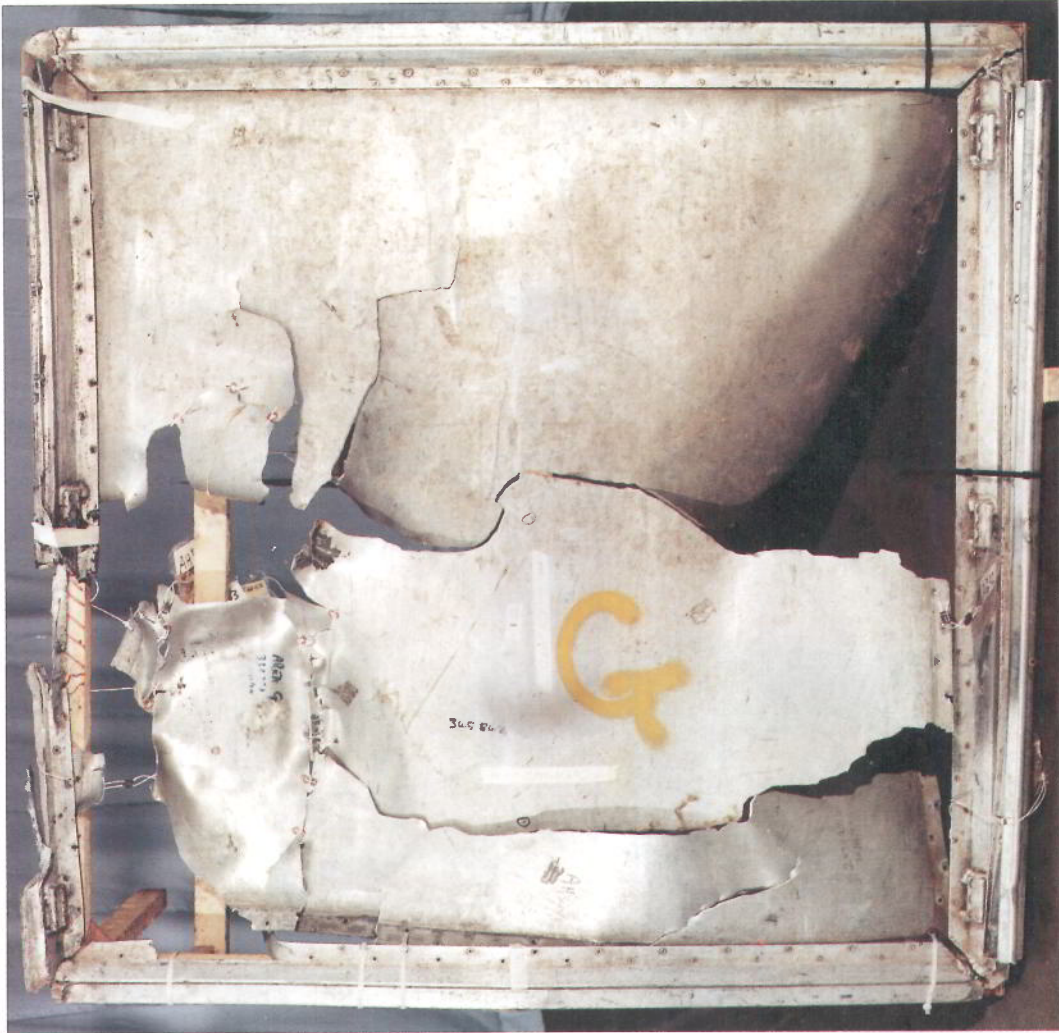
Maximum Door Opening 57 W x 62 H 145 W x 157 H

- All dimensions and weights rounded off to nearest whole number.
- Inside dimensions are 3 to 7 inches (8 to 18 cm) less than base and maximum height.



Lower Deck Container
Half Width—Cargo

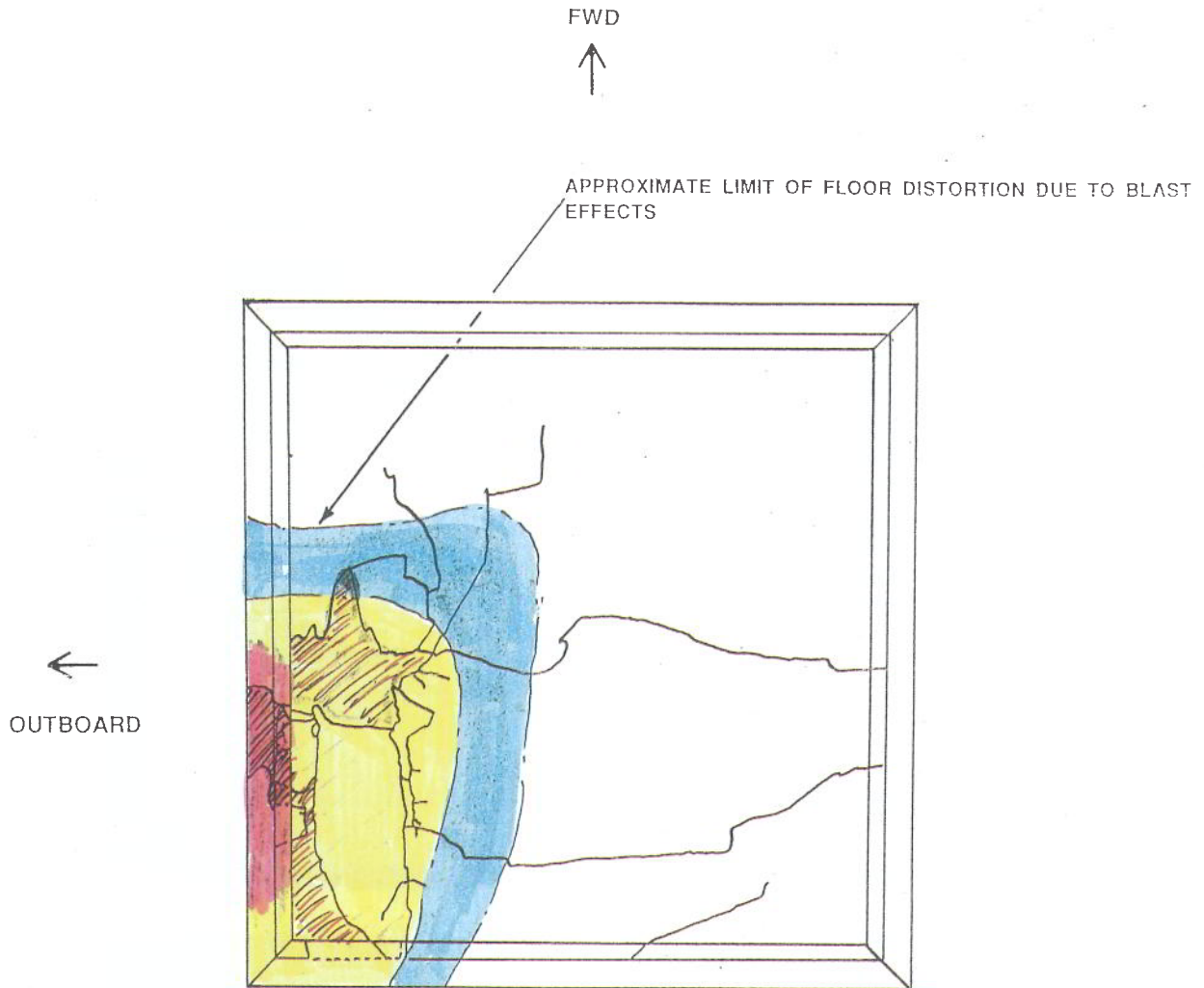
Figure F-2



Detail of Damage to Container Floor

Figure F-3

BAGGAGE CONTAINER FLOOR DAMAGE DIAGRAM



N739PA - FLOOR PANEL MAP FROM CONTAINER

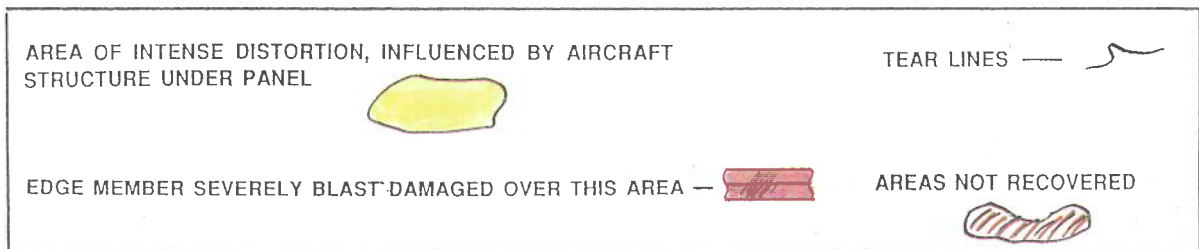
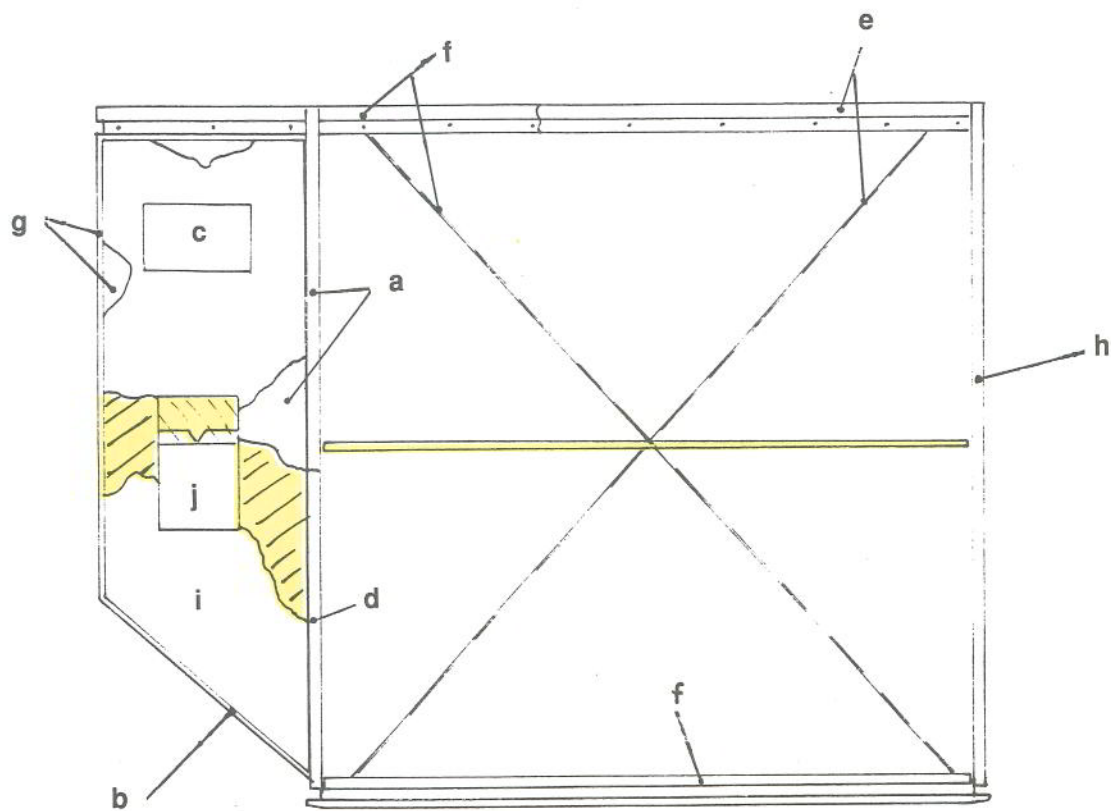


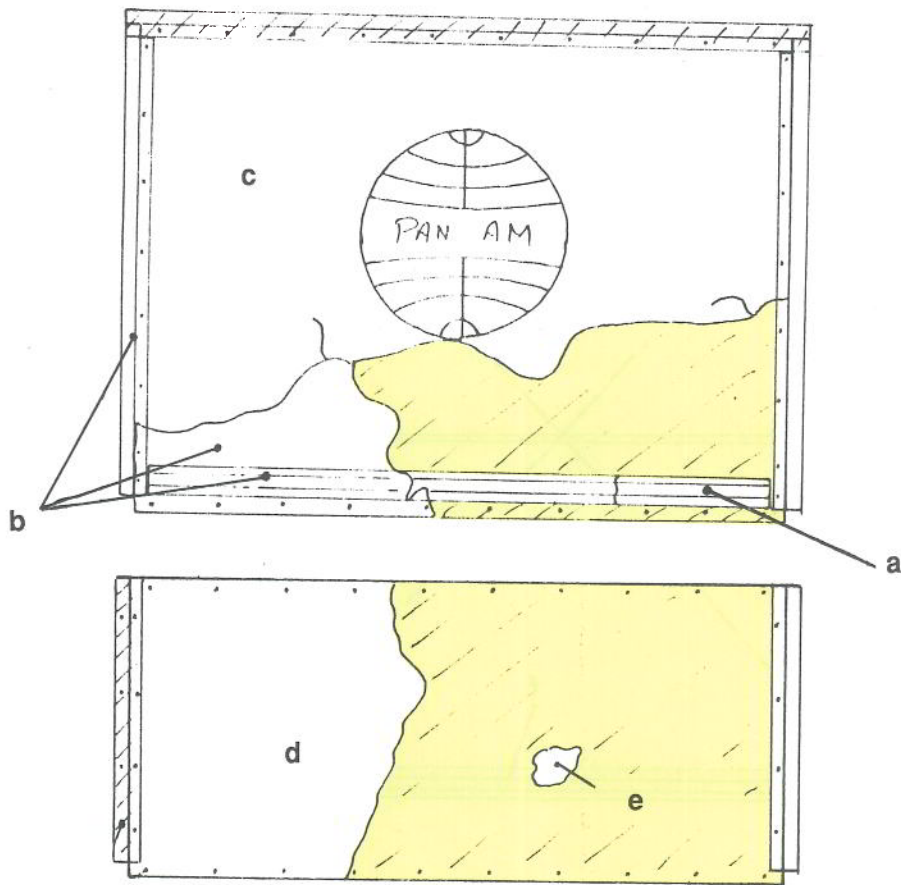
Figure F-4



- a Curtain aperture left side vertical edge member, upper half
- b Sloping face edge member
- c Container manufacturer's data plate containing burnt piece of material which itself contained a fragment of circuit board
- d Curtain aperture left side vertical edge member, lower half
- e Upper edge member, right half, attached to roof edge member and one curtain bar
- f Upper edge member, left half, attached to roof edge member, cutrain wire and lower curtain bar
- g Left edge vertical member
- h Curtain aperture right side vertical member
- i Left side lower skin section adjoining sloping face
- j Soot stained plastic sheet

**Aft face of container AVE 4041 PA, view
looking forward**

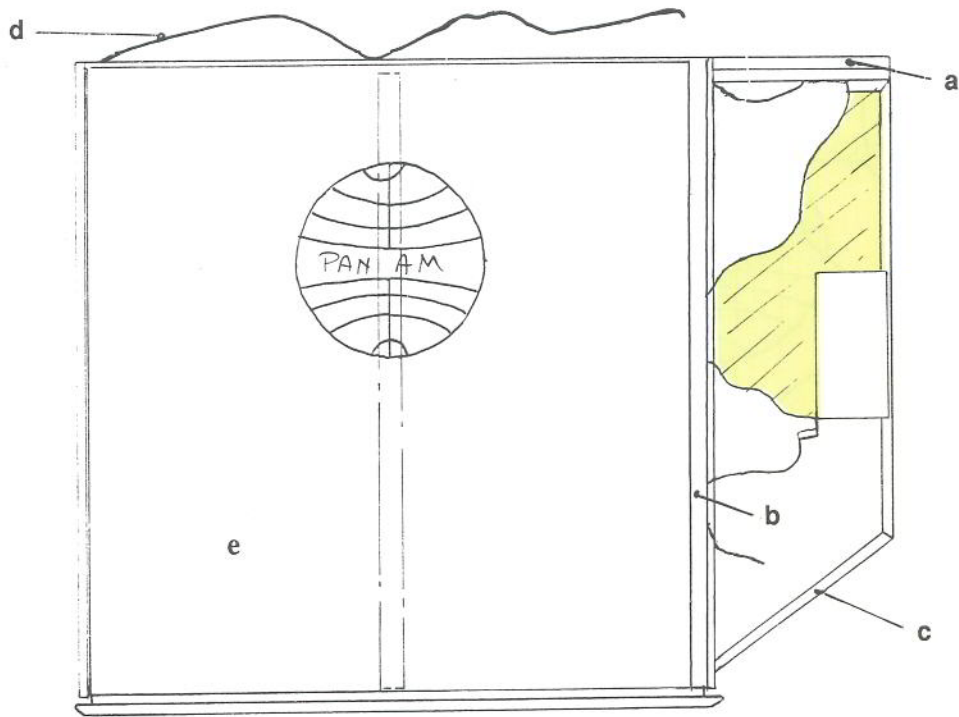
Figure F-5



- a Stiffener section from base of vertical face
- b Vertical face forward edge member, lower stiffener section and skin fragment
- c Distorted upper section of vertical face skin
- d Forward section of sloping face skin, severely distorted
- e Fragment of container skin, provisionally thought to be part of sloping face skin.

Outboard faces of AVE 404

Figure F-6



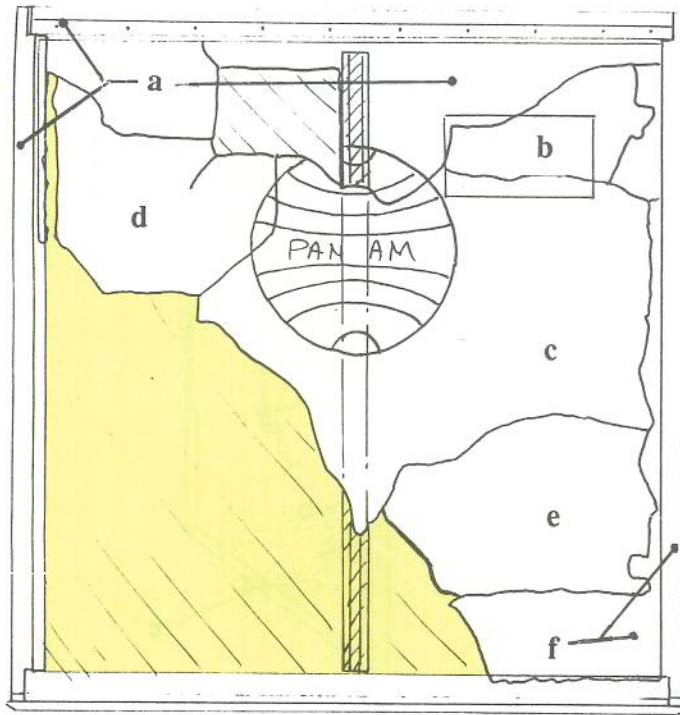
Outboard section of roof edge member

- b Forward face outboard skin, attached to vertical edge member
- c Forward edge member of sloping face
- d Roof skin panel, complete except for aft outboard corner
- e Forward face panel, complete with top, left and lower edge members



Forward face of AVE 4041 PA

Figure F-7

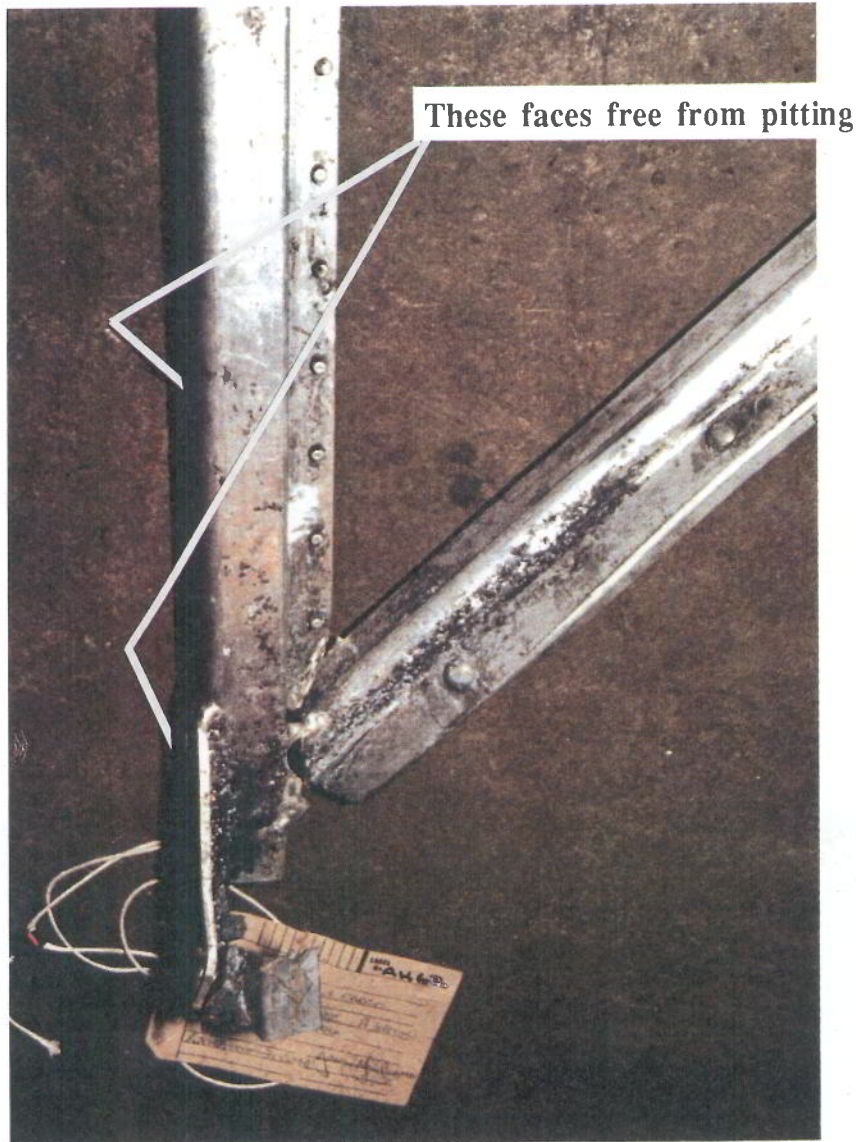


- a Aft, top and roof edge members including upper section of skin
- b Repair patch from upper right side
- c Mid section of skin including stiffener section
- d Upper skin section
- e Lower skin section
- f Right side vertical edge member attached to lower piece of skin



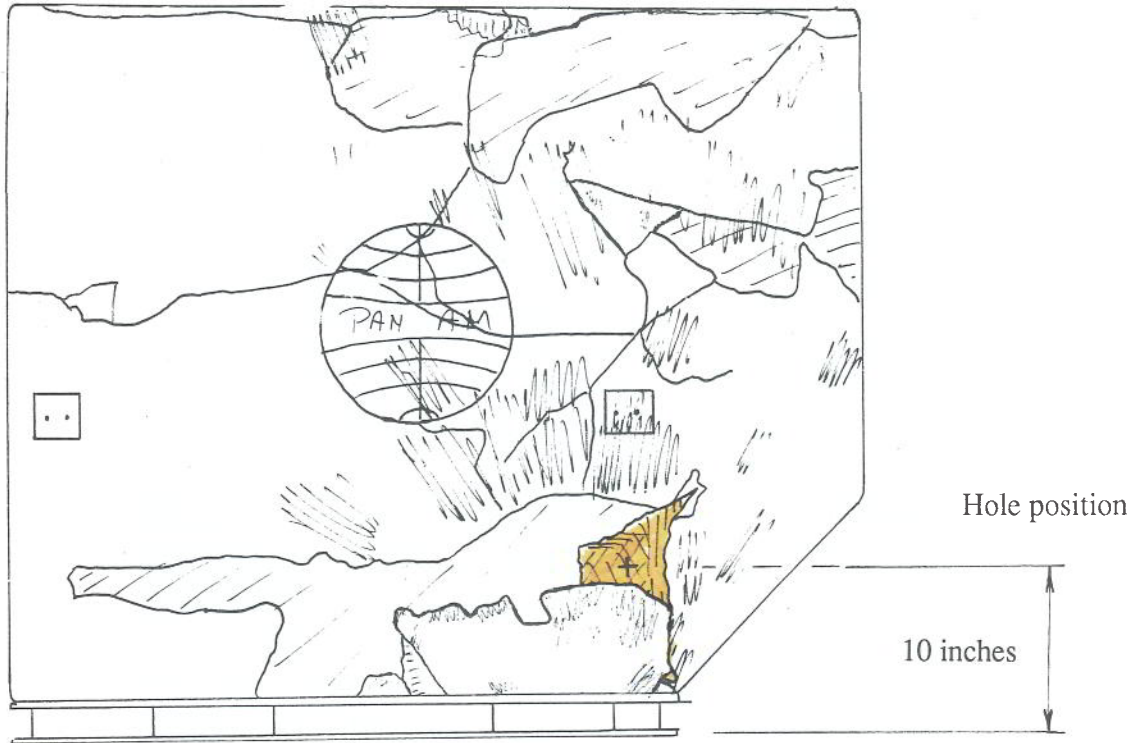
Inboard face of container AVE 4041 PA

Figure F-8



**Detail of items from aft face of container
AVE 4041 PA showing evidence of blast
damage**

Figure F-9



**Forward face of container AVN 7511 PA,
view looking aft**

Figure F-10



Installation of container floor inside fuselage reconstruction

Figure F-11

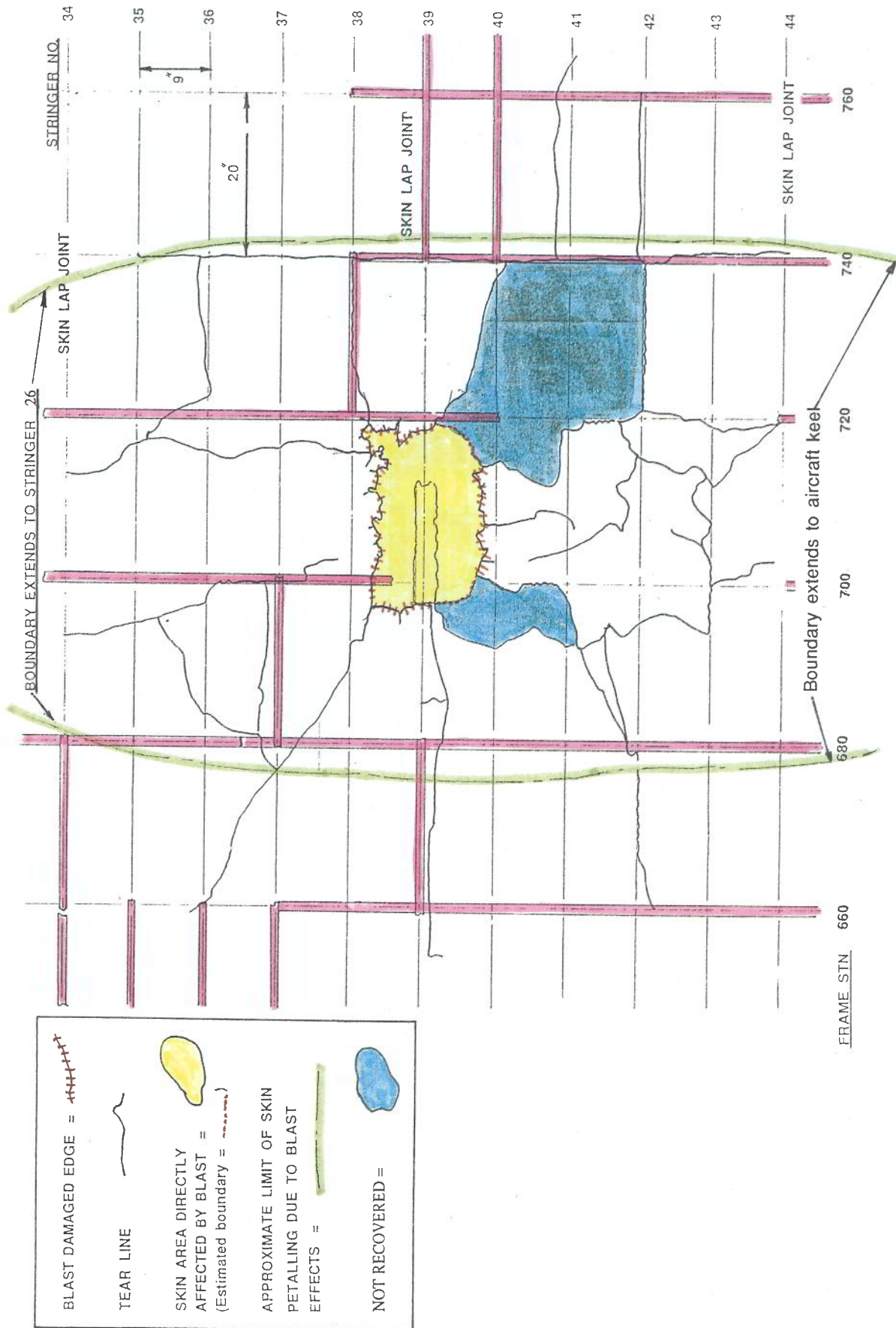


Figure F-12

N739PA Skin Structure Damage Diagram

Likely lateral and vertical position of the IED

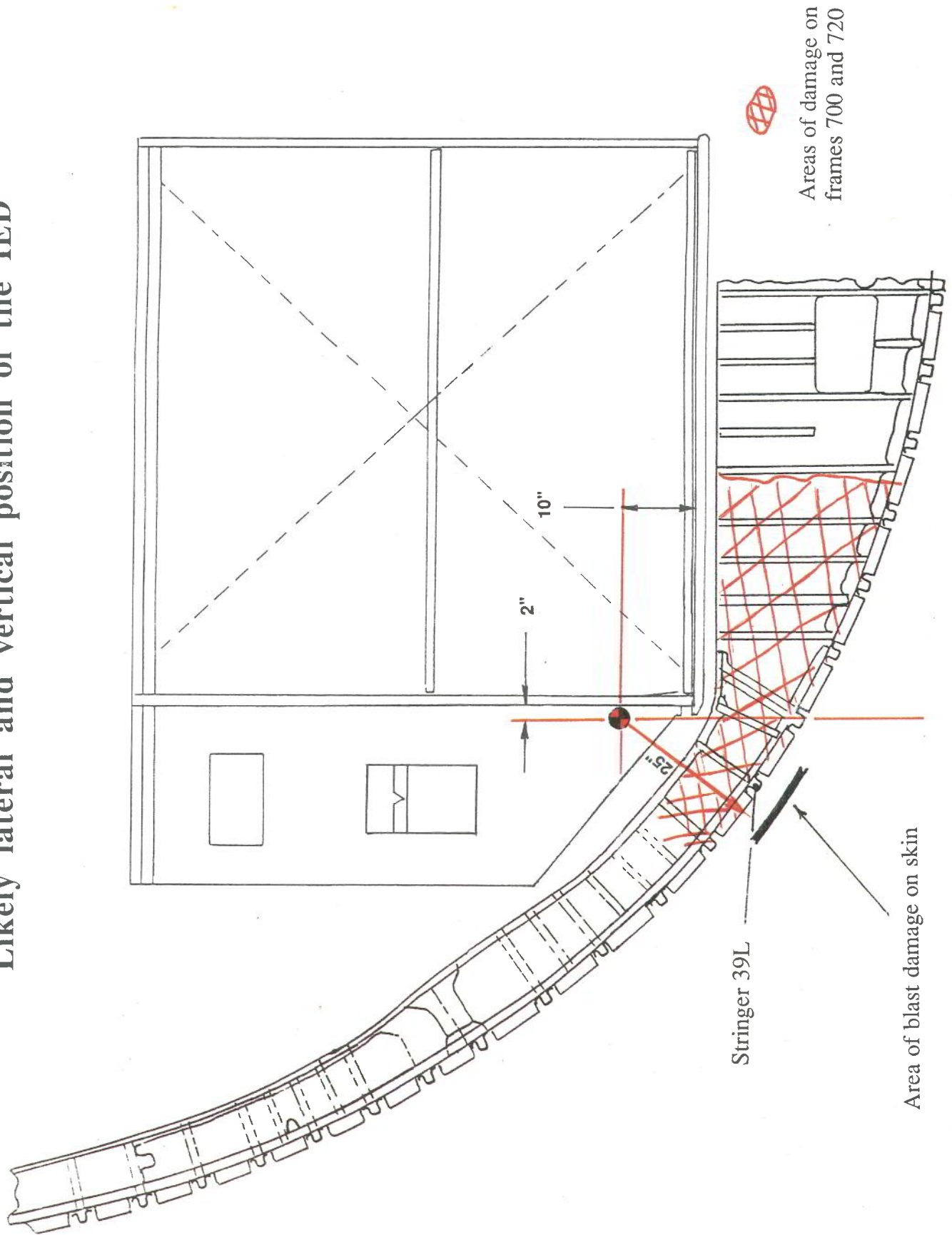


Figure F-13

MACH STEM SHOCK WAVE EFFECTS

1. Introduction

An explosive detonation within a fuselage, in reasonably close proximity to the skin, will produce a high intensity shock wave which will propagate outwards from the centre of detonation. On reaching the inner surface of the fuselage skin, energy will partially be absorbed in shattering, deforming and accelerating the skin and stringer material in its path. Much of the remaining energy will be transmitted, as a shock wave, through the skin and into the atmosphere but a significant amount of energy will be returned as a reflected shock wave, which will travel back into the fuselage interior where it will interact with the incident shock to produce Mach stem shocks - re-combination shock waves which can have pressures and velocities of propagation greater than the incident shock.

The Mach stem phenomenon is significant for two reasons. Firstly, it gives rise (for relatively small charge sizes) to a geometric limitation on the area of skin material which the incident shock wave can shatter. This geometric limitation occurs irrespective of charge size (within the range of charge sizes considered realistic for the Flight PA103 scenario), and thus provides a means of calculating the standoff distance of the explosive charge from the fuselage skin. Secondly, the Mach stem may have been a significant factor in transmitting explosive energy through the fuselage cavities, producing damage at a number of separate sites remote from the source of the explosion.

2. Mach stem shock wave formation

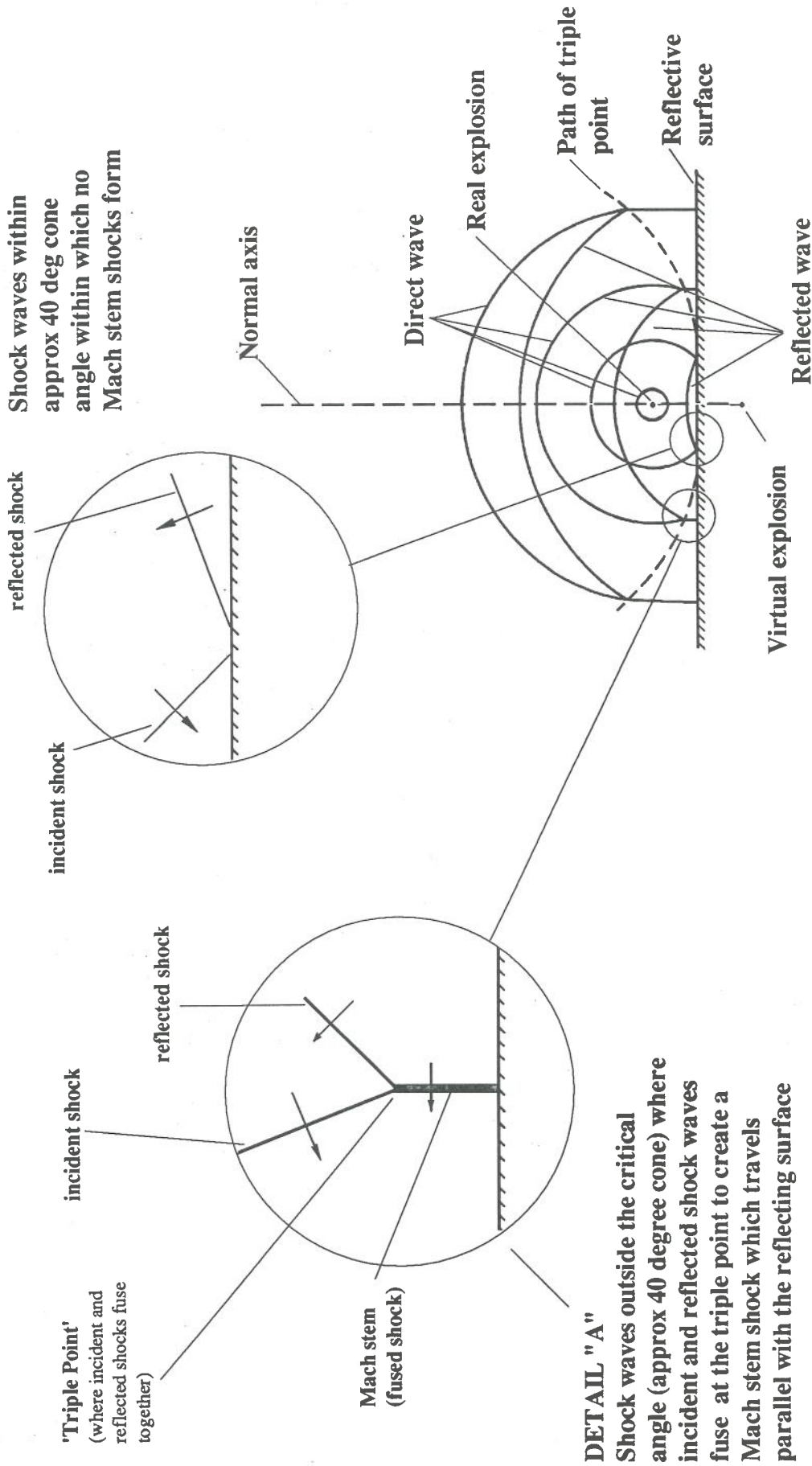
A Mach stem shock is formed by the interaction between the incident and reflected shock waves, resulting in a coalescing of the two waves to produce a new, single, shock wave. If an explosive charge is detonated in a free field at some standoff distance from a reflective surface, then the incident shock wave expands spherically until the wave front contacts the reflective surface, when that element of the wave surface will be reflected back (Figure G-1). The local angle between the spherical wave front and the reflecting surface is zero at the point where the reflecting surface intersects the normal axis, resulting in wave reflection directly back towards the source and maximum reflected overpressure at the reflective surface. The angle between the wave front and the reflecting surface at other locations increases with distance from the normal axis, producing a corresponding increase in the oblique angle of reflection of the wave element, with a corresponding reduction in the reflected overpressure. (To a

first order of approximation, explosive shock waves can be considered to follow similar reflection and refraction paths to light waves, ref: "Geometric Shock Initiation of Pyrotechnics and Explosives", R Weinheimer, McDonnell Douglas Aerospace Co.) Beyond some critical (conical) angle about the normal axis, typically around 40 degrees, the reflected and incident waves coalesce to form Mach stem shock waves which, effectively, bisect the angle between the incident and reflected waves, and thus travel approximately at right angles to the normal axis, i.e. parallel with the reflective surface (detail "A", figure G-1).

3. Estimation of charge standoff distance from the fuselage skin

Within the constraint of the likely charge size used on Flight PA103, calculations suggested that the initial Mach stem shock wave pressure close to the region of Mach stem formation (i.e. the shock wave *face-on* pressure, acting at right angles to the skin), was likely to be more than twice that of the incident shock wave, with a velocity of propagation perhaps 25% greater. However, the Mach stem out-of-plane pressure, i.e. the pressure felt by the reflecting surface where the Mach stem touches it, would have been relatively low and insufficient to shatter the skin material. Therefore, provided that the charge had sufficient energy to produce skin shatter within the conical central region where no Mach stems form, the size of the shattered region would be a function mainly of charge standoff distance, and charge weight would have had little influence. Consequently, it was possible to calculate the charge standoff distance required to produce a given size of shattered skin from geometric considerations alone. On this basis, a charge standoff distance of approximately 25 to 27 inches would have resulted in a shattered region of some 18 to 20 inches in diameter, broadly comparable to the size of the shattered region evident on the three-dimensional wreckage reconstruction.

Whilst the analytical method makes no allowance for the effect of the IED casing, or any other baggage or container structure interposed between the charge and the fuselage skin, the presence of such a barrier would have tended to absorb energy rather than re-direct the transmitted shock wave; therefore its presence would have been more critical in terms of charge size than of position. Certainly, the standoff distance predicted by this method was strikingly similar to the figure of 25 inches derived independently from the container and fuselage reconstructions.



Shock waves within
approx 40 deg cone
angle within which no
Mach stem shocks form

reflected shock

incident shock

incident shock

reflected shock

'Triple Point'
(where incident and
reflected shocks fuse
together)

Mach stem
(fused shock)

DETAIL "A"

Shock waves outside the critical
angle (approx 40 degree cone) where
incident and reflected shock waves
fuse at the triple point to create a
Mach stem shock which travels
parallel with the reflecting surface

Normal axis

Direct wave

Real explosion

Path of triple
point

Reflective
surface

Virtual explosion

Reflected wave

Mach Stem Shock Formation

Figure G-1